Thien An Huynh

CAN PROCESS INTENSIFICATION CHANGE THE FUTURE OF BIODIESEL?

CAN PROCESS INTENSIFICATION CHANGE THE FUTURE OF BIODIESEL?

Thien An Huynh

CAN PROCESS INTENSIFICATION CHANGE THE FUTURE OF BIODIESEL?

DISSERTATION

to obtain

the degree of doctor at the Universiteit Twente,

on the authority of the rector magnificus,

Prof. dr. ir. A. Veldkamp,

on account of the decision of the Doctorate Board

to be publicly defended

on Thursday 22 September 2022 at 14.45 hours

by

Thien An Huynh

born on the 18th of November, 1987

in Ho Chi Minh city, Vietnam

This dissertation has been approved by:

Supervisors

Prof. dr. ir. E. Zondervan
Prof. dr. ing. M.B. Franke

The research described in this thesis was carried out at the Laboratory of Process Systems Engineering in the Sustainable Process Technology group of the Faculty of Science and Technology, the University of Twente, the Netherlands.

Cover design:	Thien An Huynh
Printed by:	Gildeprint
Lay-out:	Thien An Huynh
ISBN:	978-90-365-5421-3
DOI:	10.3990/1.9789036554213

Graduation Committee:

Chair:	Prof. dr. J.L. Herek University of Twente
Supervisors:	Prof. dr. ir. E. Zondervan University of Twente
	Prof. dr. ing. M.B. Franke University of Twente
Committee Members:	Prof. dr. ir. D.W.F. Brilman University of Twente
	Prof. dr. ir. W.G.J. van der Meer University of Twente
	Prof. dr. F. Gallucci Eindhoven University of Technology
	Prof. dr. D.R. Lewin Technion-Israel Institute of Technology

Acknowledgements

This thesis marks the end of my PhD journey. It is really an emotional moment. I cannot make it this far without the support of many people who I would like to express my deep sense of gratitude.

First, I would like to thank my first promoter, Prof. Edwin Zondervan. Edwin gave me an opportunity which I do not think anyone would give me. His kind support and instruction were invaluable during the project, especially in the turbulent time when we moved from Bremen University to the University of Twente. He always listens to my complains and whining with great patience and understanding. Of course, I would also like to thank my second promoter, Prof. Meik B. Franke. His support and pragmatic industrial view have contributed greatly for the success of this thesis. I have learnt a lot from his experience and knowledge.

The next person I would like to thank is my wife, Hang. Without her love, support and encouragement, I could not overcome all of the difficulties in the PhD journey and in life. Thank you, my love, for always being with me.

In my PhD journey, I have met and made friends with many wonderful people. I am grateful that we have kept our contacts until this day and in the future.

In Bremen, I would like to thank the former colleagues in the Bremen University, especially, Mahmoud, Christopher, Mar, Paolo and Philipp. The landlady, Ms. Gabi, was very nice and help me a lot during the time when I first came to Germany. Grazia was my colleague for only 3 months but we have become friend and keep our contact until today.

In the University of Twente, I would like to thank the colleagues in SPT Group who I shared a lot of my weird and sometimes creepy taste of foods. This was one of the best times of my life. My thanks to Shahab (the party master) and Jasper for being my paranymphs, a long list of colleagues: Martijn, Tessa, Tim, Eline, Albertus, Rick, Hilbert, Vahideh, Kim, Romolo, Christian, Dooli, Peter, Mahsa, Dwi, Yordi, Michel, Enrico, Mario, Austin and all those I do not name here. My thanks to Yvonne for her kind support in all matters relating to paperwork and procedures. I would also like to thank Louis for his help with all the matters relating to software license and Friday scientific meetings which I have learnt many things from.

I had a very good time working with the master students in different projects. I have learnt many things from them, from the innovative way of solving problems to new cultures. I would like to express my many thanks to Vincent and Mattia for their works and friendship. Those two are amazing students and friends. I also would like to thank Wisse for joining our team and we have done a good job.

There is a nice colleague and friend, from Bremen to Twente, who I would like to express my thanks. She is Maryam. It was fun to have you in the team.

Life would be so boring if there are no friends and parties. I am glad that I met nice friends here in Enschede. My many thanks to party team: Maiander (the Dutch Viking), Tasos and Aditya.

I would also like to thank the members of the promotion committee: Prof. J.L. Herek (University of Twente), Prof. D.W.F. Brilman (University of Twente), Prof. W.G.J. van der Meer (University of Twente), Prof. F. Gallucci (Eindhoven University of Technology) and Prof. D.R. Lewin (Technion-Israel Institute of Technology). I am honoured that you are willing to participate in my promotion.

My mother, father and brother are the ones who always give me a lot of support during the hardest moments in my life. Thank you for everything.

Finally, here is the biodiesel team of cats.

University of Twente
TNW | SPT | PSE LAB

LABORATORY OF PROCESS SYSTEMS ENGINEERING

Biodiesel Superstructure - Team of Cats

Edwin – The professor cat

Vincent – The coding cat

An – The planning cat

Mattia – The data cat

Summary

While electricity has been identified as a sustainable solution for future mobility, biodiesel still has an important role to reduce the greenhouse gas emission in the European transport sector, at least, until 2050. The consumption of biofuel in Europe has increased nearly 10 times from 2004 to 2020. In 2020, the share of biodiesel is three quarters of total renewable energy consumption in transportation. However, the demand for fossil fuels is still high due to their low prices. To achieve the environmental targets and replace the fossil fuels, the costs of biodiesel production have to be reduced.

Biodiesel is a type of renewable fuel derived from green sources through chemical reactions. The conventional biodiesels produced from vegetable oils such as rapeseed oil and palm oil are designated as the first generation. Due to debates on food-or-fuel and deforestation by palm-oil farmers, the first generation biodiesel is gradually replaced by the second generation which is produced from waste and residual feedstocks such as used cooking oil and animal fats. With recent advances in biotechnology, the third generation of biodiesel from bioengineering feedstocks such as algae is under development. Overall, the feedstock greatly affects the biodiesel production process and contributes about 80% of the total production cost.

The most common biodiesel is the mixture of fatty acid methyl esters (FAME) which is conventionally produced from vegetable oils and methanol. The biodiesel production is in either batch- or continuous type which includes reaction and purification processes. Depending on the level of free fatty acid content in the feedstock, the reaction is transesterification or esterification with base or acid catalysts, respectively. Innovative production technologies such as membrane reactor, reactive distillation, supercritical reactor, etc. are important for improving the biodiesel production in terms of costs, energy requirement and environmental impact.

The membrane reactor is a process intensification technology which has appeared in many studies to improve the biodiesel production. The advantages of the membrane reactor include higher conversion rate and purity of the biodiesel product. However, membrane fouling severely affects the performance of the reactor. Process systems engineering tools such as mathematical programming can be used to reduce the impact of membrane fouling in term of operating costs. Chapter 2 presents two novel mathematical models for biodiesel production, a membrane reactor model with dynamic functions of reversible and irreversible fouling, and a dynamic membrane cleaning model. The results of solving the models show that the fouling severely reduces the performance of the membrane reactor and an optimal operating cycle can be identified in the balance of cleaning costs and production capacity.

Chapter 3 brings the optimization of biodiesel production from equipment level to process level with superstructure optimization. The superstructure is a network of different alternative options which can be used to form possible processing routes. In this work, the superstructure model serves as a bridge between three generation feedstocks and innovative biodiesel production technologies. The optimal route to produce biodiesel from tallow with reactive distillation and heterogenous acid catalyst is found by solving the superstructure optimization problem.

In chapter 4, the superstructure model is used to analyse the impacts of different uncertainties such as the prices of feedstock and products, and the production capacity on the total profit of a biodiesel refinery. By assessing different scenarios, the reactive distillation is identified as a potential technology for biodiesel production in terms of production costs and flexibility. From the technical assessment, the process intensification technologies such as reactive distillation are important to biodiesel production in particular and process industries in general.

Chapter 5 discusses about the potential of process intensification and digital twin applications in the energy transition through their applications in the process industries. While process intensification and digital twin represent the advances of technology in physical and digital forms, their deployments in process industries are not always smoothly. There are barriers such as conservative management, high investment costs and lack of capability with exist plants. The chapter presents the idea of combining the two concepts to improve individual strong points and overcome the barriers. The digital twin offers high quality and dynamic models which can be used to develop, test and improve not only the process intensification designs but also their operating conditions. Therefore, the combination reduces the investments for prototypes and pilot plants as well as the costs of adjusting the physical equipment.

Samenvatting

Hoewel elektriciteit is geïdentificeerd als een duurzame oplossing voor toekomstige mobiliteit, speelt biodiesel nog steeds een belangrijke rol bij het verminderen van de uitstoot van broeikasgassen in de Europese transportsector, in ieder geval tot 2050. Het verbruik van biobrandstof in Europa is sinds 2004 tot 2020 bijna tien keer zo groot geworden. In 2020 is het aandeel biodiesel driekwart van het totale verbruik van hernieuwbare energie in het transport. De vraag naar fossiele brandstoffen is echter nog steeds groot vanwege de lage prijzen. Om de milieudoelstellingen te halen en de fossiele brandstoffen te vervangen, moeten de kosten van de productie van biodiesel omlaag.

Biodiesel is een soort hernieuwbare brandstof die via chemische reacties uit groene bronnen wordt gewonnen. De conventionele biodiesels geproduceerd uit plantaardige oliën zoals koolzaadolie en palmolie worden aangeduid als de eerste generatie. Door discussies over voedsel of brandstof en ontbossing door palmolieboeren, wordt de eerste generatie biodiesel geleidelijk vervangen door de tweede generatie die wordt geproduceerd uit afval en restgrondstoffen zoals gebruikt frituurvet en dierlijke vetten. Met de recente vooruitgang in de biotechnologie is de derde generatie biodiesel uit bio-engineeringgrondstoffen zoals algen in ontwikkeling. Over het algemeen heeft de grondstof een grote invloed op het productieproces van biodiesel en draagt het ongeveer voor 80% bij aan de totale productiekosten.

De meest voorkomende biodiesel is een mengsel van vetzuurmethylesters (FAME) dat conventioneel wordt geproduceerd uit plantaardige oliën en methanol. De productie van biodiesel is batch-gewijs of continu, inclusief reactie- en zuiveringsprocessen. Afhankelijk van het gehalte aan vrije vetzuren in de voeding, vind er een omestering of verestering met respectievelijk base- of zure katalysatoren plaats. Innovatieve productietechnologieën zoals membraanreactoren, reactieve destillatie en superkritische reactoren zijn belangrijk voor het verbeteren van de biodieselproductie in termen van kosten, energiebehoefte en milieu-impact.

De membraanreactor is een proces intensificatie technologie die in veel onderzoeken is genoemd als technologie om de productie van biodiesel te verbeteren. Voordelen van de membraanreactor zijn onder meer een hogere conversie en zuiverheid van het biodieselproduct. Membraanvervuiling heeft echter een ernstige invloed op de prestaties van de reactor. Gereedschappen voor process systems engineering, zoals mathematisch programmeren, kunnen worden gebruikt om de impact van membraanvervuiling in termen van investerings- en operationele kosten te verminderen. In hoofdstuk 2 worden twee nieuwe wiskundige modellen voor de productie van biodiesel, een membraanreactormodel met dynamische functies van omkeerbare en onomkeerbare vervuiling, en een dynamisch membraanreinigingsmodel geïntroduceerd. De resultaten laten zien dat de vervuiling de

prestaties van de membraanreactor ernstig vermindert en dat een optimale operationele cyclus kan worden geïdentificeerd die de reinigingskosten en productiecapaciteit balanceert.

In hoofdstuk 3 wordt de optimalisatie van de productie van biodiesel van apparaat niveau naar procesniveau met optimalisatie via superstructuren besproken. De superstructuur is een netwerk van verschillende opties waarmee mogelijke verwerkingsroutes kunnen worden gevormd. In dit hoofdstuk dient het superstructuur model als een brug tussen drie verschillende grondstoffen (verschillende generaties biomassa) en innovatieve biodieselproductietechnologieën. De optimale route om biodiesel te produceren uit talg met reactieve destillatie en een heterogene zuurkatalysator wordt gevonden door het probleem van de optimalisatie van de superstructuur op te lossen.

In hoofdstuk 4 wordt het superstructuur model gebruikt om de effecten te analyseren van verschillende onzekerheden, zoals de prijzen van grondstoffen en producten, en de productiecapaciteit op de totale winst van een biodieselraffinaderij. Door verschillende scenario's te evalueren, wordt de reactieve distillatie geïdentificeerd als een potentiële technologie voor de productie van biodiesel in termen van productiekosten en flexibiliteit. Uit de technische evaluatie blijkt dat de proces intensificatie technologieën zoals reactieve distillatie belangrijk zijn voor de productie van biodiesel in het bijzonder en de procesindustrie in het algemeen.

Hoofdstuk 5 bespreekt het potentieel van proces intensificatie en digital twin toepassingen in de energietransitie via hun toepassingen in de procesindustrie. Hoewel procesintensivering en digital twin de technologische vooruitgang in fysieke en digitale vormen vertegenwoordigen, verloopt hun implementatie in de procesindustrie niet altijd soepel. Er zijn belemmeringen zoals conservatief management, hoge investeringskosten en gebrek aan capaciteit binnen bestaande fabrieken. Die kunnen worden gebruikt voor procesregeling en optimalisatie. Dit hoofdstuk introduceert het idee om de twee concepten te combineren om zo individuele sterke punten te verbeteren en de barrières te overwinnen. De digital twin biedt hoogwaardige en dynamische modellen die kunnen worden gebruikt om niet alleen de ontwerpen voor proces intensificatie, maar ook hun operationele condities te ontwikkelen, testen en verbeteren. En daarmee worden de investeringen voor prototypes en proeffabrieken, evenals de kosten voor het aanpassen van de fysieke apparatuur sterk gereduceerd.

Table of Contents

1. Introduction

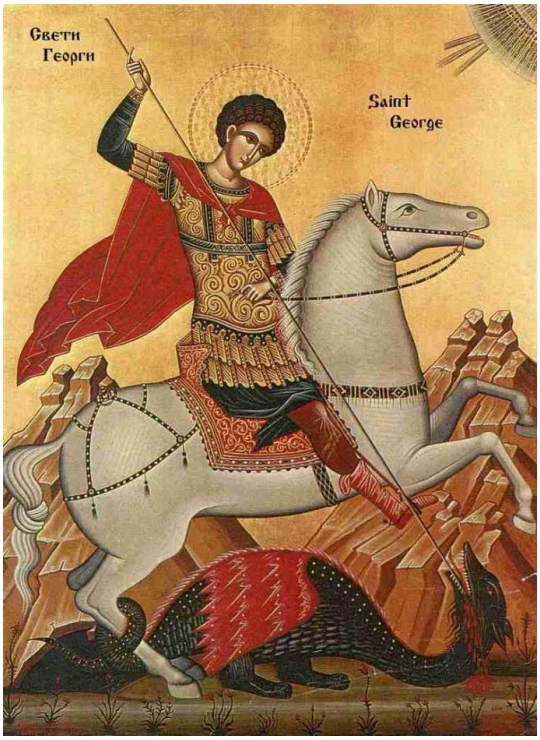

“A pessimist sees the difficulty in every opportunity, an optimist sees the opportunity in every difficulty.” - Winston Churchill

Abstract

This chapter presents a brief overview of the strategy to reduce greenhouse gas emission and biofuel production in Europe. Biodiesel which is the most consumed biofuel in transportation is considered a cornerstone in the strategy to reduce greenhouse gas emission in the transport sector. However, the price of biodiesel is still higher than fossil fuels, thus posing challenges for cost reduction in biodiesel production. This research brings solutions for the cost optimization problem with process intensification technology and process systems engineering tools such as membrane reactor modelling and superstructure optimization.

1.1. Background

Greenhouse gas (GHG) emissions are the main culprit behind many environmental problems which the world has faced in the last few decades such as rising global temperature, increasing sea level, air pollution and hostile weather patterns [1]. It is identified that more than 16% of the global GHG emission comes from the transport sector [2]. Thus, reduction of transportation GHG emissions is one of the targets of the European Commission (EC) renewable energies directive (2018/2001/EU) known as "RED II" [3]. RED II has defined that the renewable energy share in the transport sector need to be at least 14% in 2030 [3]. Nearly 75% of total GHG emissions are carbon dioxide emissions which stem largely from fossil fuels [1]. Therefore, studies to find renewable and cleaner fuels have gained more attention from governments, industries and researchers. Electricity from renewable sources such as wind, solar and hydrogen fuel cell technology are potential candidates to replace traditional fossil fuels. However, electric mobility requires heavy investments in infrastructure which is not readily available in many countries. Passenger transport apart, applications of electric vehicles in other areas such as farming, goods transport, construction, etc. are still immature. Ergo, the contribution of biofuels is still important to reach the target of RED II at least until 2030.

Biofuels, which are mostly produced from plant-based sources, are considered CO_2 neutral due to the CO_2 circulation [4]. CO_2 released from combustion engines returns to the atmosphere and is absorbed by plants which, in turn, become feedstocks for biofuel production, thus making the whole process into a CO_2 cycle [4]. The biofuel consumption in the European Union (EU) transport sector increased significantly from 1,847 kilo tonnes oil equivalent (ktoe) in 2004 to 11,924 ktoe in 2010 as shown in Figure 1.1 [3]. The biofuel consumption has increased slowly between 2010 and 2020. Aside from the exceptional situation in 2020 (i.e. the COVID crisis), the reasons of this trend include, but are not limited to; the shifting focus to electric mobility, the demand of changing feedstocks, the low oil price and the high production cost of biofuels.

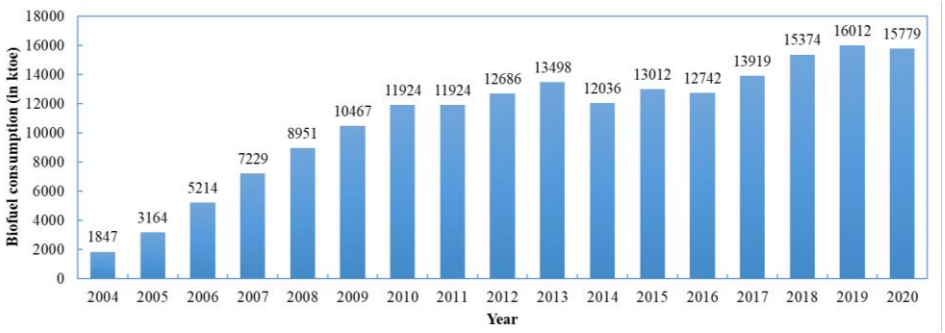

Figure 1.1: Biofuel consumption in the EU transport sector [3]

Biodiesel which shared 74% of the total renewable energy used in the EU transport sector in 2020 is still considered a cornerstone in the EU strategy to reduce the use of fossil fuels in transportation. Besides the energy contents, RED II also specified the target of feedstock for biofuels which requires a gradual replacement of edible- with non-edible feedstocks. Therefore, alternative feedstocks and innovative production processes become realistic and attractive for biofuel producers and researchers.

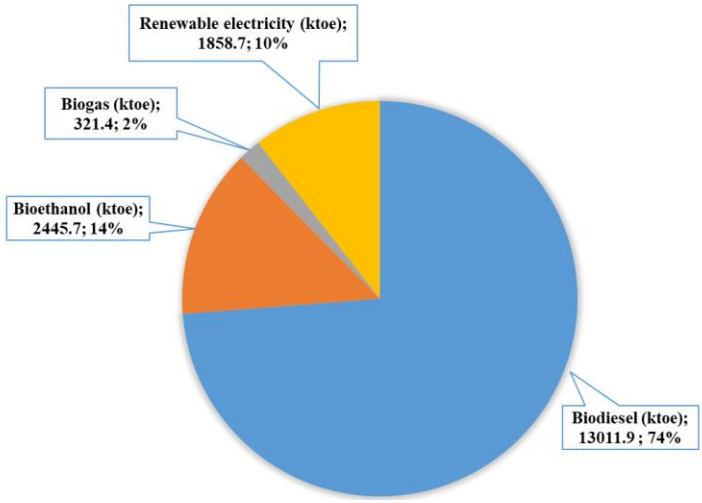

Figure 1.2: The shares of renewable energy used in EU transport sector in 2020 [3]

1.2. Biodiesel

The first reference of vegetable oils being used as fuels for diesel engines can be found in the book, "*Die Entstehung des Dieselmotors*", by Rudolf Diesel, the famous inventor of the engine that shared his name [5]. The book described a diesel engine, which was built at the request of French government by the French Otto Company, powered by peanut oil in the

Paris trade fair 1900 [5]. However, it was discovered that the direct use of vegetable oils caused operational problems such as engine deposit because of the high kinetic viscosity of the oils [5]. Many researches were conducted to raise the performance of vegetable oils as fuels, thus leading to the first development of modern-day biodiesel in 1937 by C.G. Chavanne (University of Brussels) [5].

Biodiesel is basically a mixture of fatty esters and can be industrially produced through chemical reactions of biobased feedstocks with alcohol in the presence of a catalyst [6]. The renewable nature of biodiesel comes from its wide range of green feedstocks such as vegetable oils, animal fats, waste cooking oil, and algae oil. Methanol is usually used in the biodiesel production due to its availability and low price, thus, making the mixture of fatty acid methyl esters (FAME) the most common biodiesel [7]. The production of FAME in EU reached 11,374 million litters in 2020 [3].

FAME is usually synthesized through a transesterification process of triglycerides (TG) and methanol (MeOH) with alkaline catalysts or an esterification process of free fatty acids (FFA) and MeOH with acid catalysts [6]. The biodiesel transesterification is a series of three reversible reactions which creates diglycerides (DG) and monoglycerides (MG) as intermediate products besides the main product, FAME and the by-product, glycerol (GL) [6]. The transesterification can be presented as a summarized reaction as follows [6]:

$$TG + 3\ MeOH \leftrightarrow 3\ FAME + GL \qquad (1.1)$$

The biodiesel esterification is considered simpler than the transesterification but requires higher reaction temperature and higher costs of equipment and acid catalyst. The esterification of FFA with MeOH and acid catalyst to produce FAME and water is presented as in Equation 1.2 [6].

$$FFA + MeOH \leftrightarrow FAME + H_2O \qquad (1.2)$$

In addition to be a renewable fuel, biodiesel has several advantages over the fossil fuels. While its properties are similar to traditional diesel, biodiesel has no sulphur, higher flash point and better lubricity [7]. These characters make biodiesel non-toxic, safe for storage and well compatible with unmodified engines [7]. However, the price of biodiesel is still higher than fossil fuels, thus making a serious challenge for increasing the share of the renewable fuel in the transport sector.

Biodiesel produced from different feedstocks can be classified into three generations. The first generation biodiesel is produced directly from plant oils such as rapeseed oil and palm oil. The second generation biodiesel is produced from residual and waste sources such as waste cooking oil and animal fat. The third generation biodiesel is produced from microalgae [8]. Besides defining the type of biodiesel, the feedstock also contributes

approximately 80% of the total cost of biodiesel production [9]. Therefore, the selection of feedstock is crucial to the process design and the economic feasibility of biodiesel production.

Depending on feedstock and production scale, biodiesel production is typically done batch wise or continuously with a reaction step and several purification processes. The reaction process is decided by the presence of FFA and water in the feedstock [10]. Additional treatments, different reactant ratios, high reacting temperature and/or acid catalyst are usually applied for the biodiesel production with high FFA feedstock such as waste cooking oil [10]. The crude biodiesel product of the reaction process is going through a purification process to achieve the quality as defined in the standard EN 14214 of the European Committee for Standardization. The purification process which comprises different separation, neutralization and washing steps accounts for 60 to 80% of the total biodiesel processing cost [11].

1.3. Challenges of biodiesel production

High vegetable oil price, food-fuel debates and targets for "advanced biofuels" of RED II are challenges and motivations for finding alternative biodiesel feedstock [3]. Waste cooking oil and residual animal fat from food production have been used increasingly in the biodiesel production [12]. While the waste materials are inexpensive, environmentally friendly and not food competitive, they contain a high amount of FFA and impurities. Accordingly, their usage for biodiesel production requires additional chemical treatments and washing steps, thus posing challenges of production costs and environmental impacts.

Microalgae have attracted a lot of attention as the future feedstock for biodiesel production. These microorganisms can transform CO_2 in the atmosphere and sunlight into energy with their photosynthetic pigments [13]. The advantages of microalgae are their high growth rate and adaptability which allows them to thrive in almost any aquatic and terrestrial environment including the wastewater [13]. However, the production cost is still high as compared to conventional fuels and it becomes a challenge to industrialize algae biodiesel [14].

The major challenges for biodiesel are its high selling price as compared to fossil fuels and the requirement for advanced and economic feedstocks. These challenges have attracted researchers from different fields such as biology, chemistry and economy. There are many publications to address these challenges for example, the studies on feedstocks such as the microalgae [15] and non-edible oils [16] and the techno-economic assessments of biodiesel production [17]. However, the publications focus mostly on individual aspects of the biodiesel production while a combined strategy has not received sufficient attention. The main reason is that researchers report mainly on their fields of expertise and made little connections with other fields. For example, the researches on the biodiesel feedstocks are

about characters of the raw material and product and mention the production process as simple reaction and separation steps. Another example is the technological and economic analysis of the biodiesel production which assesses different technologies and processes but with only one or two types of feedstock. The combination of feedstock selection and production optimization for biodiesel are rarely mentioned and becomes a knowledge gap in the literature. Therefore, this thesis fills the gap of knowledge by systematically combining the selection of appropriate feedstocks including three generations of feedstocks and innovative technologies such as membrane reactor into a superstructure model for biodiesel production optimization.

1.4. Scope of the thesis

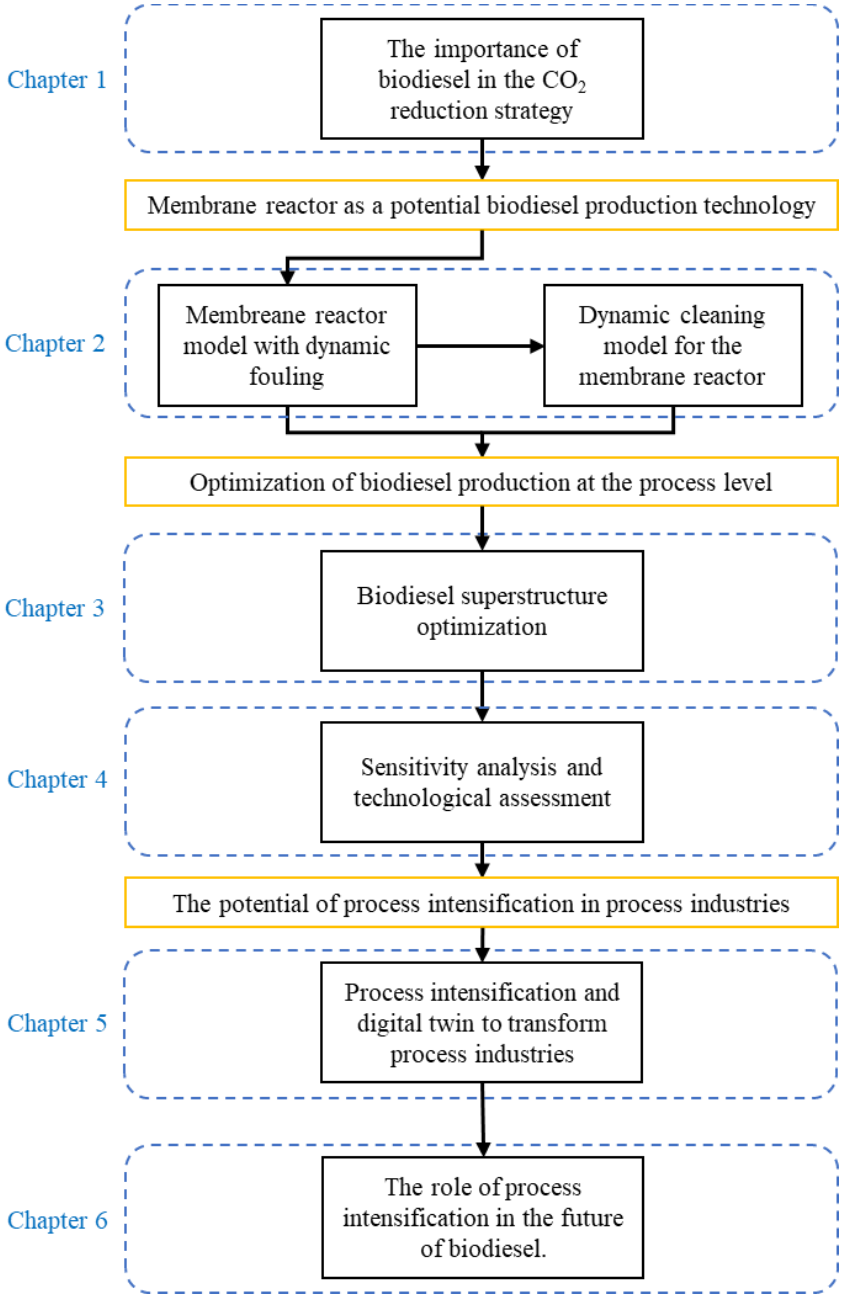

Figure 1.3: The scope of the thesis

The research presented in this thesis addresses the challenge of reducing the biodiesel production cost with process systems engineering methods, process intensification technologies and computational tools. At the equipment level, mathematical modelling and optimization are applied to improve the performance of the membrane reactor which is a process intensified technology for biodiesel production. At the process level, superstructure optimization is applied to identify the most efficient production route for biodiesel in terms of total profit, raw material consumption and energy requirement.

The membrane reactor has several advantages over traditional reactors that ensures a promising route to produce biodiesel. However, the operating cost of the membrane reactor are still high due to the fouling and costly cleaning processes. Although there are many researches related to membrane fouling and reactor in biodiesel production, the connection between the membrane fouling and reactor model is not evident. Therefore, this research develops a novel membrane reactor model with dynamic fouling functions and a membrane cleaning model for backwashing and chemical cleaning. The developed models can be used to evaluate the effect of design and operating conditions on biodiesel production. Based on the models, a tool for simulating the cyclic operation of the biodiesel membrane reactor is coded in MATLAB®.

The superstructure contains different feedstock from three biodiesel generations and various reaction- and separation technologies including membrane reactor, reactive distillation and different type of catalysts. The heat integration is an innovative function of the superstructure model which calculates the heat recovery and reduces the utility requirement. The superstructure optimization is a Mixed-Integer Nonlinear Programming (MINLP) which is solved with the Branch-And-Reduce Optimization Navigator (BARON) in the Advanced Interactive Multidimensional Modeling System (AIMMS). The results are an optimal design of a biodiesel production process and a new tool for optimizing process design under different economic and technical conditions.

This thesis answers the following questions.

- Can the cyclic operation of the membrane reactor be captured with mathematical modelling and improved with dynamic cleaning models?
- Can the superstructure model become a bridge for the biodiesel feedstock selection and process optimization in term of profit and energy requirement?
- What are the roles of process intensification and digital tools such as digital twin in the energy transition of process industries?
- Can process intensification change the future of biodiesel?

1.5. Thesis outline

Chapter two presents two new mathematical models for the membrane reactor in biodiesel production. The first is a membrane reactor model which combines a filtration model with dynamic fouling functions, component balances and reaction kinetics. The results of the model show the decline in membrane flow rate over time and the requirement of an optimized cleaning schedule to reduce the fouling, thus leading to the development of the second model, a new dynamic cleaning model for biodiesel membrane reactor. The cleaning model is used to evaluate effects of backwashing and chemical cleanings on the cleaning costs which include chemical consumption, energy requirement and production lost. An optimized operation strategy is derived from the results of the membrane reactor model and the cleaning model. Chapter three brings the optimization of biodiesel production to the process level with a new superstructure model. The superstructure includes various feedstocks from three biodiesel generations and different reaction and separation technologies from traditional to process intensification equipment. The addition of the heat integration function is an innovative feature which reduces the requirement of heating and cooling utilities by matching hot and cold streams in the process. Chapter four addresses the uncertainty of biodiesel production in term of the availability of feedstocks and technologies, the prices of raw materials, biodiesel and glycerol. A sensitivity analysis is performed to evaluate the influence of different parameters on the objective function and decision variables. Then, the optimization problem is solved with different scenarios to identify optimal process design for biodiesel production in compliance with conditions such as the availability of feedstock and technology. The influence of technology can be evaluated by doing the technological assessment. In chapter five, an overview of process intensification (PI) and digital twin (DT) in process industries is presented. In addition to individual applications, the combination of PI and DT brings potential improvements for both concepts and process industries, including biofuel production. Finally, chapter six brings the conclusion of the research and the suggestion for future works.

2. Membrane reactor and cleaning models for cyclic operation of biodiesel production

“We cannot solve our problems with the same thinking we used when we created them.” - Albert Einstein

This chapter was published in:

Huynh, T.A. and Zondervan, E., 2021, "*Dynamic modeling of fouling over multiple biofuel production cycles in a membrane reactor*", Chemical Product and Process Modeling, pp. 20200093, https://doi.org/10.1515/cppm-2020-0093

Huynh T.A., Raeisi M., Franke M.B. and Zondervan E., 2021, “*Novel Dynamic Cleaning Model for Cyclic Operation of Biodiesel Membrane Reactors*”, Chemical Engineering Transactions, 88, 883-888, https://doi.org/10.3303/CET2188147

Abstract

A membrane reactor produces high-quality biodiesel by combining both reaction and separation in a single unit. However, the reactor has disadvantages such as high operating expense and reduced efficiency over time due to membrane fouling. To solve this issue, frequent cleaning with physical and chemical methods is required. Membrane cleaning contributes to the reactor's operating cost to a large extent, including energy, chemicals and even production loss. Although there have been studies undertaken focusing on improving membrane cleaning, optimizing the performance of the membrane reactor in biodiesel production has received limited attention.

This chapter presents novel mathematical models for an intensified separation-reaction process and membrane cleaning operations of the membrane reactor in biodiesel production. The membrane reactor model is a combination of a membrane filtration model, component balances and reaction kinetics models. A unique feature is that the proposed model can capture the dynamics of membrane fouling as function of both reversible and irreversible fouling, which leads to cyclic behaviour. With an appropriate membrane cleaning model, the operational strategy can be optimized from evaluating the effects of backwashing and chemical cleaning on the membrane reactor.

In the case study of biodiesel production, the developed model was validated with experimental data. The model was in good agreement with the data, where R-squared values are 0.96 for the permeate flux and 0.95 for the biodiesel yield. From a further analysis, the period between two backwashes, or an operating cycle is a crucial factor to improve the productivity of the reactor and reduce the cleaning cost.

The result shows that the total operating time rose 2 to 3 times when the operating cycle reduced from 70 min to 15 min. The biodiesel yield increased significantly due to the extended operation. However, longer operating time led to an accumulation of more irreversible fouling, which could not be removed by backwashing. The cost of chemical cleaning rose as the irreversible fouling level increased. Regarding the cost-to-yield ratio of the biodiesel reactor, the best operating conditions were found at the operating cycle of 25 minutes between 2 backwashes. Overall, the models allow the prediction of fouling effects and reduction of the cleaning expense of the membrane reactor, thus increasing its potential as a biodiesel production technology significantly.

2.1. Introduction

Since its introduction in 1930s, biodiesel (basically a mixture of fatty esters) has become one of the most prominent renewable fuels with several advantages over petroleum diesel [5]. It is safe, renewable, non-toxic, biodegradable and a better lubricant. The renewable nature of biodiesel is indicated by its production from green sources such as vegetable oils, animal fat or even used cooking oil from the food industry.

The most challenging issue of biofuel is much higher costs of production and feedstock when comparing to mineral fuels. The price of biodiesel follows the price of edible vegetable oils closely which comprises approximately 80% of feedstock for biodiesel production in the world. The feedstock price is influenced by the type of vegetable oil, the production volumes and processes and government supportive policies. Utilizing non-edible feedstock sources is a viable way to reduce the price of biodiesel [18]. The production cost, which include the costs of equipment, operation and energy requirement, are affected by production method.

Process systems engineering tools can be used to design innovative processes for renewable fuel production while reducing costs and improving sustainability. The use of process intensification such as reactive separation can drastically decrease energy costs, both the size and number of process units and increase the yield of downstream processes. However, the investment and operating costs of intensified processes are still remarkably high and would need to be reduced before they can be applied in actual production [19].

Membrane technology has gone through significant developments in the past decades. It has the potential to improve biofuel production with the ability to combine both reaction and separation in a single unit. Dubé et al. (2007) [20] reported that a membrane reactor can be successfully used for the transesterification of canola oil into biodiesel. The reaction products (biodiesel and glycerol in methanol) are separated from the original canola oil feed because the oil droplet size is larger than the membrane pore size. A two-phase state is reported as a requirement for the operation of the membrane reactor.

Cao et al. (2009) [21] constructed a mathematical model of reaction kinetics and demonstrated that the rate of transesterification is enhanced by using a membrane reactor. The work of Cheng et al. (2010) [22] showed the effects of temperature, methanol-to-oil molar ratio and catalyst concentration on canola oil methanolysis and obtained reaction kinetics data of the membrane reactor. Chong et al. (2013) [23] developed and analyzed a model of a membrane reactor with the integration of a chemical phase equilibrium (CPE). In addition to homogeneous catalysis, Gao et al. (2017) [24], and Hapońska et al. (2019) [25] reported the effects of heterogeneous catalyzed transesterification in membrane reactors.

Overall, the membrane reactor produces higher quality biodiesel than traditional reactors due to its high conversion rate and selectivity of the desirable product [26]. Biodiesel production using a membrane reactor requires fewer downstream processing stages than conventional processes [17]. The application of membrane technology has economic and environmental benefits in reducing energy consumption, material for equipment, wastewater and the chemicals used in biodiesel production.

However, an important drawback of membrane technology is the fouling problem which affects its performance. Membrane fouling occurs when filtrated materials in the feed stream deposit and accumulate on membrane surface and/or within membrane pores. The consequences of membrane fouling are the decline of filtration flux, increased transmembrane pressure, and/or changed membrane selectivity. Although there are authors such as Cheng et al. (2012) [27], Xu et al. (2014) [28], and Abdurakhman et al. (2018) [17] who published on the operating conditions of membrane reactor, the research on the mathematical model development that describes membrane fouling for biodiesel production is rather limited. Due to the complexity of the fouling phenomena, the development of membrane fouling models is usually in the form of empirical relationships. Such empirical models have a limited predictive capability. In addition, the empirical models do not incorporate degrees-of-freedom such as the operating cycle and permeate flux that limits the productivity of membrane reactors. Degrees-of-freedom are needed to optimize the operational strategy of the membrane reactor.

Membrane fouling can be categorized into reversible and irreversible fouling. Reversible fouling is normally the formation of cake or gel layer on the membrane surface and can be removed by means of hydraulic cleanings such as backwashing. Irreversible fouling is caused by filtrated materials that penetrates the membrane pores and becomes lodged in the membrane pores and adsorbed onto the pore walls. Chemical cleaning agents are required to restore the flux in case of irreversible fouling [29].

Therefore, membrane cleaning is critical [30]. Although the cleaning cost is driving the operational cost of the membrane reactor (chemical cost, lost productivity, etc.), physical and chemical cleaning procedures are mainly determined from experience without precise prediction of results [31]. Prediction and optimization of membrane reactor cleaning are challenging tasks due to the complex relationship between membrane properties, membrane fouling, and operating conditions [32]. Research into fouling control and membrane cleaning optimization is urgently needed.

The membrane cleaning process has been studied by several researchers such as Zondervan et al. [33], and Madaeni et al. [34] in the field of water filtration and Popovic et al. [35] in dairy industry. However, the relationship between membrane fouling and cleaning in membrane reactors, especially for biofuel production has not been studied. In this

contribution, this gap is filled by setting up and connecting a novel membrane fouling- and backwashing model that can be used to simulate and optimize cyclic processes. In turn, these models can also be used to optimize decisions regarding the strategy for the long term performance of the membrane reactor which depend on the chemical cleaning policy.

In this chapter a novel dynamic mathematical model of the membrane reactor and membrane cleaning process is proposed. To provide an accurate simulation of the separation-reaction process with limited experimental data, the dynamic fouling model of membrane fouling is coupled to a reactor model. The model parameters are determined by a genetic algorithm using experimental data. After construction of the model, the transesterification process is simulated to investigate the effects of membrane fouling and process conditions in the reactor. Next, the model is used to identify the irreversible and reversible types of fouling from experimental data that could not be achieved with other membrane reactor models. Subsequently, the calculated fouling resistances are inputs of the membrane cleaning model.

The cleaning model of a membrane reactor can capture the dynamic states of membrane fouling during the physical and chemical cleaning processes. The cleaning cost, i.e., the cost of energy, chemicals, and production loss, is calculated from the relationship between the fouling level, the cleaning duration, and the utility consumption for cleaning. Consequently, the optimal cleaning conditions can improve membrane reactor efficiency in terms of operating cost and productivity.

2.2. Theory

2.2.1. Kinetic model of transesterification

The high viscosity of oil extracted directly from the seeds prevents them being used in engines as a fuel. There are different processes which can be used to produce biodiesel from various feedstocks, such as pyrolysis, micro-emulsification, dilution, and transesterification. The transesterification of triglycerides with alcohols, which is catalyzed by acid or base, is the most used method in biodiesel production. In commercial production, the most commonly used alcohols are methanol and ethanol because of their availability and low cost [36]. The large branched triglycerides (TG) reacts with the methanol to produce smaller, straight-chain molecules of methyl esters and the by-product of glycerol (GL). The transesterification process includes three reversible reactions with intermediate formation of diglycerides (DG) and monoglycerides (MG) resulting in the production of 3 mol of fatty acid methyl esters (FAME) and 1 mol of GL [37]. The stepwise reactions are as shown in equation (2.1), (2.2) and (2.3).

$$TG + MeOH \underset{k_2'}{\overset{k_1'}{\rightleftarrows}} DG + FAME \quad (2.1)$$

$$DG + MeOH \underset{k_4'}{\overset{k_3'}{\rightleftarrows}} MG + FAME \quad (2.2)$$

$$MG + MeOH \underset{k_6'}{\overset{k_5'}{\rightleftarrows}} GL + FAME \quad (2.3)$$

The reversible nature of the transesterification process creates at least two problems; the reaction time is relatively long, and the product has to be purified due to the presence of leftover oil and saponified by-products. With the aim of improving conversion rate and efficiency, the relationship of different process conditions, especially in the case of membrane reactor, and reaction kinetics has been studied by several researchers. The work of Rashid and Anwar (2008) [38] shows that alkaline-catalyzed transesterification is usually preferred to acid-catalyzed due to the higher activity and the lower process temperatures required. Most industrial biodiesel production processes are using homogeneous basic catalysts such as KOH and NaOH because of economic reasons. The ideal temperature for alkaline alcoholysis of vegetable oils is at 65 ^{o}C which is near the boiling point of methanol. A higher temperature should be avoided because it leans to accelerate the saponification of glycerides with the base catalyst [38]. Cao et al. (2009) [21] studied the effects of process conditions on the rate of transesterification of canola oil in a membrane reactor. The results show that reaction kinetics are not affected by the residence time while the increase of catalyst loading raises the reaction rate constants. Chong et al. (2013) [23] reported the importance of MeOH:oil at the feed side so that methanol becomes the continuous phase and the failure of membrane operation in the event of phase inversion if TG becomes the continuous phase. The critical point of phase inversion is expressed in terms of volume fraction of methanol (MeOH), Φ_{MeOH} to TG, Φ_{TG} ratio [23]:

$$\frac{\Phi_{MeOH}}{\Phi_{TG}} = 1.22\left(\frac{\eta^{o}_{MeOH}}{\eta^{o}_{TG}}\right)^{0,29} \quad (2.4)$$

The volume fraction ratio of MeOH to TG is calculated as 0.44 if the values for the viscosities of pure MeOH, $\eta_{MeOH}{}^{o}$ and TG, $\eta_{TG}{}^{o}$ at 333 K are substituted into equation (2.4). Thus, the most important process limitation to the membrane reactor is the MeOH to TG ratio which should be maintained at $\Phi_{MeOH}/\Phi_{TG} > 0.44$ to prevent phase inversion. With excessive amount, methanol is regarded as solvent and other components are regarded as solute [23]. Cheng et al. (2010) [22] investigated the effects of the methanol to oil molar ratio and catalyst concentration on the reaction kinetics. The work demonstrated that a high conversion can be obtained with a molar ratio of MeOH to oil of 24:1 and the ultralow NaOH concentration of 0.05 wt.%. With the experimental results, Cheng et al. [22] developed a mathematical model

for the relationship between reaction rate constants and the catalyst concentration as shown in the equation (2.5).

$$k'_i = k_i\, C \tag{2.5}$$

where the effective reaction constants k'_i with i = 1, 2, … 6 is a product of the catalyst concentration C and the reaction constants k_i. The effect of temperature on the reaction constants is expressed by the Arrhenius equations for k_i [22].

$$k_i = A_i e^{-Ea_i/RT} \tag{2.6}$$

where A_i, E_{ai}, and R are the pre-exponential factor, the activation energy of the reaction and the gas constant, respectively. The values of A_i and E_{ai} are as shown in Table 2.1.

Table 2.1: Activation energies and pre-exponential factors of the NaOH-catalyzed transesterification of canola oil [22]

	TG → DG	DG → TG	DG → MG	MG → DG	MG → FAME	FAME → MG
(E_a) (J/mol)	65431.2	58403.2	105093.0	102958.6	92540.5	67587.6
A	2.0e + 10	0.9e + 10	5.0e + 17	1.7e + 17	2.2e + 15	3.4e + 9

The kinetic model of transesterification in terms of reaction rate for each component are presented in equations (2.7) – (2.12) [27].

$$r_{TG} = \frac{dC_{TG}}{dt} = -k_1 C_{TG} C_{MeOH} + k_2 C_{DG} C_{FAME} \tag{2.7}$$

$$r_{MeOH} = \frac{dC_{MeOH}}{dt} = -k_1 C_{TG} C_{MeOH} + k_2 C_{DG} C_{FAME} - k_3 C_{DG} C_{MeOH} + k_4 C_{MG} C_{FAME} \dots$$
$$\dots - k_5 C_{MG} C_{MeOH} + k_6 C_{GL} C_{FAME} \tag{2.8}$$

$$r_{FAME} = \frac{dC_{FAME}}{dt} = k_1 C_{TG} C_{MeOH} - k_2 C_{DG} C_{FAME} + k_3 C_{DG} C_{MeOH} - k_4 C_{MG} C_{FAME} \dots$$
$$\dots + k_5 C_{MG} C_{MeOH} - k_6 C_{GL} C_{FAME} \tag{2.9}$$

$$r_{DG} = \frac{dC_{DG}}{dt} = k_1 C_{TG} C_{MeOH} - k_2 C_{DG} C_{FAME} - k_3 C_{DG} C_{MeOH} + k_4 C_{MG} C_{FAME} \tag{2.10}$$

$$r_{MG} = \frac{dC_{MG}}{dt} = k_3 C_{DG} C_{MeOH} - k_4 C_{MG} C_{FAME} - k_5 C_{MG} C_{MeOH} + k_6 C_{GL} C_{FAME} \tag{2.11}$$

$$r_{GL} = \frac{dC_{GL}}{dt} = k_5 C_{MG} C_{MeOH} - k_6 C_{GL} C_{FAME} \tag{2.12}$$

where C_i is the concentration and r_i is the rate of reaction for component i (namely, TG, MeOH, FAME, DG, MG and GL).

2.2.2. Filtration model

The applications of membrane technology in biofuel production are either membrane reactors or membrane filtration units as final means of separation and purification. There are studies investigating the efficiency of production by membrane separation-reaction systems (Dubé et al. (2007) [20], Cheng et al. (2012) [27], and Hapońska et al. (2019) [25]) and the reduction of costs of refining and purifying the final product by using membrane separation systems (Gomes et al. (2010) [39], Alves et al. (2013) [40], and Noriega et al. (2018) [41]). In biodiesel production, the ceramic membrane is commonly applied due to its chemical and mechanical resistance to the components involved in the transesterification reaction [42]. Ultrafiltration and microfiltration are two most used methods in biodiesel separation [43]. Choi et al. (2005) [44] reported that membrane fouling occurs more often in microfiltration processes than ultrafiltration processes due to the effect of membrane pore size . If the particles have the same or smaller size comparing with the membrane pore size, those particles could easily reach and deposit on membrane surface and inside the pores. In contrast, the particles could roll off the membrane surface under the shearing force of cross-flow velocity rather than getting stuck in the pores if the pores are much smaller than the particles [44]. Therefore, development and application of membrane technology in biodiesel production focuses on ultrafiltration which is environmentally friendly and economically attractive [43].

The equation that describes the ultrafiltration flux is given by the Darcy equation [45]:

$$J = \frac{\Delta P}{\mu R_{total}} \tag{2.13}$$

where J is the filtration permeate flux, μ is the viscosity of the fluid and R_{total} is the total resistance of the membrane. Due to the complexity of the fouling phenomenon, the fouling resistance is often presented by an empirical or experimental parameter in membrane reactor modelling.

The goal of this chapter is to develop a dynamic model for the membrane reactor with fouling resistances that allow an accurate simulation and optimization of the separation-reaction process. Historically, membrane fouling has been divided into four different patterns usually known as blocking filtration laws: (1) pore blocking, (2) standard pore fouling, (3) intermediate blocking and (4) cake filtration [46]. Figure 2.1 shows the schematic view of four fouling mechanisms.

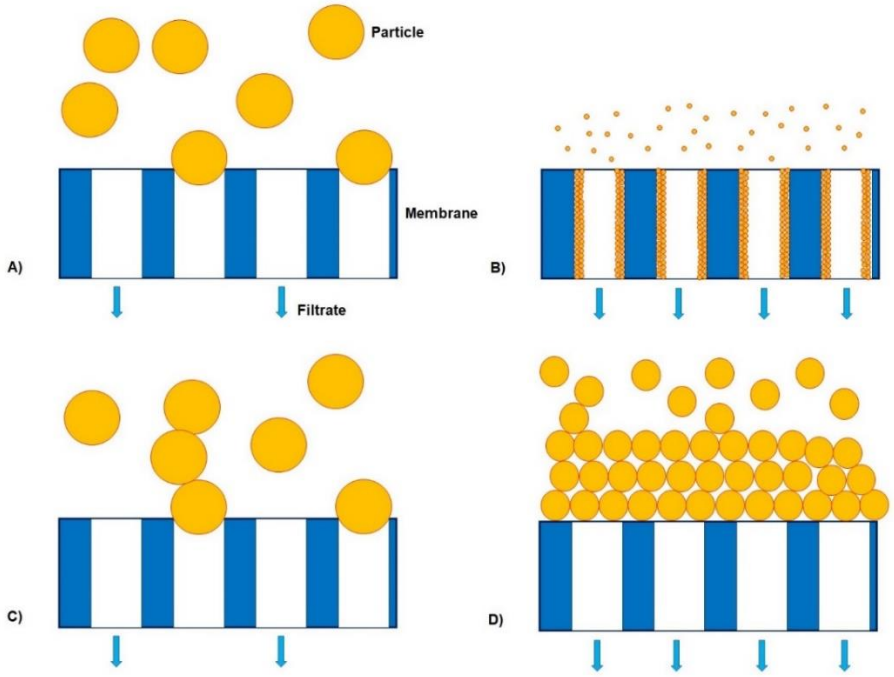

Figure 2.1: Four fouling patterns: (A) pore blocking, (B) standard pore fouling, (C) intermediate blocking, and (D) cake filtration [46]

There are a number of studies into the fouling mechanisms of membrane filtration of oil-water systems (Ghaffour (2004) [47], Das et al. (2017) [48], Salama (2019) [49]) and vegetable oil (Ariono et al. (2018) [50]). These studies indicate that most of the oil droplets accumulate on the membrane surface and contribute to membrane fouling. With the increase in the accumulation of droplets at the surface of the membrane, the fouling develops because: 1) the incoming flux of oil droplets combing with those already at the surface forms a larger oil layer, which contribute to the formation of cake layer, and 2) the pinning of droplets onto pore openings and the breaking up of droplets inside the pore contribute to pore blocking. Therefore, two dominant fouling mechanisms can be identified: 1) pore blocking and 2) cake formation which can be used to represent the total resistance. These two fouling phenomena occur simultaneously and reduce the area available for the filtration.

To simplify the model, the pore blocking fouling is considered irreversible fouling and cake filtration is reversible fouling. The total resistance, R_{total}, can be expressed as the sum of reversible and irreversible fouling.

$$R_{total} = R_m + R_c \qquad (2.14)$$

where R_m is the irreversible membrane resistance and considered the sum of intrinsic and pore blocking resistance. R_c is the reversible fouling and attributes solely to cake filtration.

To account for these kinds of fouling, Daniel et al. (2011) [51] developed cake and pore fouling models for cross-flow filtration from Hermia's common characteristic equation of flux decay. The assumption is that the irreversible fouling is leads to pore blocking and that reversible fouling is cake filtration effect in respect of back-pulsing. The following differential equation captures the flux decay for all four fouling mechanisms [51].

$$\frac{d^2t}{dV^2} = k\left(\frac{dt}{dV}\right)^n \; or \; \frac{dJ}{dt} = -kJ(A_FJ)^{2-n} \tag{2.15}$$

where V, t, A_F are the permeate volume, time and the filtration area, respectively. k is a constant and n is the blocking index, which takes the value of 0 for cake filtration, 1 for intermediate blocking, 1.5 for standard blocking and 2 for complete blocking [51].

For membrane filtration under pore blocking conditions (n = 2, as used by Daniel et al. (2011) [51]), equation (2.15) becomes

$$\frac{dJ}{dt} = -k_bJ \tag{2.16}$$

where kb is a pore blocking associated constant. Daniel et al. (2011) [51] assumed that pore blocking (R_m) is the sole fouling mechanism (i.e., R_c = 0) and combined equation (2.16) with equation (2.13) and (2.14) to yield

$$\frac{\Delta P}{\mu}\frac{d(1/R_m)}{dt} = -k_bJ \tag{2.17}$$

Equation (2.17) be further simplified to

$$-\frac{1}{R_m^2}\frac{dR_m}{dt} = -k_mJ \; or \; \frac{dR_m}{dt} = k_mJR_m^2 \tag{2.18}$$

where k_m is the effective capture-rate constant which incorporates permeate viscosity and transmembrane pressure. The rate of increase in pore blocking resistance is proportional to the filter flux term, J.

Daniel et al. (2011) [51] proposed that the membrane resistance of cake formation in cross-flow filtration was proportional to the flux ($k_{c1}J$) and the rate of material removal from the filter (k_{c2}) due to cross-flow shearing forces. This gives:

$$\frac{dR_c}{dt} = k_{c1}J - k_{c2} \tag{2.19}$$

Because two fouling mechanisms occur simultaneously in the membrane reactor, equation (2.18) and (2.19) need to be solved together to predict the permeate flux, J. To find

a solution, it is assumed that there is an initial flux, J_0 associated with initial membrane resistance $R_{m,0}$. With the assumption that cake fouling does not occur on the membrane surface at the start of filtration process, $R_c = 0$ at t = 0, $R_{m,0}$ can be presented as

$$R_{m,0} = \frac{\Delta P}{\mu J_0} \tag{2.20}$$

To be suitable for simulation and optimization of a separation-reaction process, a membrane reactor model should meet the following requirements: (a) capture the dynamics of both transesterification and filtration, (b) incorporate variables that can be used to control/optimize the process, for example, diameter and length of the reactor, in-feed flow rate, pressure, temperature, reaction time and permeate flux limit (c) have only few parameters that need to be estimated.

2.3. Modeling the membrane reactor for biodiesel production

The membrane reactor model is presented by a process model of a plug flow tubular reactor with additional terms of product removal by the effect of membrane filtration. The dynamic filtration model plays an important role in the calculation and evaluation of fouling effects on the biodiesel production.

2.3.1 Process model

Tubular membrane reactors as shown in Figure 2.2 often give a higher conversion than conventional batch reactors for the same reaction conditions because the products are continuously removed from the reaction. Therefore, they yield a high quantity and purity of biodiesel by shifting the reaction equilibrium.

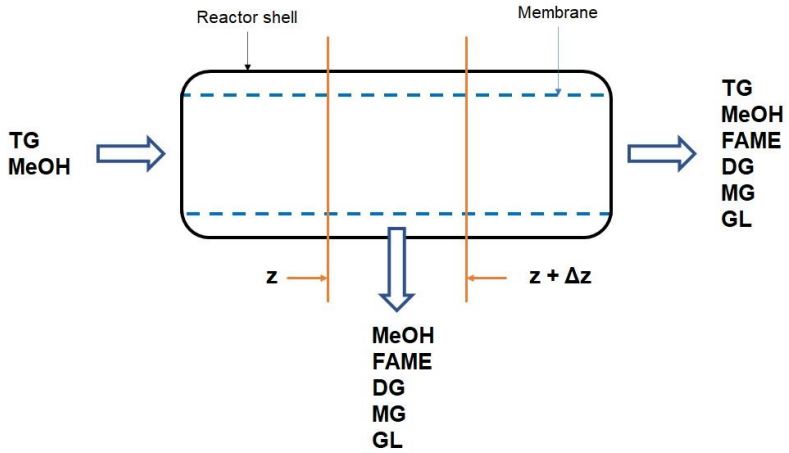

Figure 2.2: A sketch of a membrane reactor for biodiesel production by transesterification

The following assumptions are made to limit the complexity of the model.

a. From the researches of Cheng et al. (2010) [22], Portha et al. (2012) [52] and Chong et al. (2013) [23], the transesterification reactions are only slightly exothermic or almost athermic. Therefore, the separation-reaction process is assumed to be isothermal. No heat transfer in relation with time was calculated.
b. The transesterification is a pseudo-homogenous second ordered reversible reaction.
c. The diffusivity and viscosity do not depend on the concentration of the components in the fluids.
d. The fluid is incompressible in nature.
e. Pore fouling is completely irreversible and cake fouling is completely reversible.
f. The concentration of the gel layer represents the deposition of a solute which becomes both pore and cake fouling.
g. The fouling resistance and the permeate flux are evenly distributed throughout the length of the reactor.
h. Only the FAME-rich methanol phase can be permeated through the membrane. There is no oil in the permeate.

The model of the membrane reactor presented here is based on the component balance over the reaction period, Δt, for six components within the reactor. The general balance equation can be written as.

$$\begin{bmatrix} Accumulation\ of \\ component\ i \\ during\ \Delta t \end{bmatrix} = \begin{bmatrix} Component\ in \\ during\ \Delta t \end{bmatrix} - \begin{bmatrix} Component\ out \\ during\ \Delta t \end{bmatrix} \pm \begin{bmatrix} \frac{Generation}{consumption} \\ of\ component \\ during\ \Delta t \end{bmatrix} \quad (2.21)$$

The component balance for TG can be written in mathematical terms as

$$A_c \Delta z \left[C_{TG,(t+\Delta t)} - C_{TG,t}\right] = v_z A_c C_{TG,z} \Delta t - v_{z+\Delta z} A_c C_{TG,z+\Delta z} \Delta t + r_{TG} A_c \Delta z \Delta t \ldots$$
$$\ldots + D_{TG} \frac{\partial C_{TG}}{\partial z} A_c \Delta t - C_{TG,gel} J A_{membrane} \Delta t \quad (2.22)$$

where J is the permeate flux which can be determined by filtration model, C_{TG} is the concentration of TG in the reactor, v is the axial velocity of the medium, A_c is the cross sectional area of the membrane, D_{TG} is the axial diffusion coefficient of TG in MeOH and $C_{TG,gel}$ is concentration of TG in the gel layer.

The gel layer concentration can be calculated by using the film theory, which is a simple and commonly used theory for modeling flux in pressure independent, mass transfer-controlled systems. The relation between the concentration of TG in the bulk media and gel layer is presented by equation (2.23) [45].

$$C_{TG,gel} = C_{TG}\, exp\left(\frac{J}{K}\right) \tag{2.23}$$

where K is the mass transfer coefficient which is determined by the flow regime of the media in the reactor. For turbulent flow, when Re > 4000, K can be calculated by equation (2.24) and for laminar flow by equation (2.25) [45].

$$K = 0.023\left(\frac{D^{0.67}v^{0.8}\rho^{0.47}}{d_h^{0.2}\mu^{0.47}}\right) \tag{2.24}$$

$$K = 1.86\left(\frac{D^{0.67}v^{0.33}}{d_h^{0.33}L^{0.33}}\right) \tag{2.25}$$

where D is the diffusion coefficient, v is cross flow velocity, ρ is the density, d_h is the hydraulic diameter (membrane internal diameter in this case) and L is the length of the reactor. It is the basic assumption in the film theory that the mass transfer coefficient is constant as the bulk concentration increases [45].

The balance equation of component i (i = MeOH, FAME, DG, MG, GL) which permeates through the membrane can be described by the expression

$$A_c\Delta z\left[C_{i,(t+\Delta t)} - C_{i,t}\right] = v_z A_c C_{i,z}\Delta t - v_{z+\Delta z}A_c C_{i,z+\Delta z}\Delta t + r_i A_c \Delta z \Delta t \ldots$$
$$\ldots + D_i\frac{\partial C_i}{\partial z}A_c\Delta t - C_{i,permeate}A_{membrane}\,J\Delta t \tag{2.26}$$

where $C_{i,permeate}$ is the concentration of component i in the permeate stream.

Using the boundary layer film model by assuming that a thin layer of unmixed fluid with thickness δ separates the region of higher concentration near the membrane surface and the uniform concentration bulk solution, the mass balance equation between solutions in the bulk and the permeate can be written as [53]

$$\frac{C_{i,o}-C_{i,permeate}}{C_{i,bulk}-C_{i,permeate}} = exp\left(\frac{J\delta}{D_i}\right) \tag{2.27}$$

where $C_{i,bulk}$ and $C_{i,o}$ are the concentrations of solute in the bulk solution and at the membrane surface, respectively.

The enrichment factor, E, and the intrinsic enrichment of the membrane without the boundary layer, E_o, can be defined as following

$$E = \frac{C_{i,permeate}}{C_{i,bulk}} \tag{2.28}$$

$$E_o = \frac{C_{i,permeate}}{C_{io}} \tag{2.29}$$

And Equation (2.27) can be written as

$$\frac{C_{i,permeate}}{C_{i,bulk}} = \frac{E_o exp\left(\frac{J\delta}{D_i}\right)}{1+\left(exp\left(\frac{J\delta}{D_i}\right)-1\right)E_o} \tag{2.30}$$

In the equation (2.30), the diffusion coefficient of a component i in a solvent, D_i, is calculated in the Appendix A-2.1

The flow rate balance of membrane reactor's section is presented as

$$F_z = F_{z+\Delta z} + F_{permeate} \tag{2.31}$$

where F_z and $F_{z+\Delta z}$ are the flow rate of medium at the input and output of the section. $F_{permeate}$ is the flow rate of the permeate stream through membrane section with length Δz.

Equation (2.31) can be written is term of fluid velocity as

$$v_z A_c = v_{z+\Delta z} A_c + J A_{membrane} \tag{2.32}$$

Or

$$v_{z+\Delta z} = v_z - \frac{2}{R} \cdot J \cdot \Delta z \tag{2.33}$$

where R is the membrane internal radius and $A_{membrane}$ is the area of membrane and defined by equation (2.34)

$$A_{membrane} = 2\pi R \Delta z \tag{2.34}$$

2.3.2. Solution method

The MATLAB® Genetic Algorithm (GA) is a solver for smooth or non-smooth optimization problems with any types of constraints, including integer constraints [54]. This algorithm inspired by Charles Darwin's theory of natural evolution which includes the principles of survival of fittest. GA simulates the natural evolutionary process by modifying a population of individual solutions. Over successive generations, the population evolves toward an optimal solution. Therefore, GA represents an intelligent exploitation of a random search within a defined search space to solve a problem [55].

The filtration model (equations 2.13, 2.14, 2.18, 2.19 and 2.20) contains three unknown rate constants k_m, which represents the rate of pore blockage or irreversible fouling, k_{c1}, and k_{c2}, that represent the rate of formation and removal of cake layer or reversible fouling. Estimation of these constants from experimental data is conducted with the use of Matlab® genetic algorithm function (`ga`). In this case, the Matlab® GA solver determines the values of k_m, k_{c1}, and k_{c2} that minimize the fitness function, which is the sum of squared errors (SSE) defined by equation 2.35 [56].

$$\sum_i (d_i)^2 = \sum_i \left(J_i - J_{experiment,i}\right)^2 \qquad (2.35)$$

where d_i is the absolute error, sometimes called the residual, J_i is the measured data of permeate flux and $J_{experiment,i}$ is the predicted result of the model.

The values of R_m and R_c are numerically calculated by using Matlab® tool `ode45`. The permeate flux, J, is then predicted as a function of time by the Matlab® curve fitting toolbox. At the end of a production cycle which is evaluated in this study, the backwashing process is performed and the value of R_c is reset to zero. The value of R_m at the end of current cycle becomes the new $R_{m,0}$ of the next cycle.

The production process of the membrane reactor includes many production cycles. When the value of J reaches a pre-determined flux limit which marks the end of a production process, the reactor needs to be stopped for chemical cleaning to restore its productivity.

By rearrangement and combination with equations (2.22), (2.29) and (2.33), the component balance equations (2.21) and (2.25) of TG and five other components (MeOH, FAME, DG, MG and GL) can be written in terms of a system of partial differential equations (PDEs).

$$\frac{\partial C_{TG}}{\partial t} = -v_{z+\Delta z}\frac{\partial C_{TG}}{\partial z} + D_{TG}\frac{\partial^2 C_{TG}}{\partial z^2} + r_{TG} - \frac{2}{R}J\left(exp\left(\frac{J}{K}\right)C_{TG} - C_{TG,z}\right) \qquad (2.36)$$

$$\frac{\partial C_i}{\partial t} = -v_{z+\Delta z}\frac{\partial C_i}{\partial z} + D_i\frac{\partial^2 C_i}{\partial z^2} + r_i - \frac{2}{R}J\left(\frac{E_o exp\left(\frac{J\delta}{D_i}\right)}{1+E_o\left[exp\left(\frac{J\delta}{D_i}\right)-1\right]}C_i - C_{i,z}\right) \qquad (2.37)$$

The intrinsic enrichment factor, E_o, is estimated by using Matlab® GA solver with the fitness function being SSE of the calculated and experimental total permeate productivity. The membrane reactor PDEs can be solved with Matlab® PDE solver, which is called `pdepe`, with the Danckwerts boundary conditions at the reactor inlet and outlet [57]. The total permeate productivity, $m_{permeate}$, of the membrane reactor can be calculated according to

$$m_{permeate} = \sum_i C_{i,permeate} M_i F_{permeate} \qquad (2.38)$$

where $C_{i,permeate}$ is the concentration of component i (i = MeOH, FAME, DG, MG, GL) in the permeate stream which are from the results of equations 2.29, 2.36 and 2.37; M_i is the

molecular weight of component *i* and $F_{permeate}$ is the flow rate of the permeate stream through the total membrane area.

2.4. Membrane cleaning model

The membrane cleaning model can predict the state of cleaning chemical, reversible and irreversible fouling as functions of time, washing flow and chemical inlet concentration. The cleaning model is capable of characterizing the effects of backwashing and chemical cleaning by combining with a membrane reactor model.

2.4.1. Model development

The membrane cleaning model is developed basing on the relationship of the fouling resistances, the cleaning flow and the reaction between a cleaning chemical and the irreversible fouling material [33]. The fouling state of the membrane $x_f(t)$ is related to the fouling resistance according to:

$$x_f(t) = \frac{R_f(t)}{R'_f} \tag{2.39}$$

where $R_f(t)$ is the fouling resistance during cleaning at a specified pressure and R'_f is the fouling resistance at the beginning of the cleaning.

Backwashing is commonly used to enhance the permeate flux by periodically removing the reversible fouling. The outlet of the permeate channel is closed, and the permeate is pumped back to the feed channel of the membrane module, thus, lifting the fouling off the membrane surface [29]. The decay of the reversible fouling state, $x_{f,r}$, is described by:

$$\frac{dx_{f,r}}{dt} = -k_r \cdot F_r \cdot x_{f,r} \tag{2.40}$$

where k_r is the correlation constant between the removal of fouling layer and fouling resistance and F_r is the dimensionless reversal permeate flow:

$$F_r = \frac{F_{r,in}}{F_{r,ref}} \tag{2.41}$$

where $F_{r,in}$ and $F_{r,ref}$ are the pumped flow at the inlet of the permeate channel and the reference flow based on the pump capacity.

Chemical cleaning is applied when the irreversible fouling that the backwashing cannot remove reaches a critical level. A typical chemical cleaning process includes physical washing with high-temperature solvent or water and dissolving the foulant with a chemical

reaction. The change of irreversible fouling state, $x_{f,ir}$, during the chemical cleaning is represented as [33]:

$$\frac{dx_{f,ir}}{dt} = -k_{ir} \cdot F_{ir} \cdot \left(x_{f,ir} - x_{f,\infty}\right) - r_c \quad (2.42)$$

Where $x_{f,\infty}$ is the fouling state of the membrane at infinite cleaning time, k_{ir} is the physical washing constant and F_{ir} is the dimensionless washing flow calculated from the inlet flow of the chemical cleaning stream Fir,in and the reference flow $F_{ir,ref}$:

$$F_{ir} = \frac{F_{ir,in}}{F_{ir,ref}} \quad (2.43)$$

The reaction between the irreversible fouling and cleaning chemical is assumed to be first order. The reaction rate, r_c, is calculated by:

$$r_c = k'_1 \cdot x_c \cdot \left(x_{f,ir} - x_{f,\infty}\right) \quad (2.44)$$

where k'_1 is the reaction rate constant and x_c is the state of the cleaning chemical which is dimensionless and defined by the concentration of cleaning chemical at the start, $C_{chemical,0}$ and during the cleaning, $C_{chemical}(t)$.

$$x_c(t) = \frac{C_{chemical}(t)}{C_{chemical,0}} \quad (2.45)$$

The state of the chemical agent during the cleaning process is defined as [33]:

$$\frac{dx_c}{dt} = k_{ir} \cdot F_{ir} \cdot \left(x_{c,in} - x_c\right) - n_c \cdot r_c \quad (2.46)$$

where $x_{c,in}$ is the state of chemical cleaning at the inlet of membrane module and n_c is a pseudo-stoichiometric constant for the fouling decomposition.

2.4.2. The cleaning cost

The cost of cleaning can be determined from production loss, energy and chemicals consumption. The cost relating to biodiesel loss during the cleaning time, $Cost_{BD}$, is calculated as:

$$Cost_{BD} = m_{f,av} \cdot t_c \cdot W_{BD} \quad (2.47)$$

where $m_{f,av}$ is the average mass flow of biodiesel produced from the membrane reactor, t_c is the cleaning duration, and W_{BD} is the price of biodiesel. The energy consumption includes the pumping and heating of cleaning fluid. The cost of energy, C_E, is a function of the washing stream, $F_{ir,in}$, specific pumping energy consumption, E_P, and specific heating energy consumption, E_H. The energy cost is presented as:

$$Cost_E = F_{ir,in} \cdot t_c \cdot W_E \cdot (E_P + E_H) \quad (2.48)$$

where W_E is the price of energy. The cost of cleaning chemicals, $Cost_C$, is defined as:

$$Cost_C = F_{ir,in} \cdot t_c \cdot W_C \cdot C_{chemical,in} \quad (2.49)$$

where W_C is the price of chemical and $C_{chemical,in}$ is the concentration of cleaning chemical at the inlet.

2.4.3. Model solution

The filtration model above can be used to predict the value of reversible and irreversible fouling resistances over time and at the end of a filtration cycle, that will be the initial values of the cleaning model. The cleaning model parameters k_r, k_{ir}, k'_1 and n_c can be estimated from experiments and simulation data.

The model is solved with the `ODE45` solver of Matlab®. The results of the cleaning model are used to estimate the cleaning time and chemical consumption that contribute to the cleaning cost. The states of fouling after cleaning are the initial condition for a new operation cycle of the membrane reactor. This data can be used to calculate the biodiesel production per cycle by using the membrane reactor model as proposed in section 2.3. The results are useful to evaluate long term effects of backwashing and the operating cycle on the membrane reactor's productivity and irreversible fouling accumulation.

2.5. Case study

2.5.1. System definition

First, the membrane reactor model is fitted by adjusting the values of the parameters to the experimental data. Subsequently, to test the predictive capabilities of the model, simulations are carried out to check the membrane reactor performance in terms of the permeated biodiesel flux at experimental conditions.

The developed model is applied to simulate an experimental membrane reactor in biodiesel production from the work of Cheng et al. (2012) [27]. The transesterification experiment was conducted in a system of a membrane reactor integrated with a pre-reactor. The experimental feedstocks including canola oil and its biodiesel come from Taiwan NJC Corporation. The operating conditions of the membrane reactor were controlled at methanol to oil molar ratio in the feed of 24:1, the catalyst (NaOH) concentration to the oil of 0.05wt% at 65 ^oC. The data of the tube ceramic membrane reactor are as shown in Table 2.2 [27].

Table 2.2: The parameters of the tubular membrane reactor [27].

The membrane reactor	Range
Feed flow rate (F_{feed}, L/min)	0.2
Number of tubes (N)	1
Inner radius of the membrane tube (R, mm)	4.2
Length of membrane tube (L, m)	0.6
Transmembrane pressure (ΔP, kPa)	12.67

The results of the experiment carried out by Cheng et al. (2012) are shown in Figures 2.3 and 2.4 [27]. The experimental data shows that the permeate is free of TG and the FAME concentration increases while the MeOH concentration decreases with the increase of the operating time [27]. The permeate compositions and total productivity of the membrane tube length 0.6 m are used to estimate the parameters of the membrane reactor in this work.

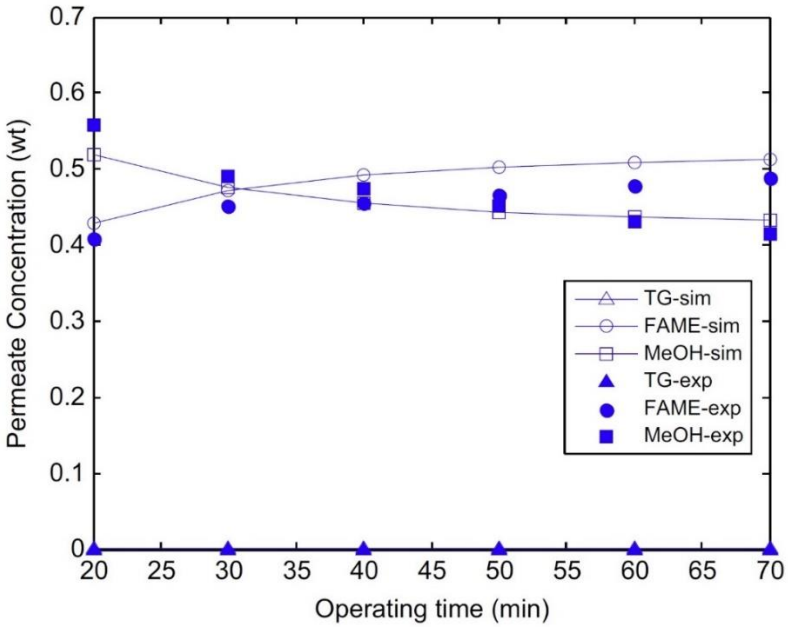

Figure 2.3: The permeate composition of TG, FAME and MeOH over the operating time of the membrane reactor with the tube length 0.6 m [27]

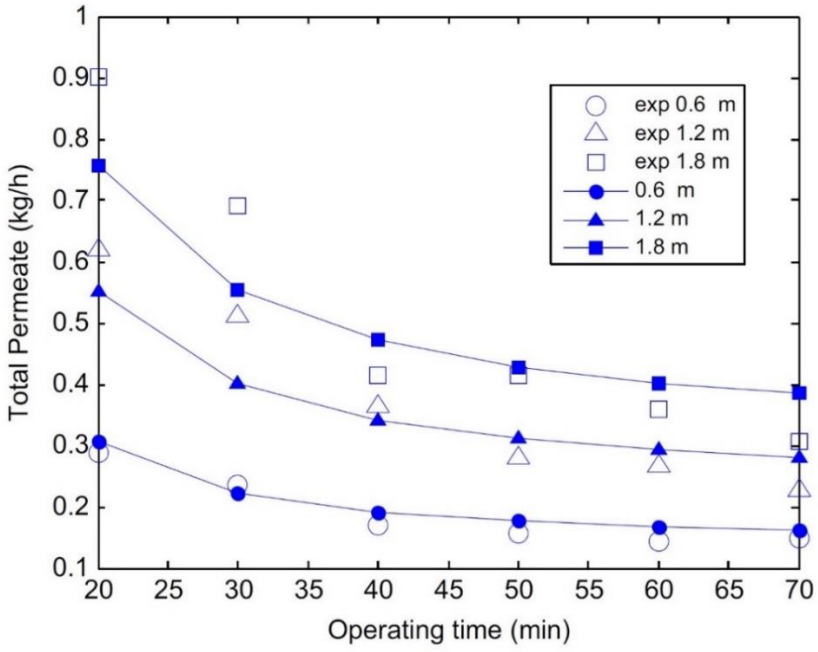

Figure 2.4: The total permeate productivity over the operating time of the membrane reactor with different tube lengths [27]

2.5.2. Results

To determine three adjustable parameters: k_m, k_{c1}, and k_{c2}, the combined-fouling flux model was fitted against the actual measured flux data by using genetic algorithm function of Matlab® as shown in Figure 2.5. The values of these parameters are 1.48×10^{-12}, 4.5×10^{14} (m^{-2}) and 1.03×10^{7} ($m^{-1}\ s^{-1}$) for k_m, k_{c1}, and k_{c2}, respectively.

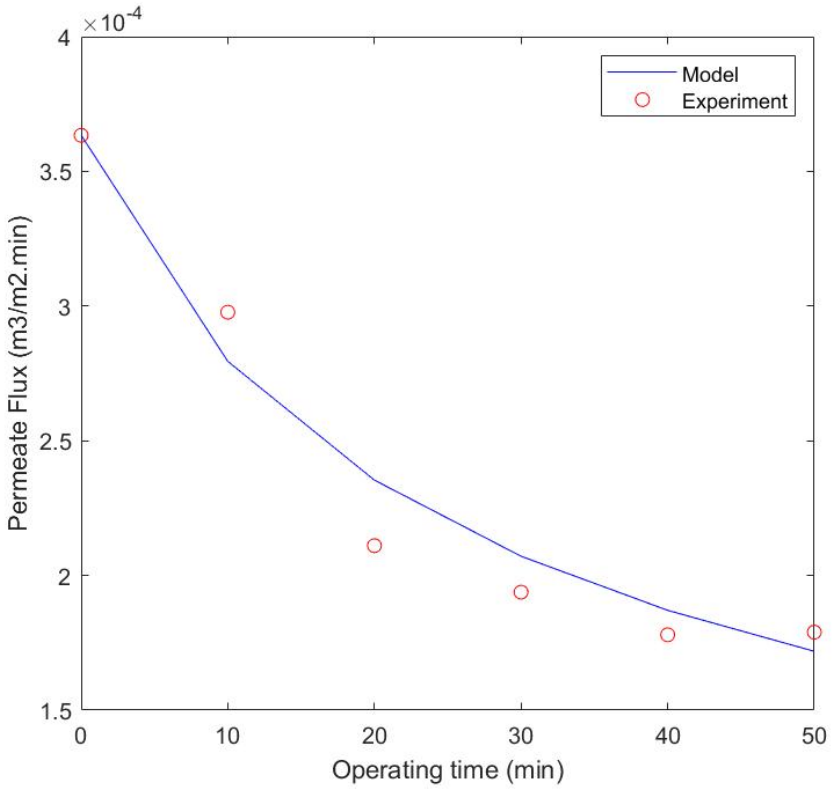

Figure 2.5: Comparison between the experimental data and calculated results by using the filtration model

The ANOVA table for the residual analysis is provided in Table 2.4 [56]. The R-squared (R^2) value between the calculated values and experimental data in Table 2.3 indicates that there is a good agreement between data and model.

Table 2.3: ANOVA table for the filtration model

Source	Degrees of freedom	Sum of squares	F-value	R^2
Regression	3	SSR = 1.34×10^{-12}	15.7	0.9575
Residual	2	SSE = 5.71×10^{-14}		
Total	5	SST = 1.17×10^{-12}		

From the experimental data of membrane reactor productivity, the membrane intrinsic enrichment constant, E_o, is estimated a value of 1.09. Figure 2.6 shows the comparison between the model prediction generated by using E_o to the experimental values of reactor

productivity. The statistical analysis data reported in Table 2.5 shows that the proposed model was capable to model the experimental data over the entire process of separation-reaction.

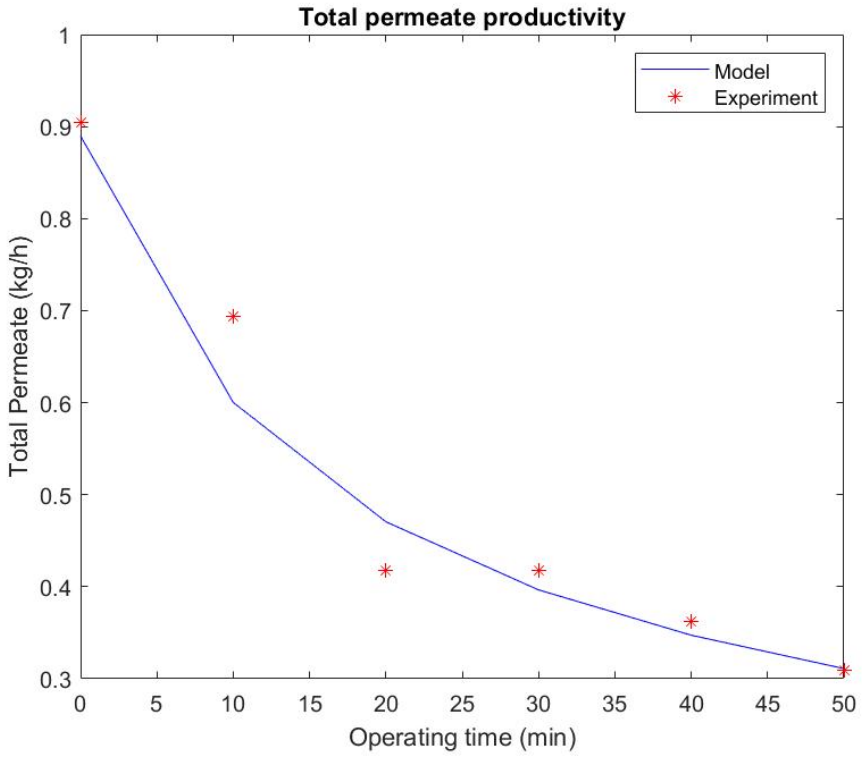

Figure 2.6: Comparison of experimental data of the total permeate productivity of the membrane reactor to the results of the model using estimated E_o

Table 2.4: ANOVA table for the membrane reactor model

Source	Degrees of freedom	Sum of squares	F-value	R^2
Regression	1	SSR = 0.04469	86.12	0.9535
Residual	4	SSE = 0.002		
Total	5	SST = 0.0387		

Figures 2.5 and 2.6 show the serious effect of membrane fouling on the reactor's performance. The permeate flux and productivity reduce by a factor 2, during the 50 minutes of operation. To restore the original flux, the membrane reactor needs to be cleaned by backwashing and chemical cleaning i.e., to remove reversible fouling and irreversible fouling. The results of the reversible fouling resistance, R_c, and the irreversible fouling resistance, R_m, are calculated from the model and allow to simulate the cleaning effects on

the membrane reactor operation. The backwashing process is simulated by assuming that R_c = 0 after backwashing and that $R_m = R_{m,0}$ for the next production cycle. The final value of the irreversible fouling resistance can be used in a follow-up study to simulate and evaluate the chemical cleaning process.

One of the intended uses of the model developed in this chapter is to assess optimal backwashing conditions. To achieve this, the effect of reaction time was evaluated. A permeate flux limit of the membrane reactor of 2.39 x 10^{-6} m^3/m^2s and a back washing duration of 1 minute are assumed [58]. The relationship between membrane fouling, permeate flux and FAME yield from membrane reactor for experimental conditions is shown in the Figure 2.7. It is found that the FAME production decreases with an increase of the membrane fouling. The simulated results show the effect of backwashing on the restoration of the flux. However, the FAME yield of each production cycle is less than the previous one because of increasing of irreversible membrane fouling.

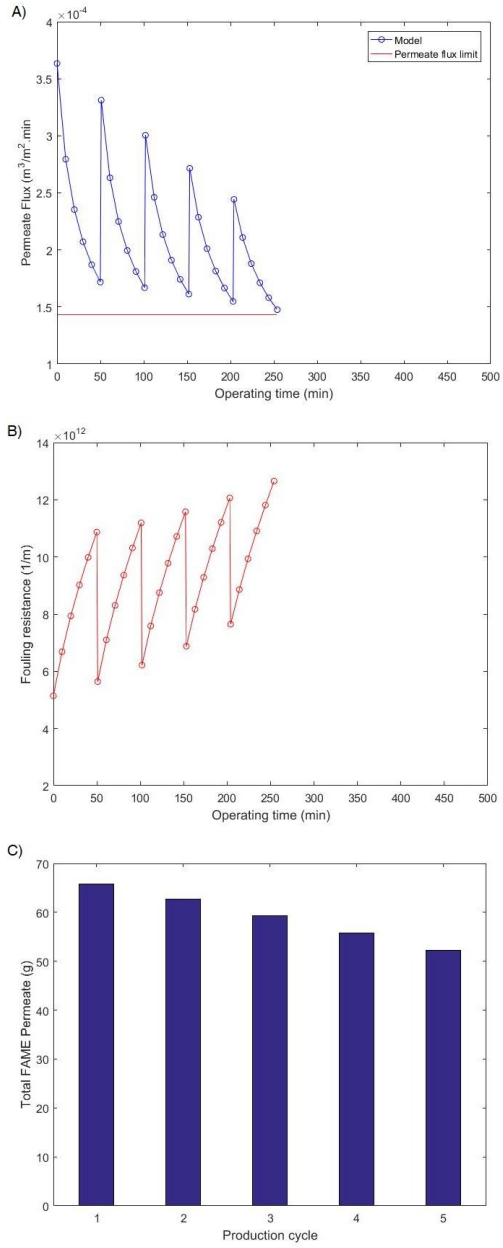

Figure 2.7: Simulation of biodiesel production process with a production cycle of 50 minutes: A) The permeate flux, B) the fouling resistance and C) the FAME yield of each cycle

Table 2.5 shows the effect of changing the duration of an operating cycle where the FAME productivity and the irreversible fouling for each test case from 15 to 70 minutes per cycle with a step of 5 minutes is shown. As can be seen, the FAME productivity increases when the duration of operating cycle is reduced or the backwashing frequency is increased. The total FAME production from the reactor increases from 164.05 g at low frequency (< 0.5 backwashing per hour) to 415.74 g at high frequency (> 3.5 per hour). However, the operating time is longer with a higher backwashing frequency leading to a higher irreversible fouling resistance at the end of the membrane operation.

Table 2.5: Simulation results for the membrane reactor model

Operating cycle (min)	Operating time (min)	Total FAME production (g)	Number of backwashing	FAME production rate (g/min)	Irreversible fouling resistance (1/m)
70	141	164.05	1	1.172	6.59×10^{12}
65	197	226.42	2	1.161	7.38×10^{12}
60	182	214.04	2	1.189	7.21×10^{12}
55	223	260.53	3	1.184	7.91×10^{12}
50	254	295.88	4	1.183	8.53×10^{12}
45	275	320.88	5	1.188	9.04×10^{12}
40	286	336.16	6	1.200	9.39×10^{12}
35	323	375	8	1.190	10.38×10^{12}
30	309	367.42	9	1.225	10.19×10^{12}
25	337	396.91	12	1.221	11.06×10^{12}
20	335	399.48	15	1.248	11.16×10^{12}
15	351	415.74	21	1.260	11.73×10^{12}

The correlation between the FAME production rate, irreversible fouling resistance and the operating cycle is shown in Figure 2.8. The results proof that the production rate decreases with the irreversible fouling resistance. This irreversible fouling is only recovered by cleaning the membrane reactor with a suitable chemical agent. To identify the optimized operating conditions for the reactor, the productivity needs to be considered together with maintenance costs such as power and lost production during backwashing and chemical cleaning. The simulation and analysis were performed with the data from the bench-scale system. However, the system parameters for the full-scale system may be measurably different.

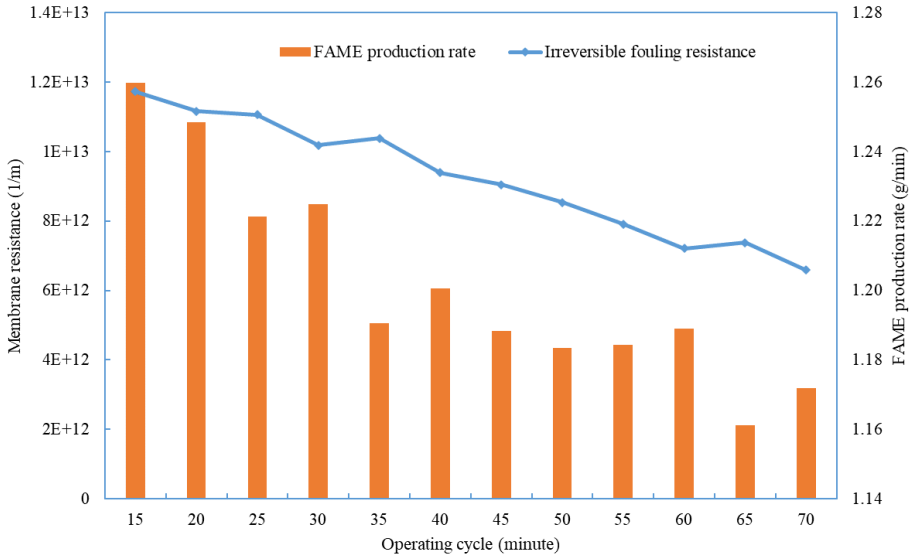

Figure 2.8: Effect of the backwashing frequency on the FAME productivity and membrane irreversible fouling resistance

The filtration model was validated with the experimental data of biodiesel production in a membrane reactor from [27]. The constants of the chemical cleaning model were estimated from a cleaning simulation based on an experimental cleaning curve of an ultrafiltration membrane [33]. The cleaning model parameters are shown in Table 2.6.

Table 2.6: Parameters of the cleaning model

Parameter	k_r	k_{ir}	k'_1	n_c
Cleaning model	0.0055 (s^{-1})	1.026 x 10^{-4} (s^{-1})	0.1415 (s^{-1})	0.4566 (s^{-1})

To determine the chemical cleaning duration, it is assumed that the chemical cleaning will reduce 100 % of irreversible fouling resistance. The inlet flowrate of cleaning fluid is 2 times the normal flowrate of filtration to ensure the removal of foulant, $F_{ir,in}$ = 0.4 L/min. The cleaning chemical is sodium hydroxide 1 % Wt. and the cleaning temperature is 70 ºC.

The relationship between the number of backwashes per hour with the irreversible fouling and chemical cleaning duration is shown in the Figure 2.9(a). The graphs show that more irreversible fouling accumulates with shorter operating cycle or higher number of backwashes per hour, demanding longer chemical cleaning times. However, Figure 2.9(b) shows that the estimated cleaning cost per tonne of biodiesel is increasing with the increase of operating cycle. The reason is that the biodiesel production rate and the total production time rise with more backwashing occurred during the operation.

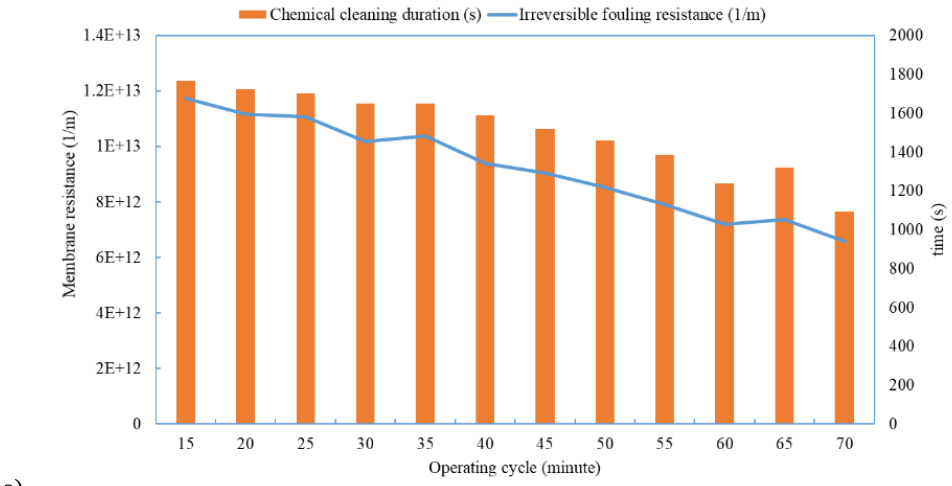

a)

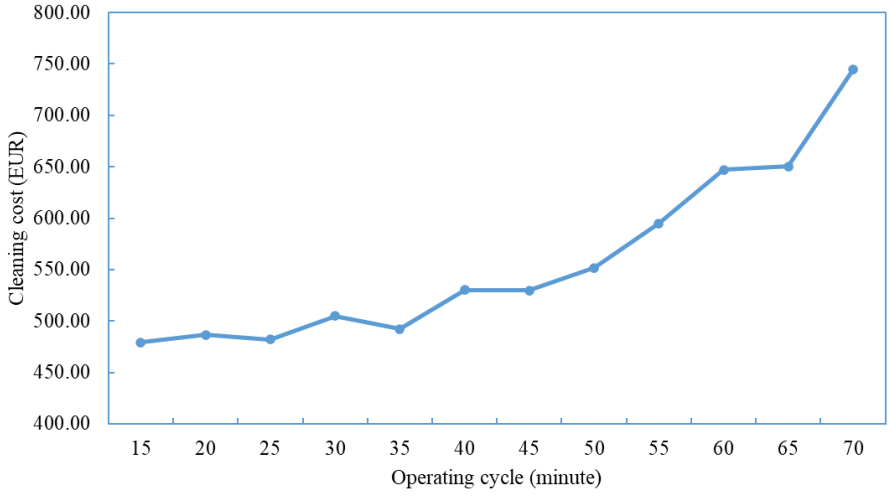

b)

Figure 2.9: The relation between the backwashing frequency and (a) the irreversible fouling and the chemical cleaning time; (b) the cleaning cost per ton of FAME produced

The results show that the cleaning cost per t of biodiesel is reduced from 745 to 482 EUR/t by reducing the operating cycle from 70 min to 25 min. However, the cleaning cost of the membrane reactor cannot be reduced further when the operating cycle reduces from 25 min to 15 min or the number of backwashes increases from 2 to 4h. The biodiesel production rate only slightly increases as compared to the accumulation rate of fouling. This can be explained by the fact that the membrane reactor nearly reaches its capacity limit, which can

be risen by increasing the filtration area or using different membrane materials. The prolonged chemical cleaning time will reduce the membrane lifetime.

2.6. Conclusions

A novel model of the membrane reactor with dynamic membrane fouling and a dynamic cleaning model which defines the cleaning and fouling states as functions of time, cleaning flow, reversible and irreversible fouling resistances is developed for transesterification in biodiesel production. Experimental data from literature shows good agreement with the model outcomes. The cleaning model is proven that it is an important tool in combination with the membrane reactor model to improve the potential of membrane reactor in biodiesel production by reducing operating cost.

The models provide insights in the effects of membrane fouling and cleaning on the membrane reactor, which can be used to improve the productivity of biodiesel. Based on the results of different operating cycles, several conclusions can be drawn from this work:

The model of reversible and irreversible fouling can be effectively applied to evaluate the productivity of the membrane reactor in the short term (reversible fouling) and long term (irreversible fouling). The reactor productivity and operating time increase with decreasing operating cycle duration, from 1.17 g per minute and 141 minutes at a 70-minute operating cycle (or 1 backwashing per 2 hours) to 1.26 g per minute and 351 minutes at a 15-minute operating cycle (or 3 backwashing per hour).

The membrane fouling has a profound effect on the reactor productivity as irreversible fouling accumulates during operating time even with backwashing and forces the production to stop for chemical cleaning. An operating cycle which balances between cleaning cost and time, and productivity can be determined as 25 min. The cleaning cost per weight of biodiesel produced was reduced 35 % when the operating cycle decreased from 70 min to 25 min.

At the level of a single equipment, the membrane reactor has several advantages over traditional reactors. However, the reactors need to be place in the context of an entire production process or process level to evaluate precisely their technical and economic effects. The next chapter presents the membrane reactor and other reactors in a biodiesel production superstructure which is a process systems engineering tool for optimization at process level.

2.7. Nomenclature

A	pre-exponential factor
A_c	membrane cross sectional area (m^2)
A_F	membrane filtration area (m^2)

$A_{membrane}$	membrane surface area (m^2)
C	concentration (mol m^{-3})
$C_{chemical,in}$	chemical inlet concentration (mol m^{-3})
$Cost_{BD/E/C}$	cost of biodiesel loss/energy/chemical (EUR)
D	diffusion coefficient (m^2 s^{-1})
d_h	hydraulic diameter (m)
E	enrichment factor
E_a	reaction activation energy (J)
E_H	specific heating energy (kW m^{-3})
E_o	membrane intrinsic enrichment constant
E_P	specific pumping energy (kW m^{-3})
F	flow rate of medium (m^3 s^{-1})
F_{ir}	chemical cleaning flow (m^3 s^{-1})
F_r	backwashing inlet flow (m^3 s^{-1})
J	permeate flux (m s^{-1})
J_0	initial flux (m s^{-1})
K	mass transfer coefficient (m s^{-1})
k	reaction rate constant (m^3 mol^{-1} s^{-1})
k_{c1}	effective cake-deposition constant for fouling model (m^{-2})
k_{c2}	effective cake-erosion constant for fouling model (m^{-1} s^{-1})
k_m	effective pore-blocking constant for fouling model
L	length of membrane (m)
M	molecular weight (g mol^{-1})
$m_{f,av}$	biodiesel average mass flow (kg s^{-1})
$m_{permeate}$	total permeate productivity (kg h^{-1})

ΔP	transmembrane pressure (kPa)
r	reaction rate (mol s^{-1})
R	universal gas constant (= 8.314, J K^{-1} mol^{-1})
R_c	reversible fouling resistance (m^{-1})
R_m	irreversible fouling resistance (m^{-1})
$R_{m,0}$	initial membrane resistance (m^{-1})
R_{total}	total membrane resistance (m^{-1})
t	time (s)
t_c	cleaning duration (s)
T	temperature (K)
v	fluid velocity (m s^{-1})
V	solute molar volume at normal boiling point (m^3 $kmol^{-1}$)
$W_{BD/C}$	price of biodiesel/chemical (EUR kg^{-1})
W_E	price of energy (EUR kg^{-1})
x_c	cleaning chemical state, -
x_f	membrane fouling state, -
δ	concentration polarization layer thickness (m)
η	kinematic viscosity (m^2 s^{-1})
μ	dynamic viscosity (Pa.s)
ρ	fluid density (kg/m^3)
ϕ	association constant for solvent
Φ	volume fraction

3. Promising future for biodiesel: Superstructure optimization from feed to fuel

“If you can't explain it simply, you don't understand it well enough.” - Albert Einstein

This chapter was published in:

Thien An Huynh, Vincent Reurslag, Maryam Raeisi, Meik B. Franke and Edwin Zondervan, 2022, "*Superstructure Optimization of Biodiesel Production from Continuous Stirred Tank and Membrane Reactors*", Proceedings of the 14th International Symposium on Process Systems Engineering – PSE 2021+ June 19-23, 2022, Kyoto, Japan, page 109-114, doi: http://dx.doi.org/10.1016/B978-0-323-85159-6.50018-X.

Thien An Huynh, Mattia Rossi, Maryam Raeisi, Meik B. Franke, Flavio Manenti, Edwin Zondervan, 2022, “*Promising future for biodiesel: Superstructure optimization from feed to fuel*”, Proceedings of the 32nd European Symposium on Computer Aided Process Engineering (ESCAPE32), June 12-15, 2022, Toulouse, France, page 595-600, doi: http://dx.doi.org/10.1016/B978-0-323-95879-0.50100-4

Thien An Huynh, Meik B. Franke, Edwin Zondervan, 2022, “*Steps towards the winning formula for biodiesel: Superstructure, process intensification and heat integration*” – Is going to submit to the journal Computers & Chemical Engineering

Abstract

A superstructure is a collection of numerous alternative feedstock and equipment options that combine to form various possible process flowsheets. The superstructure can be formulated as a mathematical model by using variables, equations and constraints to describe its options and flowsheets. The best flowsheet for predefined criteria and constraints can be identified by solving the model with optimization software tools [59].

This chapter presents a superstructure model which encompasses a wide range of feedstock (e.g., waste cooking oil, tallow, rapeseed oil and algae), conventional reaction and separation equipment (e.g., continuous stirred tank reactor, decanter and vacuum distillation) and intensified operation units such as membrane reactor and reactive distillation column. The superstructure model is used for the optimization of the biodiesel production in terms of total profit, production cost, energy requirement and value of by-product glycerol. The heat integration of the superstructure model is a novel feature which allows further reduction of utility costs and energy requirement of the biodiesel production.

The superstructure model is implemented in Advanced Interactive Multidimensional Modeling (AIMMS) as Mixed-Integer Nonlinear Programming (MINLP). Three case studies are tested to verify the superstructure model, identify the optimal production route from feedstock to biodiesel and test the economic feasibility of the membrane reactor.

The results present an optimal design of a biodiesel production process from waste cooking oil and tallow with a heterogeneous acid catalyst, a reactive distillation column and additional purification steps for producing pure glycerol which is 40% higher in price than technical glycerol. The total annual profit of the biodiesel production from waste cooking oil is 2,619,038 USD and from tallow is 3,539,025 USD. The membrane reactor is a potential technology. However, it has negative annual profit, -2,007,646.1 USD, thus requiring more improvement in term of biodiesel yield.

From the results, the combination of feedstock selection and implementation of advanced processing technologies to improve biodiesel production can be achieved with the superstructure optimization method.

3.1. Introduction

The feedstocks are critical to the economic feasibility of biodiesel production because approximately 80% of biodiesel production cost comes from raw material costs [9]. The first generation feedstocks such as vegetable oils are generally expensive and lead to food concern [8]. Thus, the research of economic feedstocks for second- and third-generation biodiesel has become more important.

Besides the feedstocks, taking advantages of process intensification technologies in production can reduce the biodiesel cost. For instance, intensified reactor designs which combine reaction and separation into one operation unit have been developed to improve biodiesel conversion and purity. Catalytic reactive distillation process has many benefits for biodiesel production such as lower equipment and operating cost, high productivity and reduced waste [60]. Membrane reactor is a process intensification option which integrates a membrane separation into a cross-flow reactor to produce higher quality biodiesel than conventional reactors [26]. Supercritical methods present alternative biodiesel production routes without using a catalyst. Supercritical methanol as a reactant is a popular method which requires few equipment and can use both clean and used oil as feedstock [61].

In addition to the reaction, the purification process plays an important role in biodiesel production as it accounts for 60-80% of the total processing cost [11]. Therefore, the optimization of a biodiesel purification process has become an important research topic. For example, several biodiesel purification scenarios have been simulated and analysed to identify the optimal biodiesel production process from soybean oil [62].

To design an optimal biodiesel production process, two methods are commonly used: the heuristic approach and the superstructure-based approach. The heuristic approach is based on rules derived from experience and understanding of unit operations while the superstructure approach is based on optimization algorithms and mathematical models to identify the optimal process from all possible alternatives [59]. A disadvantage of the heuristic approach is that the interaction between different process stages and levels of detail is difficult to capture. The superstructure approach solves design problems simultaneously as a mathematical programming problem and therefore does not have this disadvantage [63].

Superstructure optimization has become more popular in recent researches of biochemical process design. AlNouss et al. (2019) used superstructure optimization to develop an economic and environmentally friendly gasification process, which produces fuels, fertilizers, and power from multiple biomass sources [64]. Galanopoulos et al. (2019) developed a superstructure framework for optimizing the design of an integrated algae biorefinery which can reduce the cost of biodiesel production up to 80% [14]. Kenkel et al. (2021) presented an open-source generic superstructure optimization for modelling and

optimizing of production process which is applied to design a cost optimal plant which produced methanol from captured CO_2 [65]. However, superstructures for biodiesel production are usually generalized with a minimum numbers of operating units and a simplified glycerol purification process.

Most of published studies focused mainly on one aspect between finding inexpensive feedstock and developing optimal processes for biodiesel production. A combined strategy of economic feedstock and innovative processes for biodiesel production has not been addressed adequately.

Therefore, in this chapter a superstructure model which connects appropriate feedstock selection with process synthesis is developed. In addition to the biodiesel production, the superstructure model comprises glycerol treatment options to increase the value of the by-product. Also, novel heat integration functions for further energy savings are setup and tested. With this superstructure model, an optimization is conducted for a production process from feedstock to biodiesel and glycerol. The results of this work will be compared to different biodiesel production processes from the literature [66].

3.2. Superstructure development

3.2.1. Problem statement

Given :

The different options for feedstock and reactants with their initial flowrates and compositions, the reaction- and separation equipment with their technical and economic specifications for producing and purifying biodiesel and glycerol.

Under conditions that:

1) Each option is assigned a binary logical decision variable which takes the value of 1 if the option is chosen and 0 if not chosen.

2) The options are connected to form possible processing routes by logical constraints.

3) The input and output flowrates of each option are calculated by mass balance constraints.

4) The utility requirement can be estimated from the heating, cooling and electricity requirement of each option which are calculated based on its flowrates and technical specifications.

5) The economics of an option including capital investment and operating costs is calculated from flowrate and utility consumption.

6) A heat integration function which is capable of matching hot and cold streams is integrated for further reduction of heating and cooling requirements.

Decide:

The superstructure optimization problem decides the optimal biodiesel feedstock and processing route while complying with logical, mass and energy constraints, and European Union (EU) standards of biodiesel product, EN 14214.

Objective:

To maximize the total profit of the biodiesel refinery and minimize environmental impacts in terms of utility consumptions and by-product improvement.

3.2.2. Superstructure topology

The superstructure has total 68 technical options which are related to 68 binary decision variables. The superstructure is presented by two parts: The first part has 54 possible options for the biodiesel production and the second part has 14 options for glycerol treatment. Figure 3.1 presents the first superstructure part for the biodiesel production from three generations of feedstocks such as rapeseed oil and canola oil (first generation), waste cooking oil, tallow and linseed oil (second generation), and algae oil (third generation). For reaction, continuous stirred tank reactor (CSTR), reactive distillation (RD) column and membrane reactor (MR) with different catalysts and supercritical operating conditions are included. For separation, options are vacuum distillations, decanters, acid and base neutralization reactors, water washing columns and hydrocyclones. After purification, the product stream has 96.5 wt.% FAME.

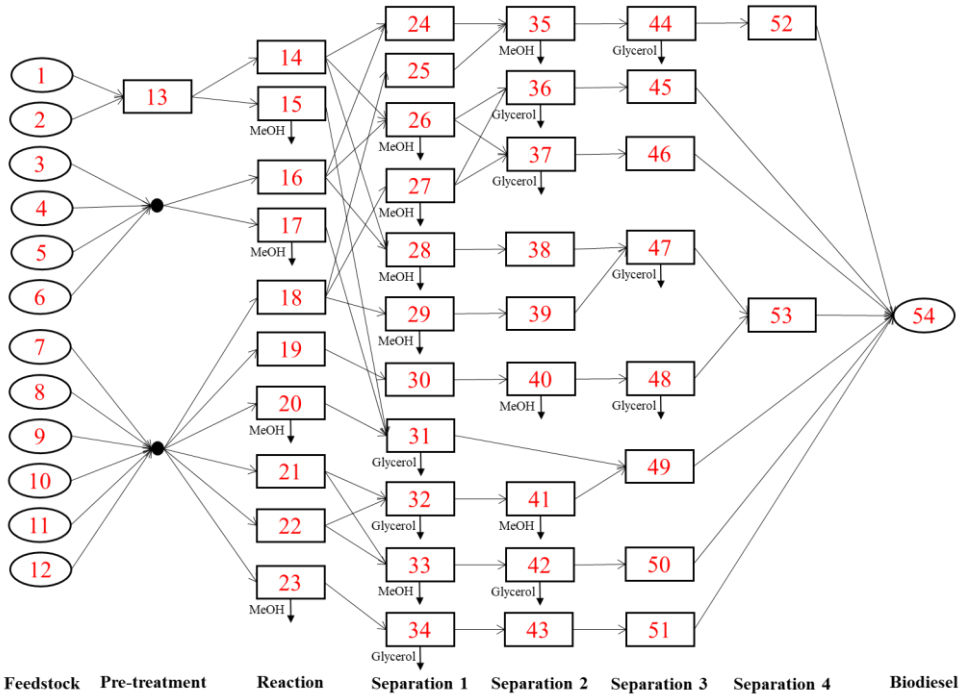

Figure 3.1: The superstructure for biodiesel production

In Figure 3.2, the second part of the superstructure for glycerol can be used to decide the treatment process depending on the quality of glycerol input and desired output. Depending on its initial purity, the glycerol separated from the biodiesel production can be disposed as a waste or purified further to sell as crude glycerol (~80 - 98 wt.%), technical glycerol (~98 - 99.5 wt.%) and pure glycerol (> 99.5 wt.%) [67].

A complete description of superstructure options with reference capacity, chemical engineering index and equipment size exponent can be found in Appendix A-3.1.

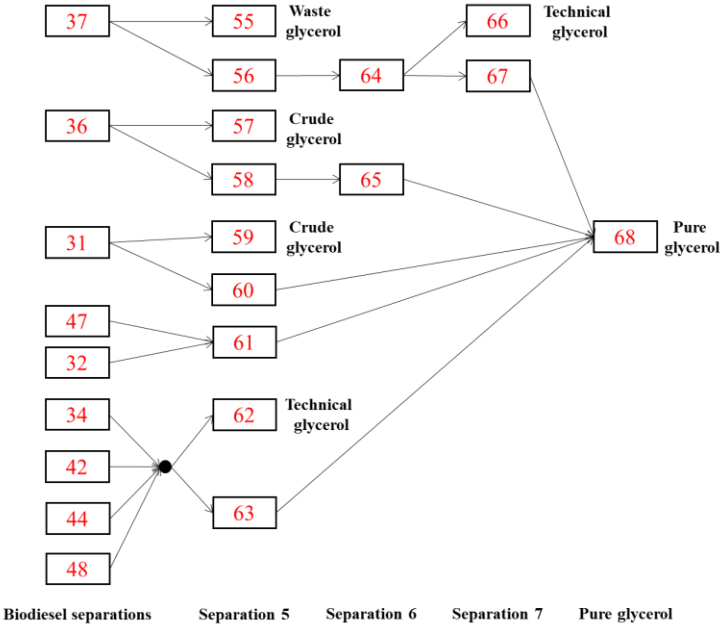

Figure 3.2: The superstructure for glycerol treatment

3.2.3. Mathematical model

Each option *j* of the superstructure has an infeed stream, *F*, and a reactant stream, *R*, which come in, and a product stream, *P*, and a waste stream, *W*, which come out, as shown in Figure 3.3. The product stream of an option will be the feed stream of the next option on the same process route.

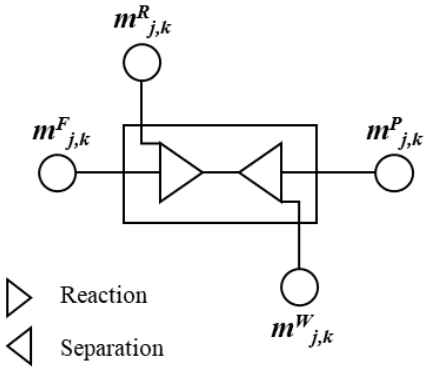

Figure 3.3: The illustration of streams which come in and out of a unit in the superstructure

The mathematical model includes mass balances of component *k* in each option *j* as shown in equations 3.1 and 3.2.

$$m_{j,k}^{P} = (m_{j,k}^{F} + m_{j,k}^{R} + M_k \cdot ER \cdot \alpha_k) \cdot SF_{j,k} \cdot y_j \quad (3.1)$$

$$m_{j,k}^{W} = (m_{j,k}^{F} + m_{j,k}^{R} + M_k \cdot ER \cdot \alpha_k) \cdot (1 - SF_{j,k}) \cdot y_j \quad (3.2)$$

where *k* is a component of the streams (e.g., FAME, MeOH, glycerol, etc.), $m^{F}_{j,k}$, $m^{R}_{j,k}$, $m^{P}_{j,k}$ and $m^{W}_{j,k}$ are mass flow rates (*kg/h*) of component *k* in feed, reactant, product and waste streams, respectively. y_j is the logical decision variable which takes the value of 1 or 0 if the option is selected or not. $SF_{j,k}$ is the split factor of component *k* based on how much k in the feed stream split into product stream. ER_j is the extent of reaction (*kmol/h*) calculated from the conversion of the main component of the feed stream into the main product of the product stream (e.g., from oil into biodiesel) as shown in equation 3.3.

$$ER_j = \frac{\theta_A \cdot \left(m_{j,A}^{F} + m_{j,A}^{R}\right)}{(M_A \cdot \alpha_A)} \quad (3.3)$$

where θ_A is the percent of component A being converted into product and α_A is the reaction stoichiometric number of A. From the extent of reaction, the conversion of another component can be calculated with the molar weight (*kg/kmol*), M_k, and the reaction stoichiometric number, α_k, of that component.

The equipment cost (*USD*), EC_j, of an option is estimated based on the order of magnitude as presented in equation 3.4 [68].

$$EC_j = EC_j^{Ref,year} \cdot \left(\frac{m_j^{F}}{m_j^{F,Ref}}\right)^{Es} \cdot \left(\frac{CE^{2020}}{CE^{year}}\right) \cdot y_j \quad (3.4)$$

where *Es* is the size exponent, $EC^{Ref,year}{}_j$ is the equipment reference cost (*USD*), $m^{F,Ref}$ is the reference capacity (*kg/h*), CE^{year} and CE^{2020} are the Chemical Engineering Index of the reference year and 2020, respectively.

The total capital investment (*USD*), *TCI*, is calculated based on the overall factor method of Lang as shown in equation 3.5 [68].

$$TCI = 1.05 \cdot f_{L,TCI} \cdot \sum_j \left(EC_j\right) \quad (3.5)$$

where $f_{L,TCI}$ is the Lang factor for fluid processing plant being 5.93 and 1.05 is to account for the delivery cost of equipment being 5% of total equipment cost [68]. The total annualized capital investment (*USD*), *TACI*, is calculated from the *TCI* with total project lifetime, *LT*, being 20 years and interest rate, *IR*, being 0.1 as described in equation 3.6

$$TACI = TCI \cdot \frac{IR \cdot (IR+1)^{LT}}{(IR+1)^{LT} - 1} \quad (3.6)$$

The annual utility consumption (*kg steam* or *kg cooling water* or *kW/year*), E^u_j, of an option is calculated as equation 3.7.

$$E_j^u = \left(m_j^F + m_j^R\right) \cdot \tau_j^u \cdot H \cdot y_j \quad (3.7)$$

where *u* is a type of utility such as heating with low- and high-pressure steams, cooling water and electricity, τ^u_j is the specific utility requirement (*kg steam or kg cooling water or kW electricity per kg infeed stream*) of the equipment, *H* is the total operating hours per year (*h*).

The utility prices, $price^u$, are taken from literature with an average inflation rate of USD being 2.26 % per year. The value of low-pressure steam is 10.2 *USD/tonne* [9]. The price of high-pressure steam is 15 *USD/tonne* [9]. The price of electricity being 0.09424 *USD/kWh* [9]. The price of cooling water is 2.23 *USD/tonne* [65]. The total annual utility cost (*USD*), *TAU*, is calculated as follows.

$$TAU = \sum_j \sum_u E_j^u \cdot price^u \quad (3.8)$$

The heat integration of the superstructure optimization model is a function based on Pinch Technology that minimizes the heating and cooling requirements of the biodiesel production. Each product or waste stream out of an option has a defined temperature with an assumption that the stream can only be heated or cooled with heat exchangers using other streams or heating and cooling utilities.

First, a series of heat intervals defined from the temperature differences of the product streams which are designated as hot streams or cold streams depending on their heating or cooling requirements. The stream heat load (*kW*), ΔH_l, of each interval *l* can be calculated from the heat capacity flow rates ($kW/^oC$) of hot stream, $CP_{Hot,j}$, and cold stream, $CP_{Cold,j}$, as in equation 3.9.

$$\Delta H_l = \left(\sum_j CP_{Hot,j} - \sum_j CP_{Cold,j}\right) \cdot \Delta T_l \quad (3.9)$$

Second, the function is used to select hot and cold streams based on the decision variable in each product stream. Then, the hot and cold streams are matched with each other according to their temperature to calculate the total heat load of heat intervals and set up the heat cascade.

Finally, the minimum hot and cold utility requirements can be predicted by balancing the negative heat interval of the infeasible heat cascade. The heat integration feature of the superstructure is to evaluate the possible energy recovery with heat exchanger network. The heat exchanger network and investment costs are at this stage not considered in the heat integration function.

The maintenance cost (*USD*), *MC*, can be considered as 2% of the total annualized capital investment [14]. The operating cost (*USD*), *OC*, can be calculated from the average hourly salary of an operator in 2020 which is 15 *USD/h* and 1 operator for 1 automatic continuous operation of fluid processing plant with capacity below 1000 tonnes of product per day [69]. The operating and maintenance cost (*USD*), *OMC*, is presented as follows:

$$OMC = MC + OC \tag{3.10}$$

The total annual operating cost (*USD*), *TAOP*, includes feedstock and reactant costs, operating and maintenance cost and total utility cost. The costs (*USD*) of feedstock, *FC*, and reactant, *RC*, are calculated by multiplying mass flow rate with cost per kg and operating hours per year. The operating and maintenance cost (*USD*), *OMC*, is calculated as equation 3.10. The total utility cost (*USD*), *TAU*, is calculated as equation 3.8. The calculation of *TAOP* is presented in equation 3.11.

$$TAOP = FC + RC + OMC + TAU \tag{3.11}$$

To include the effect of recycling methanol in the mathematical model, the pure methanol coming out of distillation options is considered a by-product which can be sold to reduce the cost of fresh methanol. The annual methanol sales (*USD*), *MES*, is calculated from the methanol stream that is separated from the biodiesel stream as in equation 3.12 with j = 15, 17, 20, 23, 26, 27, 28, 29, 33, 35, 40, 41 and 43.

$$MES = m_j^W \cdot price^{methanol} \cdot H \cdot y_j \tag{3.12}$$

Maximizing the total annualized profit (*USD*), *TAP*, is the objective function of the superstructure optimization as presented in equation 3.13.

$$\max TAP = BDS + GLS + MES - TACI - TAOP \tag{3.13}$$

where the annual biodiesel sales (*USD*), *BDS*, is defined from the biodiesel price and the flow rate of product stream out of options: 45, 46, and 49-53. The annual glycerol sales (*USD*), *GLS* is defined from the glycerol grade and the mass flow rate of the glycerol treatment. All the sales are calculated with the product market prices and the total operating hours of the refinery in a year

The superstructure optimization problem is formulated as a mixed-integer nonlinear programming (MINLP) problem. It is solved with the Branch-And-Reduce Optimization Navigator (BARON) which is a computational program designed to find the global solution of non-convex optimization problems [70].

The mathematical model includes 5,978 constraints and 6,007 variables with 68 binary variables is implemented in the software AIMMS, version 4.84.3.4 64-bit. The

optimization problem is solved in an average of 55 s with a CPU Intel(R) Core(TM) i5-8265U CPU @ 1.80 GHz and 8.00 RAM.

3.3. Results and discussion

The superstructure model is applied in three case studies:

1) In the first case, the feedstock is only waste cooking oil to verify the superstructure model by comparing with the results from literature.

2) In the second case, the feedstocks are from different generations of biodiesel to select the most cost-effective feedstock and processing route.

3) In the third case, the membrane reactor is chosen to test the economic feasibility of the potential process intensification technology for biodiesel production [17].

The biorefinery has feedstock flow rate of 1000 kg/h, 8000 operating hours per year and biodiesel output quality complied with the EU standard, EN 14214. All the prices of biodiesel and glycerol, costs of feedstocks, chemicals, utilities and equipment are calculated in the year 2020.

In the case studies, the flowrate of the feedstock is chosen based on the case study in the literature which, in turn, is based the regional availability of waste cooking oil in the United States and the same capacity as the existing continuous biodiesel plant described by Connemann and Fischer (1998) [71]. Due to the pilot scale of the biodiesel plant, the capital investment is calculated by using economies of scale on bigger equipment. It is recommended that more detailed calculations are required to identify the exact sizes and costs of the equipment resulted from this case study.

3.3.1. First case study: Waste cooking oil as the only feedstock

In the first case study, the optimal processing route is presented by the yellow blocks and orange arrow lines. In Figure 3.4, the biodiesel is produced from the transesterification of the waste cooking oil (option 7) by using reactive distillation with heterogeneous acid-based catalyst (option 20) [72]. The products of the reactive distillation process are recycling methanol and a biodiesel-rich stream which is passing through a decanter (option 31) to separate the glycerol. After separating the glycerol, the biodiesel product is purified to achieve purity standards by using a vacuum distillation column (option 49). In Figure 3.5, the separated glycerol from the decanter (option 31) is going through a vacuum distillation (option 60) to become pure glycerol. The total annual profit of the biodiesel production in this case is 2,619,038 USD per year.

The selected sequence of process makes sense as it is based on the composition of biodiesel product stream which usually contains a large amount of methanol, biodiesel, glycerol, catalyst, water and unreacted oil. Methanol has the lowest boiling point, at 65 ^{o}C, in the mixture and can be separated easily by distillation. Its separation at the beginning of the process increases methanol recycle and decreases the flowrate of processing streams for downstream equipment, thus, reducing the costs of fresh methanol, utility and capital investment. The removal of catalyst out of biodiesel product requires neutralization and washing steps which consume chemicals such as sulfuric acid and calcium oxide, utility and water. By applying the reactive distillation column which is a process intensification technology and the heterogeneous catalyst, several equipment along with their utility and chemical consumptions can be removed from the production process [72].

1 kg of by-product glycerol is produced for every 10 kg of biodiesel. In conventional production processes, the glycerol stream can contain methanol, catalyst and water. The crude- and technical-grade glycerol are not high price products, while the expensive pure-grade glycerol requires additional energy intensive equipment such as distillation column and neutralization reactor to produce. The low return of investment becomes discouragements to producers from upgrading the glycerol. In the optimal process from superstructure, the separated glycerol has higher purity than conventional processes because of the early removal of methanol and no catalyst in product stream. Therefore, it is more economic to upgrading glycerol to pure quality.

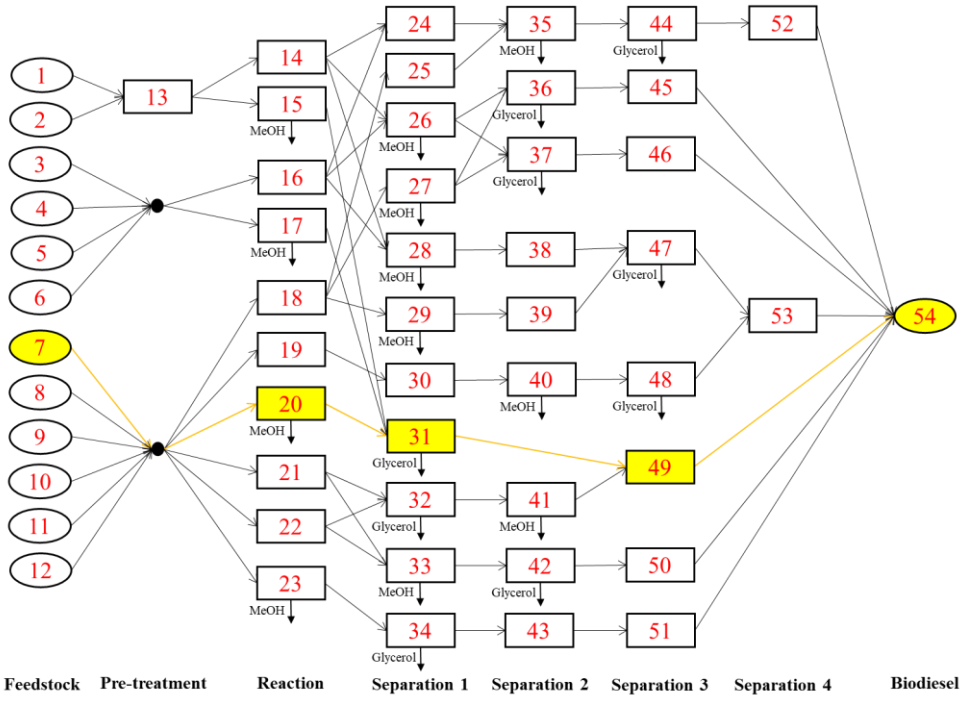

Figure 3.4: The optimal production route for biodiesel from waste cooking oil

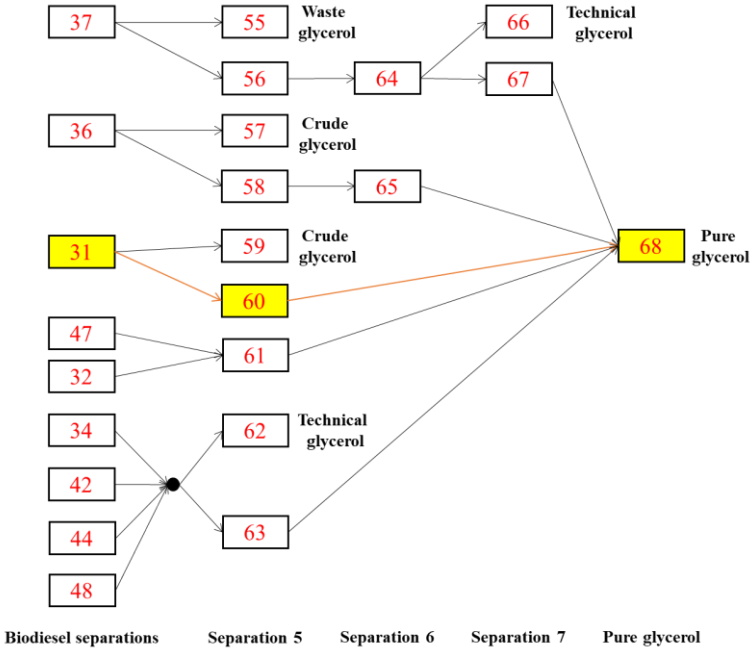

Figure 3.5: The optimal treatment routes for the glycerol separated from biodiesel production process

When comparing with the different production processes of biodiesel from waste cooking oil [66], the superstructure optimal process has higher total annual profit, as presented in Figure 3.6. There are three reasons: Firstly, the application of the heterogenous acid reactive distillation process which can be used for feedstocks with high content of free fatty acids such as waste cooking oil and tallow. This process intensified technology reduces the costs of production by removing separation steps for methanol and catalysts. Secondly, the glycerol is purified and sold as pure glycerol with higher price than in other processes. Finally, the heating and cooling costs are reduced with the heat integration. It should be noted that the cost of heat exchangers has not been included in the analysis.

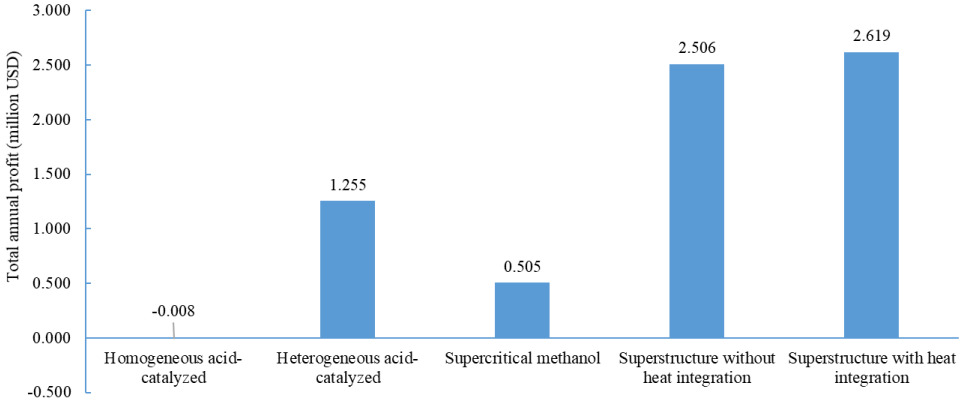

Figure 3.6: The total annual profit comparison of different biodiesel production process from waste cooking oil

Besides the total annual profit, the environmental impacts of the production process are optimized in terms of utility consumptions. With the process intensification and heat integration, the utilities required for heating and cooling can be reduced greatly. In Figure 3.7, the heating and cooling costs of the superstructure optimized processes with and without heat integration are compared with other biodiesel production processes [66]. The results show a significant decrease in heating requirement by using the heterogeneous reactive distillation process. The process with heat integration function has the total annual costs of heating and cooling 30% lower than the process without heat integration.

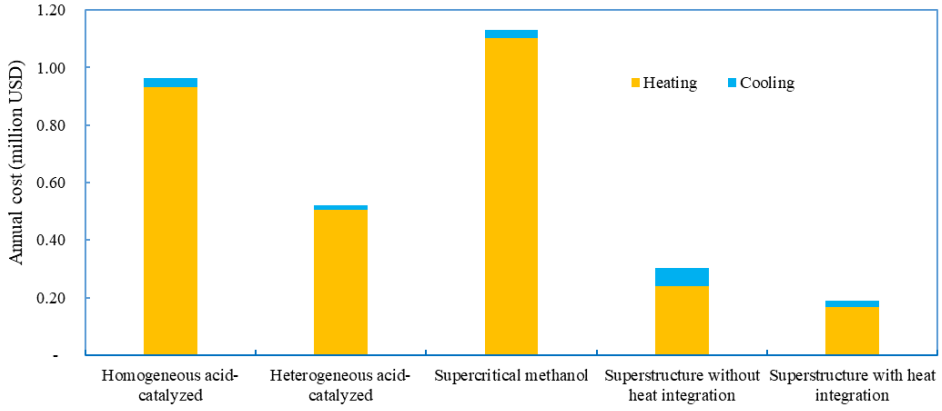

Figure 3.7: The annual heating and cooling costs of different biodiesel production process from waste cooking oil

The heat integration results in Figure 3.6 and 3.7 show that there is a difference in the production cost and utility consumption. In the case study of biodiesel produced from waste cooking oil, the heat integration does not have a profound effect on the results. The reason is that the optimal process for this case uses a reactive distillation with a heterogeneous acid catalyst which requires less equipment and utilities than other processes. This optimal process has less streams and heat waste than other processes, thus, reducing the need for heat integration. From the result, the heat integration function has worked and can be incorporated in the future work.

3.3.2. Second case study: different feedstocks from three generations

In the second case study, different feedstocks such as rapeseed oil, canola oil (first generation), linseed oil, waste cooking oil, tallow (second generation) and algae oil (third generation) are used for biodiesel production. The optimal result is the biodiesel produced from tallow (option 8) with the same processing route as the waste cooking oil. The annual profit this process is 3,539,025 USD per year which is higher than the first case because the price of tallow is lower than waste cooking oil. With the total capital investment being 1,800,834 USD, the payback time of the biodiesel plant is less than one year.

A breakdown of the annual production costs is presented in Figure 3.8. To evaluate the weight of feedstock such as tallow on biodiesel production cost, the chemicals such as methanol, neutralization acid/base, catalysts, etc. are separated from the raw material cost. The utility includes heating, cooling and electricity costs. The cost of feedstock is the decisive factor for the economic feasibility of biodiesel production which agrees with the literature [66].

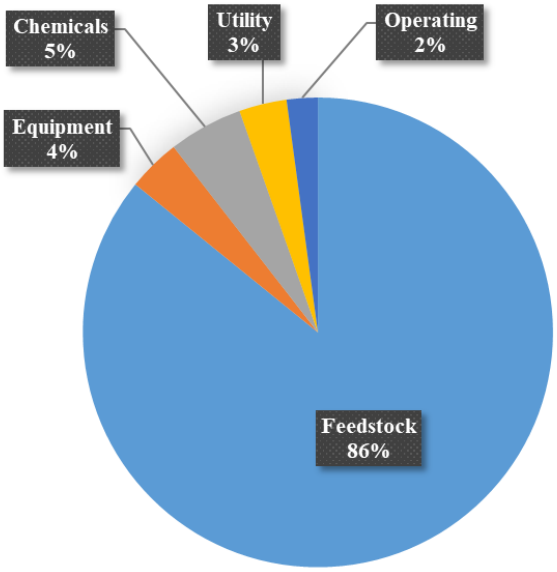

Figure 3.8: The annual cost breakdown of biodiesel production from tallow

3.3.3. Third case study: membrane reactor

In the third case study, the membrane reactor with heterogeneous acid catalyst is chosen by assigning the value 1 to the logical constraint of the equipment. With tallow (option 8) is the chosen feedstock, the product stream out of the membrane reactor (option 23) is going through the decanter (option 34) to separate the glycerol and the methanol removal (option 43) [17]. Finally, the biodiesel stream is purified by a distillation column (option 51) [17]. The glycerol stream separated from the decanter is purified by a distillation column (option 63) to become pure glycerol. Although the membrane reactor has high conversion rate and purer product stream than other reactors, it has a low product yield due to nature of membrane separation process. The biodiesel yield of the membrane reactor is only 42.6% of the reactive distillation. Therefore, the biodiesel production process with membrane reactor has negative total annual profit, -2,007,646 USD.

3.4. Conclusion

A superstructure model for biodiesel production which encompasses different generation feedstocks, conventional and process intensification technologies has been developed. The superstructure bridges the gap between feedstock selection and production process optimization in the literature. Another novelty of the superstructure model is the heat integration function which can be used to reduce the energy requirement of biodiesel production process.

The results show that the combination of waste cooking oil and tallow with reactive distillation and heterogenous acid catalyst can open a promising future for biodiesel. The membrane reactor requires more improvement in term of biodiesel yield to be economic efficiency. The feedstock has an important role in the optimization problem as it accounts for more than 80% of the total production cost. The superstructure optimization is proven as a powerful tool of process systems engineering for biorefinery design by systematically and simultaneously solving multi-constraint problems.

However, the superstructure approach relies on simplified process parameters (such as extent of reaction and split factor) and estimate calculations (such as economies of scale and Lang's factor). Therefore, the accuracy of economic results is typically between 30% and 35%. More detailed calculations are required to apply the optimal production route from the superstructure optimization.

3.5. Nomenclature

BDS	the annual biodiesel sales (USD)
CE^{year}	Chemical Engineering Index of the reference year
CE^{2020}	Chemical Engineering Index of 2020
$CP_{Cold,j}$	the heat capacity flow rates of cold stream (kW/^{o}C)
$CP_{Hot,j}$	the heat capacity flow rates of hot stream (kW/^{o}C)
E^{u}_{j}	the annual utility consumption of an option j (kg or kW/year)
EC_j	the equipment cost (USD)
$EC^{Ref,year}_{j}$	the equipment reference cost of the reference year (USD)
ER	the extent of reaction (kmol/h)
Es	the size exponent
$f_{L,TCI}$	the Lang's factor
FC	the annual cost of feedstock (USD)
GLS	the annual glycerol sales (USD)
H	the total operating hours per year (h)
IR	annual interest rate
LT	the total project lifetime (year)

$m^{F}_{j,k}$	the mass flowrate of component *k* in feed stream (kg/h)
$m^{P}_{j,k}$	the mass flowrate of component *k* in product stream (kg/h)
$m^{R}_{j,k}$	the mass flowrate of component *k* in reactant stream (kg/h)
$m^{W}_{j,k}$	the mass flowrate of component *k* in waste stream (kg/h)
M_k	the molar weight of component *k* (kg/kmol)
MES	the annual methanol sales (USD)
OMC	the operating and maintenance cost (*USD*)
$price^{u}$	the utility price (USD/kg or USD/kWh)
RC	the annual cost of feedstock (USD)
$SF_{j,k}$	the split factor of component *k*
TACI	the total annualized capital investment (USD)
TAOP	the total annual operating cost (USD)
TAU	the total annual utility cost (USD)
TCI	the total capital investment (USD)
α_k	the reaction stoichiometric number of component *k*
ΔH_l	the stream heat load of interval *l* (kW)
ΔT_l	the temperature difference of interval *l* (^{o}C)
θ_A	the percent of component *A* being converted
τ^{u}_{j}	the specific utility requirement of the equipment (kg or kW per kg infeed)

4. Technological impact assessment and sensitivity analysis

“As far as the laws of mathematics refer to reality, they are not certain; and as far as they are certain, they do not refer to reality.” - Albert Einstein

This chapter was published in:

Thien An Huynh, Meik B. Franke, Edwin Zondervan, 2022, “*Steps towards the winning formula for biodiesel: Superstructure, process intensification and heat integration*” – Is going to submit to the journal Computers & Chemical Engineering.

Abstract

In chapter 3 the superstructure optimization problem has been solved to identify the most profitable way to produce biodiesel. The result shows that the biodiesel production route from tallow with the reactive distillation technology and heterogeneous acid catalyst has the highest total annual profit. The cost of feedstock which contributes more than 85% of the total annual cost has a significant impact on the economic feasibility of biodiesel production. The fluctuation in market prices of feedstocks and products as well as the availability of technology are important uncertainties which should be addressed in the design a biodiesel production process.

This chapter firstly evaluates the effects of different parameters on the optimized design by performing a sensitivity analysis. The superstructure is used to generate various biodiesel production processes according to the different scenarios. The results show that the price of biodiesel, feedstock and the production capacity are most influencing parameters on the total annual profit. By exploring six different scenarios, the reactive distillation process is the most economic choice for biodiesel production from different feedstocks.

4.1. Introduction

The design of a biodiesel production process is mainly decided by the feedstock, technology and market prices of products. The cost of feedstock is the decisive factor in the economic calculation of a biodiesel production as it contributes more than 80% of the total production cost [9]. As presented in Figure 4.1, the prices of feedstock and biodiesel are seasonal parameters, thus reducing the accuracy of the optimized results based solely on fixed values.

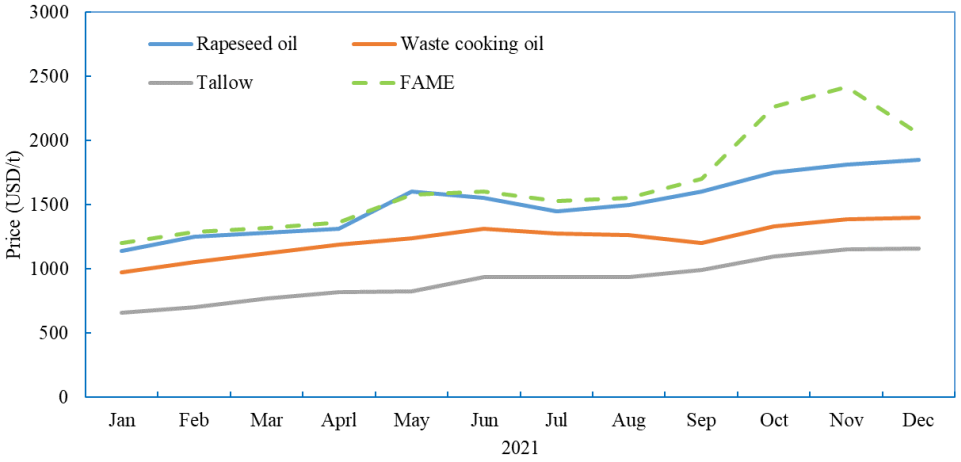

Figure 4.1: The prices of biodiesel and feedstocks in 2021 [73], [74], [75]

The difference between market prices of feedstock and biodiesel is the main motivation for optimizing the production to reduce processing costs with advanced technologies. However, process intensified and innovative technologies such as reactive distillation and supercritical reaction which have been proven in the literature and industrial applications are not always available. Therefore, the availability of technology is another important factor that affects the design of biodiesel production process.

Process design and optimization under uncertainty are in general very challenging problems in the field of process systems engineering [76]. The challenge is ensuring that the process design is feasible and optimal over a range of changing parameter values [76]. Notable efforts have been made by the process systems engineering community to develop methods for solving the problems under uncertainty [77]. One method is to analyse and maximize the flexibility of the process design in the trade-offs with costs to cope with a range of uncertainty parameters [77]. Clay and Grossmann proposed a sensitive-based successive disaggregation algorithm to solve a two-stage linear stochastic production planning problem including cost and supply/demand uncertainties [78]. The sensitivity of the uncertain parameters and the process flexibility are important factors for solving the optimization

problem under uncertainty. Therefore, this chapter has two objectives: Firstly, it is to evaluate the impact of important parameters on the optimization result through a sensitivity analysis. Secondly, different scenarios according to the availability of technology are generated to test the feasibility of the superstructure model.

4.2. Sensitivity analysis

To design and optimize models under uncertainty, sensitivity analysis is performed to evaluate the impact of changing parameters on the model outcome. From the result of cost breakdown in the chapter 3, three most influencing parameters are costs of feedstock, chemical and equipment. The cost of chemical can be calculated based on the price of methanol which is the major reactant in biodiesel production. From the literature, the prices of biodiesel and glycerol, and the production capacity i.e. the feedstock flowrate per hour are also considered important parameters [9]. The sensitivity factor, *S*, which is used to measure and compare the impact of selected parameters on the objective function is calculated as in equation 4.1.

$$S = \frac{|\Delta\%_{profit}|}{|\Delta\%_{parameter}|} \tag{4.1}$$

where $|\Delta\%_{profit}|$ is the absolute value of profit difference according to the changing parameters in percentage $|\Delta\%_{parameter}|$, including the prices of biodiesel, glycerol, feedstock, methanol and equipment, and the production capacity [9].

Each of these six parameters is evaluated within 20% range of their values which is used in chapter 3. Figure 4.2 shows the sensitivities of selected parameters on the total annual profit of the biodiesel production. The result shows that the price of biodiesel has the greatest effect on the total annual profit compared to other evaluated parameters. The second and third influencing parameters are the price of feedstock and the production capacity. The prices of glycerol, methanol and equipment have less impacts on the superstructure model outcome.

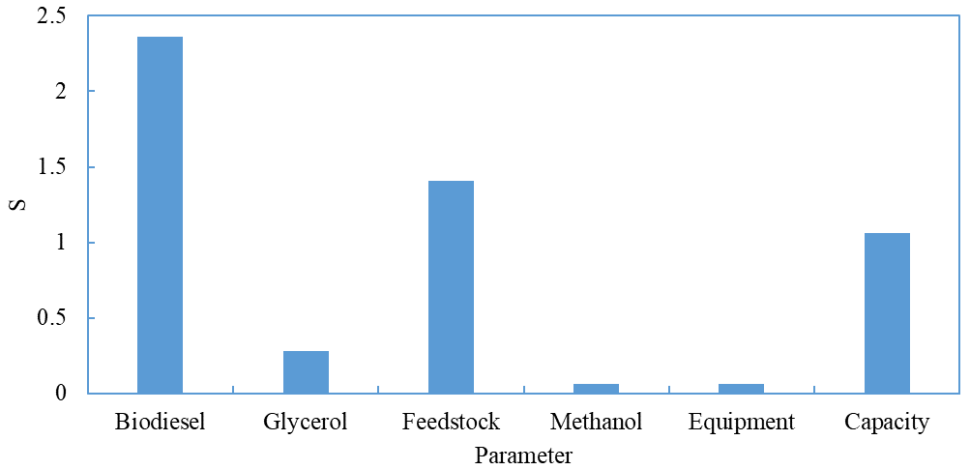

Figure 4.2: Result of the sensitivity analysis for six parameters

4.3. Technological impact assessment

The innovative production technologies have an important role in the production processes. In this section, six scenarios have been used to assess the impact of reaction technologies and catalysts on the biodiesel production. The most profitable and flexible production technology can be identified from the assessment. The optimal process as proposed in chapter 3 producing biodiesel from tallow via reactive distillation with a heterogeneous acid catalyst is chosen to be the base case in the assessment. For scenarios 1 to 4, the availability of technology is simulated by using different reaction technologies and catalysts such as supercritical reactor, multi-phase reactor, continuous stirred tank reactor, and homogeneous and heterogeneous catalysts. For example, scenario 1 uses the multi-phase reactor instead of the reactive distillation which is the optimal choice of the base case from the superstructure. Figures 4.3 and 4.4 present the results of superstructure optimization for scenarios 1, 2, 3 and 4.

For scenarios 5 and 6, the simulations are performed to evaluate the effect of technology in the situation that different feedstocks are used to produce biodiesel instead of waste cooking oil and tallow. Figures 4.5 and 4.6 show the results of scenarios 5 and 6.

4.3.1. Scenario 1

The first scenario uses the continuous stirred tank reactor (CSTR), multi-phase reactor, supercritical reactor and membrane reactor with the catalysts of acid, base and enzyme to compare with the reactive distillation in the base case. With the tallow as a feedstock with high content of free fatty acid (FFA), the heterogeneous acid catalyst is still

the best choice. The optimal process route is using the multi-phase reactor (option 19) then separating the catalyst with a hydrocyclones (option 30) [66]. After catalyst removal, the methanol is separated from the biodiesel production stream with a distillation column (option 40) and recycled to the reactor [66]. The glycerol is separated into a glycerol-rich stream by a decanter (option 48) and goes through a distillation (option 63) to remove water and methanol. The total annual profit is 3,134,732 USD.

4.3.2. Scenario 2

In the second scenario, the multi-phase reactor is excluded from the list of reactor in scenario 1. This scenario is to identify the next potential reactor after reactive distillation and multi-phase reactor. The chosen reaction technology is a supercritical reactor (option 21) with high temperature (350 ^{o}C) and large amount of methanol (methanol to oil molar ratio: 42:1) [66]. The supercritical alcohol process does not require catalysts and can tolerate high-FAA feedstocks [66]. After reaction, the biodiesel production stream goes through a methanol distillation column (option 33), then glycerol gravity separation (option 42) and finally biodiesel purification column (option 50) [66]. The separated glycerol stream contains mostly methanol and no catalyst. Therefore, it is suitable for further distillation (option 63) and sold as pure glycerol. The total annual profit of the second scenario is 2,973,252 USD.

4.3.3. Scenario 3

For the third scenario it is assumed that the reactive distillation, multi-phase reactor and supercritical reaction are not in the list of reactor of scenario 1. The next choice for producing biodiesel from tallow is the conventional continuous stirred tank reactor (CSTR) (option 18) with a homogenous acid catalyst, H_2SO_4 [66]. The product stream of the reactor is going through a distillation column (option 29) to recycle the methanol, then a neutralization process (option 39) to remove the acid catalyst and a decanter (option 47) to separate the glycerol, finally, a vacuum distillation (option 53) to purify the biodiesel. This process is sensible because the removal of alcohol at first separation stage will maximize the amount of recycling methanol and reduce the costs of downstream equipment [62]. The glycerol is further purified to be pure glycerol with distillation (option 61). In this scenario, the total annual profit is 2,295,976 USD.

4.3.4. Scenario 4

In the base case and previous scenarios, the homogeneous and heterogeneous acid catalysts are used directly at the reaction step. Scenario 4 explores the pre-treatment process which is actually used in the biodiesel industry for feedstocks with high content of FFA [6]. While scenario 4a is the conventional process of using the CSTR and homogeneous base catalyst, NaOH, (option 14) after pre-treatment process (option 13), scenario 4b uses the

process intensification technology of reactive distillation (option 15). The results show the difference in processing routes of scenarios 4a and 4b as in Figures 4.3 and 4.4. The process intensification route has higher total annual profit (2,691,672 USD) than the conventional production route (2,006,746 USD).

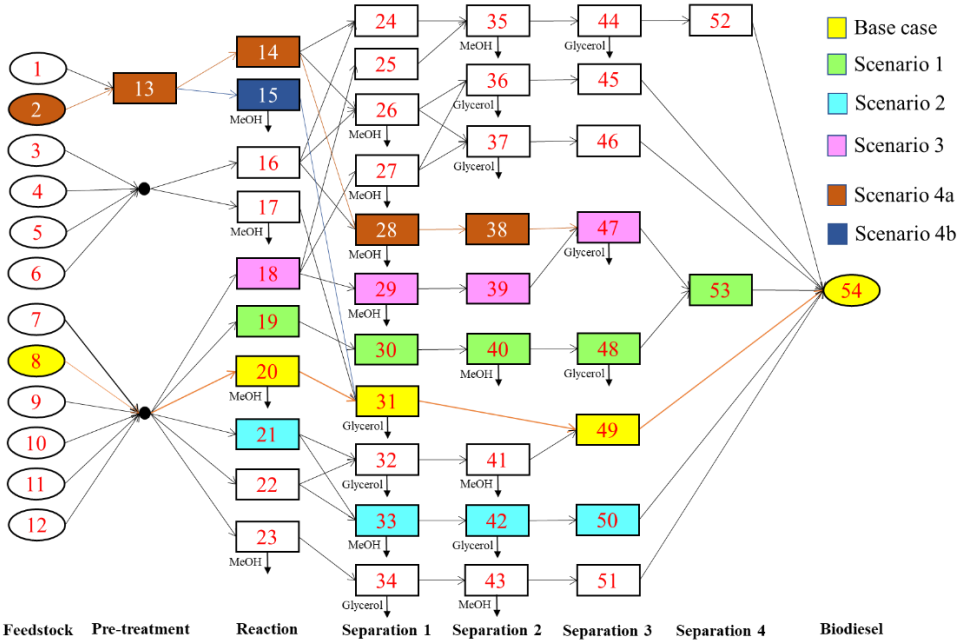

Figure 4.3: Optimization biodiesel production route of scenario 1, 2, 3 and 4

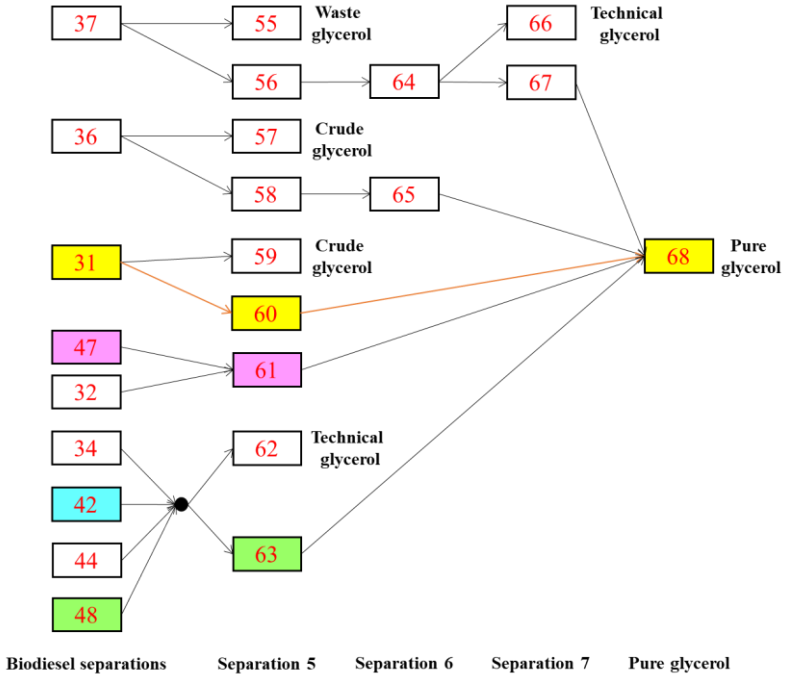

Figure 4.4: Optimization glycerol treatment route of scenario 1, 2, 3 and 4

4.3.5. Scenario 5

A feedstock such waste cooking oil and/or tallow have low costs and require the acid catalyst to deal with the high content of FFA, thus affecting the technological choice. The fifth scenario is to evaluate the feasibility of superstructure model under condition of no waste feedstock. The chosen feedstock is the canola oil (option 5) which is the cheapest one in the current model. Without FFA, the base catalyst is more economic than the acid one because NaOH is generally cheaper than H_2SO_4. The optimal production route is the reactive distillation (option 17), then the decanter to separate the glycerol (option 31) and finally, the distillation column for biodiesel purification (option 49). The glycerol treatment is a distillation column (option 60) to remove impurity. The final glycerol is sold as pure glycerol. The annual profit of the scenario 5 is 1,033,042 USD.

4.3.6. Scenario 6

The sixth scenario is used to evaluate the impact of process intensification on the model result by comparing the conventional CSTR with the reactive distillation. With the same feedstock, the scenario 6 uses more equipment, thus having lower annual profit

(333,870 USD) than scenario 5. The processing routes of scenarios 5 and 6 are presented in Figures 4.5 and 4.6.

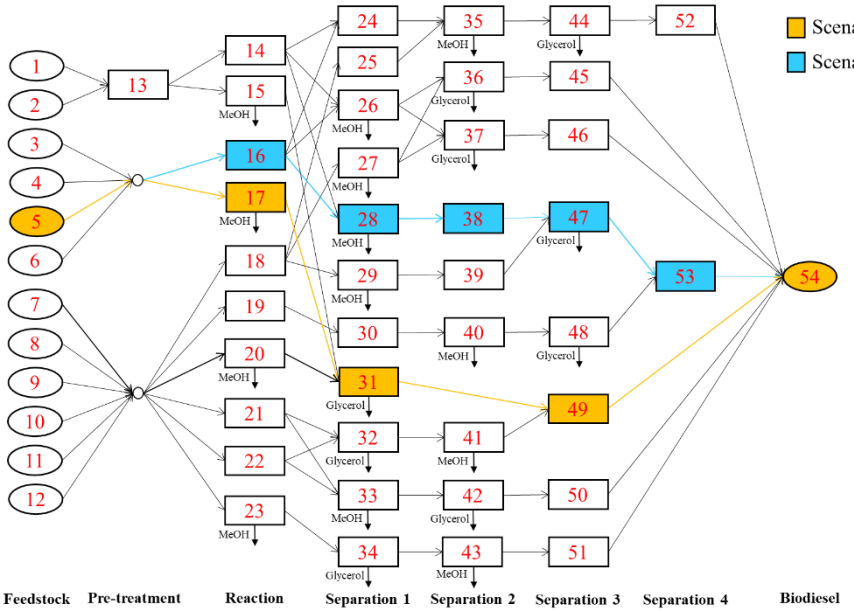

Figure 4.5: Optimization biodiesel production route of scenario 5 and 6

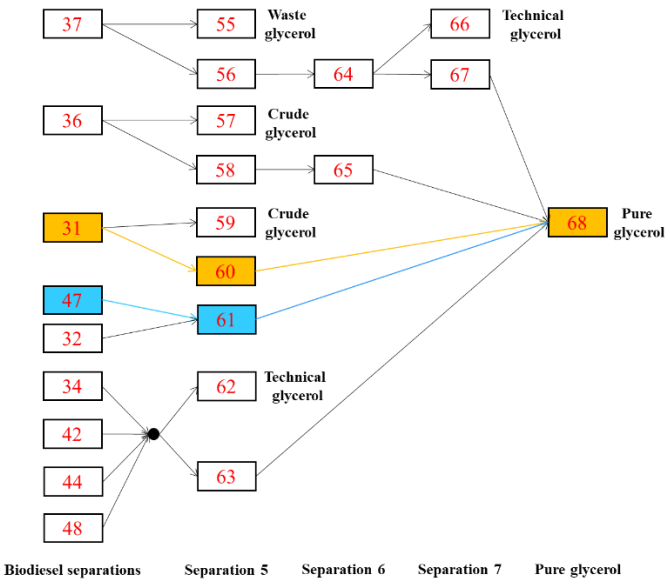

Figure 4.6: Optimization glycerol treatment route of scenario 5 and 6

4.3.7. Scenario comparison and discussion

The annual profit comparison of all scenarios is shown in Figure 4.7. The total annual profit of the base case and the sixth scenario are the highest and lowest among the assessed scenarios, respectively. The reason is the difference in feedstock and production costs. The scenarios 4a and 4b have an additional step of pre-treatment which makes them have higher production costs than other scenarios using tallow as feedstock. Scenarios 5 and 6 have lower annual profits than the rest because the price of canola oil is 52% higher than tallow. Between scenarios with the same feedstock, the ones using reactive distillation such as the base case, scenarios 4b and 5 have higher profit than others.

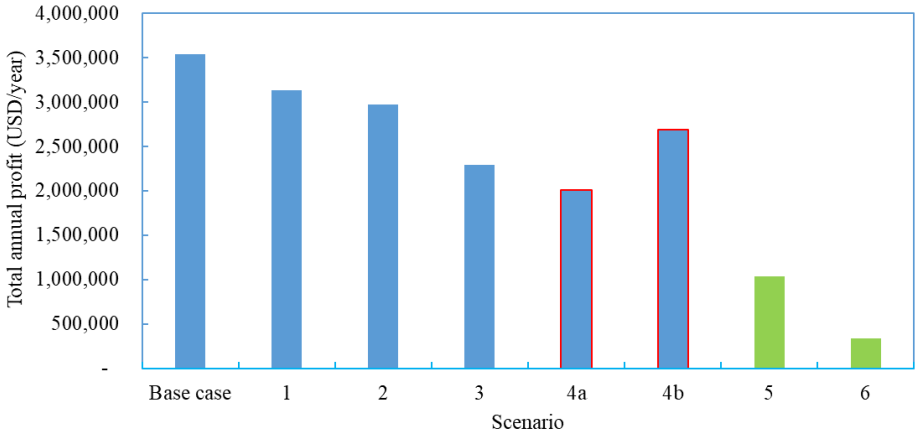

Figure 4.7: The total annual profit of biodiesel production of different scenarios

Figure 4.8 presents the breakdown of production costs without feedstock from different scenarios. Due to the high content of FFA, the conventional ways of producing biodiesel from the waste feedstocks require additional production costs as shown in the scenarios 3, 4a and 4b. The reactive distillation process reduces the equipment cost significantly but it is not always the least utility consumption process. The scenarios 4a and 6 which use conventional CSTR and the heat integration to match hot and cold streams have the lowest utility consumption. Scenario 5 has the lowest production cost because of the reactive distillation and canola oil as low FFA feedstock. However, the profit of scenario 5 is still much lower than previous scenarios due to the high price of feedstock.

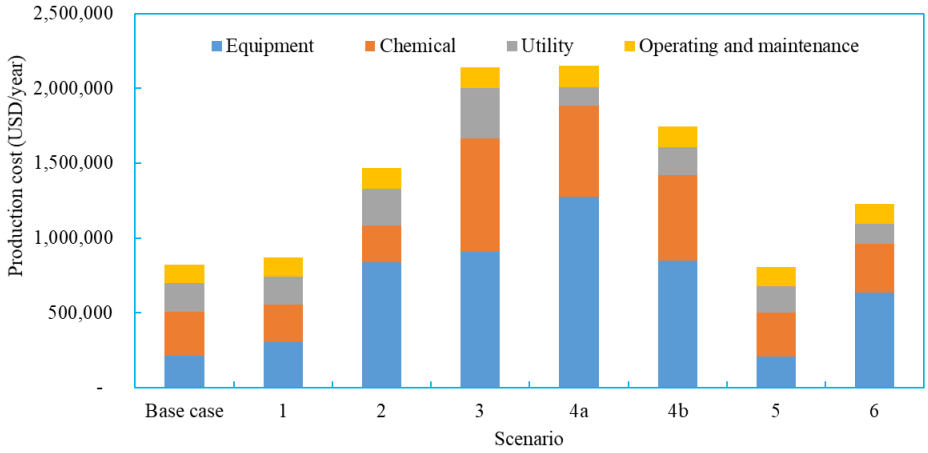

Figure 4.8: The breakdown of production costs from the scenarios

4.4. Conclusion

This chapter performs a sensitivity analysis and identifies most influencing parameters of the model. The biodiesel price, feedstock price, and the production capacity are considered important parameters due to the high sensitivity factors being 2.36, 1.41 and 1.06, respectively. Although the equipment price has lowest sensitivity factor with only 0.061, the choice of technology has great impacts on the result of the superstructure optimization. Besides testing the feasibility of the superstructure model, the technological assessment shows the importance of the process intensification with the reactive distillation being the most economic process for different kinds of feedstock. The production costs including the costs of equipment, chemicals, utility, and operating and maintenance of the base case and scenario 5 which uses the reactive distillation technology are lower than other scenarios, being 823,944 USD and 803,526 USD, respectively.

For scenarios of biodiesel produced from tallow, the annual profit of base case which uses reactive distillation with heterogeneous acid catalyst in the chapter 3 is the highest with 3,539,025 USD per year. The second best scenario with the annual profit of 3,134,732 USD is the scenario 1 which uses the multi-phase reactor and heterogeneous acid catalyst. For the scenarios of biodiesel produced from canola oil, the scenario 5 with reactive distillation and homogenous NaOH catalyst has the highest annual profit of 1,033,042 USD.

However, this is an estimate study which does not consider the real obstacles in applying new technologies in production. The next chapter explores the applications and barriers of process intensification in process industries and presents an innovative idea of combining process intensification and digital twin.

5. Process intensification and digital twin – The potential for the energy transition in process industries

“Innovation is the ability to see change as an opportunity, not a threat.” – Steve Jobs

This chapter was published in:

Huynh, T.A. and Zondervan, E., 2022, " Process intensification and digital twin – The potential for the energy transition in process industries", Physical Sciences Reviews, doi: https://doi.org/10.1515/psr-2022-0058

Abstract

In previous chapter, the results of the superstructure optimization show that process intensification technology (PI) such a reactive distillation can change the production of biodiesel drastically. However, the application of process intensified equipment in real situation is not always easy. The barriers are not just the technology but also the human aspect of the project such as conservative management and not enough skilled operators.

This chapter defines and discusses process intensification and digital twin (DT) as potential tools to accelerate the energy transition through their applications in the process industries including biofuel production. The PI technologies take advantage of innovative principles in equipment design and control to improve the physical process, while the DT offers the virtual model of the plant as an environment for production optimization. The effects of both tools on the energy transition are evaluated not only from the point of applications but also from the possibility of implementation and barriers in process industries. Although they are beneficial, the deployment of PI and DT requires not only infrastructure and capital investment but the knowledge and cooperation of different levels of plant personnel. Besides review of individual implementation, this work explores the concept of combining PI and DT which can make them the enabler of each other and bring a breakthrough in optimization of process design and control.

5.1. Introduction

Over the course of the last years, the world has been facing many challenges at an unprecedented scale, from rapidly spreading diseases to devastating natural disasters which are tied to the global pollution and climate change. Significant transformations to cope with the new situation have happened in all aspects of society from working routine to energy usage and production methods. Therefore, sustainability and renewables are the target of the energy transition in terms of production, distribution and application. Process industries which are among the most intensive energy users require drastic changes to increase energy efficiency and reduce environmental impacts. Process systems engineering in combination with the digital transformation, known as Industry 4.0, brings the required tools such as process intensification (PI) and digital twin (DT) to transform the process industries.

Even though there have been intensified processes since several decades, one of the earliest mentions of intensified processes was published in a research of Wightman et al. in the Research Laboratory of Eastman Kodak in 1925 [79]. While the initial concept was the reduction in equipment- and plant size, it was proven that the scope of PI has been expanded far beyond the miniaturization hallmark [80]. The benefits of PI for energy production are not just smaller equipment and lower investment costs but also higher reaction rate, better product quality, reduced waste generation, improved process safety and reduced environmental burdens [81]. The advantages of PI can be found in different examples. The application of membrane reactors for biodiesel production improved the reaction rate and the purity of both biodiesel and glycerol by simultaneously removing the unreacted oil during the reaction. Without the oil impurity, the equipment and energy requirement for biodiesel purification were reduced, thus, lowering investment costs and environmental impacts [82]. In coating industry, acrylic and methacrylic monomers are widely used chemicals [83]. An economic analysis by Kiss (2018) showed that the cost of acrylate can be reduced by 43.5%, from 1350 EUR/t to 762 EUR/t, by using continuous processes with reactive distillation instead of batch processes [83]. With the development of new technologies, the potential energy saving of PI is increasing over the years. The report of Kim (2017) presents the data of energy saving by applying PI in the chemical and petrochemical industries for different countries and the world as in the Figure 5.1 [84].

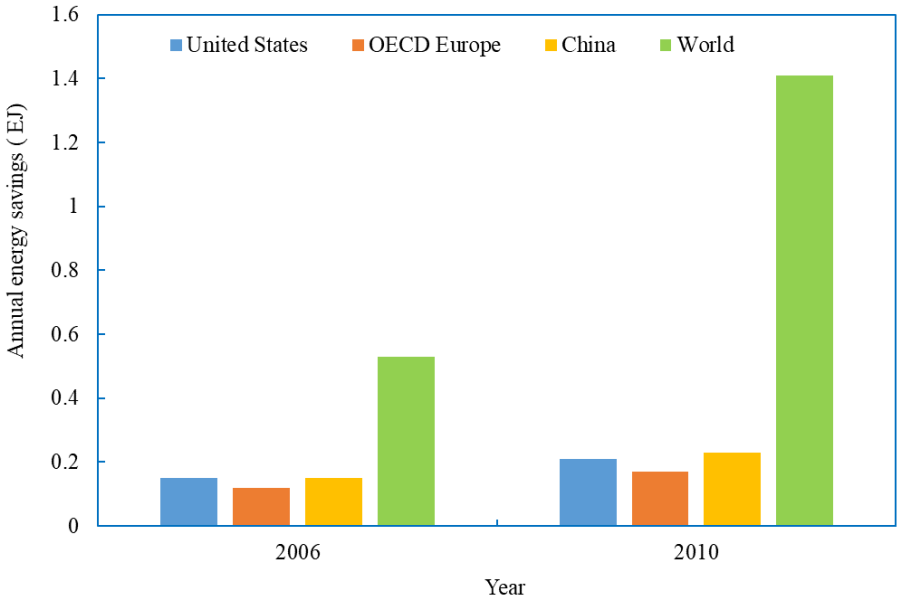

Figure 5.1: Annual energy saving of PI in the chemical and petrochemical industries (unit: EJ; 1 EJ = 10^{18} J) [84]

Digital twin is a fairly new concept compared to process intensification. It was introduced in a presentation of product lifecycle management by Michael Grieves at the University of Michigan in 2002 [85]. The DT was originally defined as a system including a physical object, a virtual replicant of that object and a link of data and information between physical and digital objects [85]. Since its introduction, the concept of DT has evolved rapidly and found its way into new applications and industries, for instance, supply chain management [86], shop floor management, prognostics, and health management of airplanes, monitoring and optimizing complex production processes [87]. Over the last ten years, the literature reported 46 DT definitions which combine the original concept with specific characterizations based on the applications [88]. Due to its ability to exchange data between the virtual models and physical objects, DT offers many benefits for a production process from real-time monitoring and analysis to intelligent update and management that can be applied in process design, maintenance and optimization [89]. Figure 5.2 illustrates the concept of DT for a production plant.

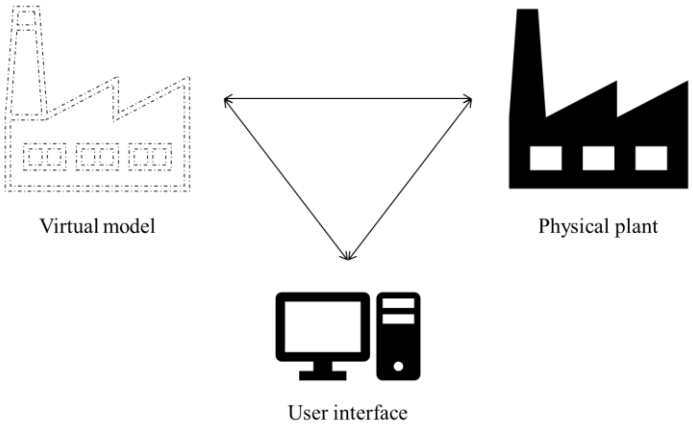

Figure 5.2: The data exchange between virtual model, physical plant and users in a DT system

Even though PI and DT have different approaches, they have the similar objective of making production process more efficient and can be combined for mutual improvement. The innovative designs of PI can be further optimized by integration with more precise and up-to-date data and information from the DT. Safdarnejad (2019) proposed a novel dynamic approach for PI application which utilized the data-driven modelling of the entire production plant [90]. The data-driven approach gave similar results while having advantages of less complexity and lower costs compared to traditional gradient-based methods [90]. The improved systems of PI can bring new challenges for the data management and digital simulation of DT, thus, leading to improvement of sensory systems, new data processing methods and simulation programs. A combination of PI and DT will bring greater benefits in terms of production capacity, investment and operation costs, and environmental impacts for process industries which require more economic and sustainable production methods. This contribution provides a literature review of PI and DT applications and the state-of-art trends of combined concepts for the energy transition in the process industries. After the introduction in section 1, more details and examples of technologies and applications relating to PI and DT in process industries are presented in section 2 and 3. Section 4 discusses the benefits of combining PI and DT. Finally, section 5 provides take-away messages of important topics and developments for future works.

5.2. Applications and effects of process intensification on energy transition.

The European Roadmap for Process Intensification presents the potential of PI which can improve the energy efficiency in several industries as in Table 5.1 [91]. The long-term potentials of PI have attracted a lot of research interest with many reviews of recent

developments and more than 12 books published since 2003 [92]. The applications of PI can be categorized as separation , reaction and separation-reaction-combined technologies.

Table 5.1: The energy efficiency increases (by percentage) over time by applying PI in different process industries [91]

	5 – 20 years	30 – 40 yeas
Petrochemicals	5 %	20 %
Pharmaceuticals	20 %	50 %
Food ingredients	25 %	75 %
Consumer foods	10 – 15 %	30 – 40 %

5.2.1. Separation technologies.

Distillation is the most used and energy intensive separation technology in process industries. The distillation is the main separation process used in oil industry and consumes globally 230 gigawatts (2.3×10^8 kilowatts) [93]. Therefore, it is considered one of the best candidates for process intensification. The dividing wall column (DWC) is one of the most preferred PI technologies in commercial application [94]. Another potential PI technology based on distillation is the cyclic distillation which has been applied in industry since 2000 [95]. Other potential separation technologies are the pressure swing adsorption (PSA) and simulated moving bed (SMB) which can be intensified for process industries [94]. The potentials of PI separation technologies do not only reduce the costs, energy requirements and environmental impacts but also present very effective ways to improve product quality [94].

Since its first industrial application in 1985, the dividing wall column which is the integration of two conventional distillation columns into one shell, has more than 100 applications and will become a standard distillation tool in the near future [96]. When changing from traditional distillation columns to DWC, it offers smaller installation footprint and lower investment costs due to the reduced number of equipment units. The saving of operating costs and energy of DWC can be up to 50% as compared to conventional units [96]. Kiss et al. presented a reactive dividing-wall column design (Figure 5.3) in an industrial case study of AkzoNobel that provided up to 35% savings of investment costs and 15% savings of energy costs [97].

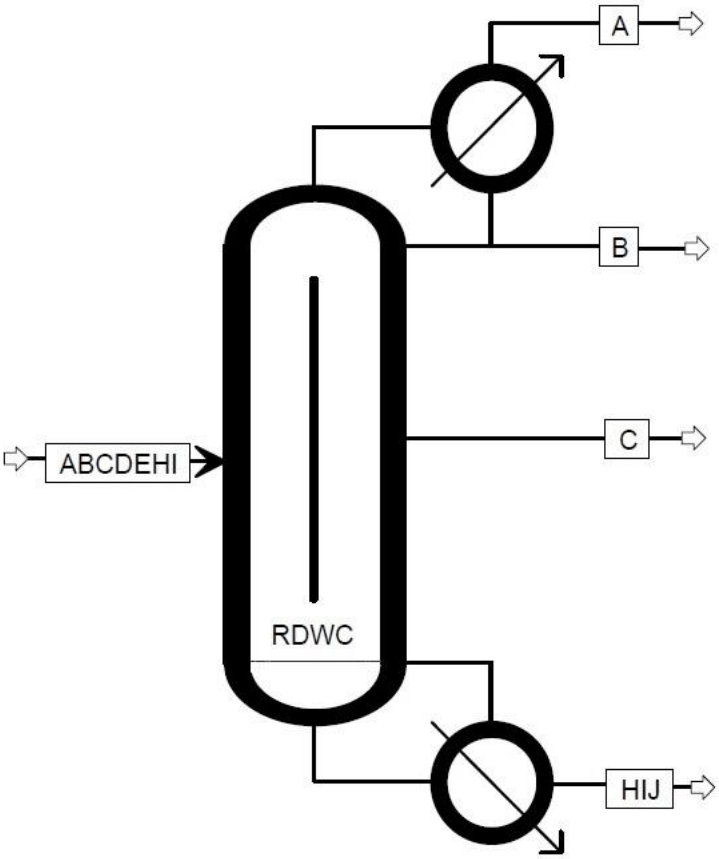

Figure 5.3: The illustration of the proposed reactive DWC [97]

Besides DWC, the cyclic distillation is a potential intensified distillation process which was proposed by Cannon et al. [98]. The operation of cyclic distillation column can be described as a cycle of a vapor period (when the vapor flows upwards and the liquid is stationary) followed by a liquid period (the liquid flows down the column while the vapor is stopped) [98]. The implementation of cyclic distillation for ethanol production has been evaluated in Eastern Europe food industry with significant results [95]. The cyclic distillation columns requires 20 – 30 % less energy and 1.5 – 2 times lower height than the traditional columns, thus greatly reducing the utility consumption and greenhouse gas emission [95].

The pressure swing adsorption is a gas separation technique based on the different adsorption forces between an adsorbent material and different components of a gas mixture [99]. It is a cyclic process of physical adsorption and desorption depending only on the gas pressure and the operating temperature [99]. PSA was mentioned in a patent in 1942 and developed widely in industry at the end of the 1960s and the beginning of the 1970s [100].

Main applications of PSA are in gas drying and purification, particularly in hydrogen production with several advantages such as high purity (up to 99.9 % in case of hydrogen purification), less capital investment as well as lower energy requirement and operating costs compared to conventional technologies [101]. The twin-or multiple-bed pressure swing adsorption is popular PI choice to improve the capacity and energy-savings of gas production [102]. Marcinek et al. (2021) presented a PI study of the twin-bed PSA plant for nitrogen production with different operating strategies which can increase the productivity up to 23.9% [102].

In chromatography, the components of a mixture are separated by their adsorption and desorption at the surface of the adsorbents such as silica and alumina. One of the popular chromatographic separations in process industries is the simulated moving bed technology which was developed in 1961 by Broughton, Gerhold, and Carson [103]. While the true moving bed technology requires the solid adsorbent to actually move in the opposite direction of the liquid, the operating principle of the SMB is the periodical shift in the position of inlet and out ports to create a similar effect of the counter-current flows as presented in Figure 5.4 [103]. The simulated moving bed reactor (SMBR) is a promising PI technology which found many applications in bio- and petrochemical industries [104]. For example, Shi et al. (2020) proposed a novel SMBR which used a homogeneous combination of catalyst and adsorbent to increase the yield of p-xylene about 25% and reduce the energy requirement by 19% [105].

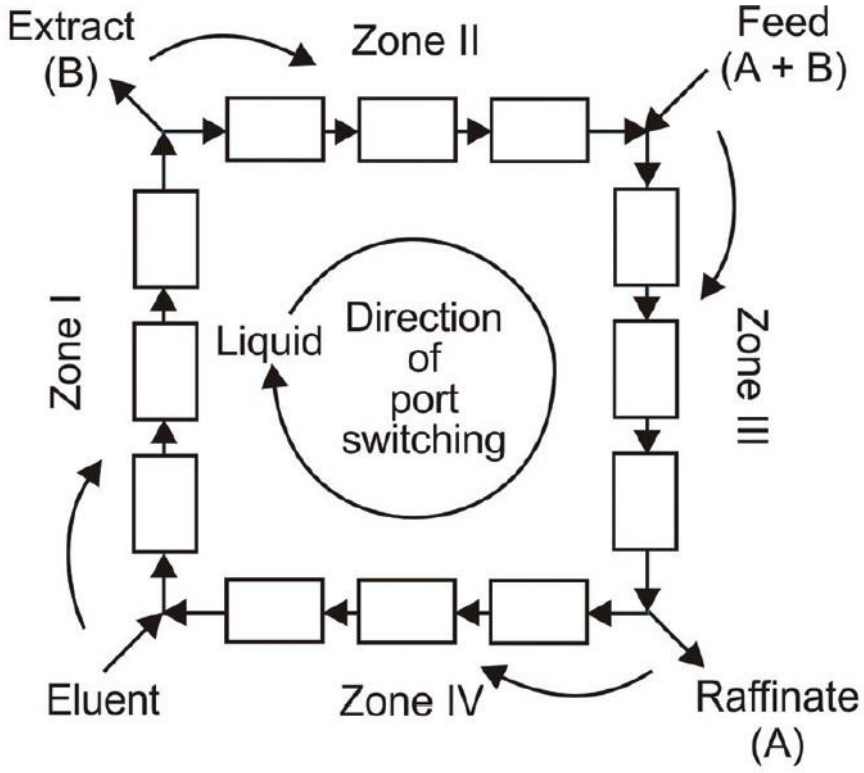

Figure 5.4: The illustration of a simulated moving bed [106]

5.2.2. Reaction technologies.

The PI reaction technologies are usually called "green" chemical reactors because they bring green benefits for industrial processes such as reduced size by combination of several reactions, continuous process, improved safety and reaction rate, decrease of waste formation, etc. [107]. The industrial applications of PI reaction technologies are including spinning disc reactors (SDR), static mixer reactors (SMR), monolithic reactors and microreactors [107].

The principles of the spinning disc reactor have been developed in the 1920s and seen more application since the 1960s [108]. By generating a very thin film of liquid on the rotating surface with the centrifugal force, the SDR creates excellent heat-, mass- and momentum transfers between liquid and gas phases, and between the liquid and the disc surface [109]. Thus, the SDR is the ideal continuous reactor for fast reactions required gas-liquid contact and an intensive mixing environment [109]. In the processing industry, the SDR is a very high performance reactor which can improve the efficiency and economics of production processes [109]. For example, compared with traditional methods, the application

of the SDR in pharmaceutical production can reduce the reaction time up to 99.97 %, plant volume up to 99.21 %, impurity level up to 93.33 % and reaction temperature up to 6.83% [110]. An example of a large scale SDR which can be used for production up to 10 tons per day is shown in Figure 5.5 [111].

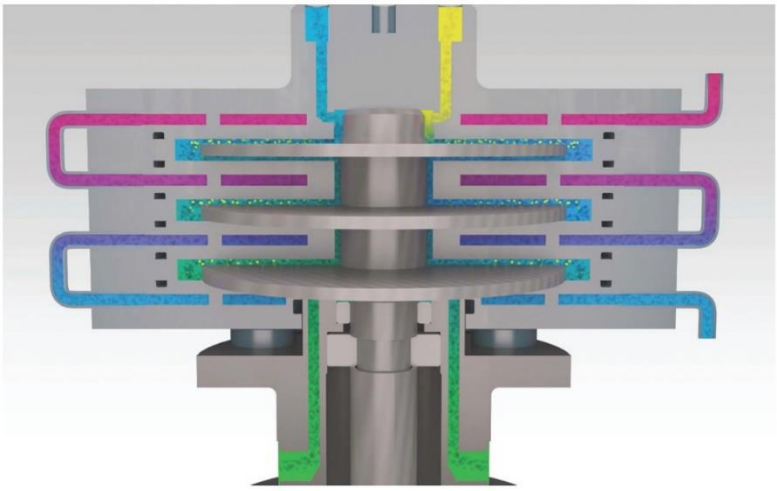

Figure 5.5: A cross section presentation of a spinning disc reactor by SPINID [111]

Although the forerunner of the static mixer reactor, a single element motionless gas mixer, was described in a patent in 1874, the reactor was not widely applied in the process industries until 100 years later [112]. The SMR has several advantages such as easily changed product types, continuous operation, smaller footprint, shorter residence time, lower equipment cost and energy requirement compared to the conventional continuous stirred tank reactor (CSTR) [112]. In a quantitative example presented by Bayer and Himmler (2005), a homogeneous mixture can be achieved with a SMR requiring only 1 kW power and 0.25 s residence time while a CSTR requires 10 kW and 1 h [113]. The continuous SMR process is commonly applied in fine chemical and polymerization plants with a 20 % - 25 % better yield than the conventional batch type process [113].

The monolithic reactor was commonly applied for automotive exhaust gas treatment since the 1970s [114]. With a simple and robust design, the monolithic reactor is considered a potential PI replacement for the conventional packed bed reactor in catalytic gas–solid reactions [115]. The monolithic catalyst is a construction of multiple narrow straight parallel channels manufactured from ceramics or metallic components which create an ease passage for the reactant flow [116]. This design reduces the pressure drop and increases the specific surface area of the reactor, thus, improving the conversion rate per unit volume and heat and mass transfer efficiency [116]. Therefore, the monolithic reactor has smaller size and requires less energy than the conventional reactor with same capacity [116].

The research and applications of microstructure devices such as microreactors, micro-heat exchangers and micromixers became more popular since the beginning of the 1990s [117]. The first industrial application of a microreactor was in 1935 in form of the falling-film microreactor for a gas-liquid reaction [94]. The potential of upscaling a microreactor has been demonstrated in a study relating the effect of oxygen addition on water-gas shift reaction by Neuberg et al. [118]. The results showed that the pilot scale microreactor retained the performance and efficiency of the laboratory scale reactor [118]. With advantages such as excellent heat and mass transfer, a continuous process with high conversion rate, easy control and compact size, the microreactor is a potential process intensification which saves a great amount of investment and energy for chemical and pharmaceutical industries that usually apply energy intensive reactions [119].

5.2.3. Reactive separation technologies.

Reactive separation technology has several definitions from different authors [120]. One of the general concepts was presented in 1967 by Balashov [120]. The concept considers that the reactive separation technology is a development of several separation and reaction processes at the same time with the target of mutual intensification, efficiency improvement and reduction of process flow sheet [120]. A notable example of the reactive separation technologies is the reactive distillation column as shown in Figure 5.6. Various strategies are applied to incorporate different separative functions into the reactor, which guarantee improvement of reaction rate and selectivity, and reduction in waste processing, equipment and energy cost [121]. A list of common reactive separation processes is given in Table 5.2.

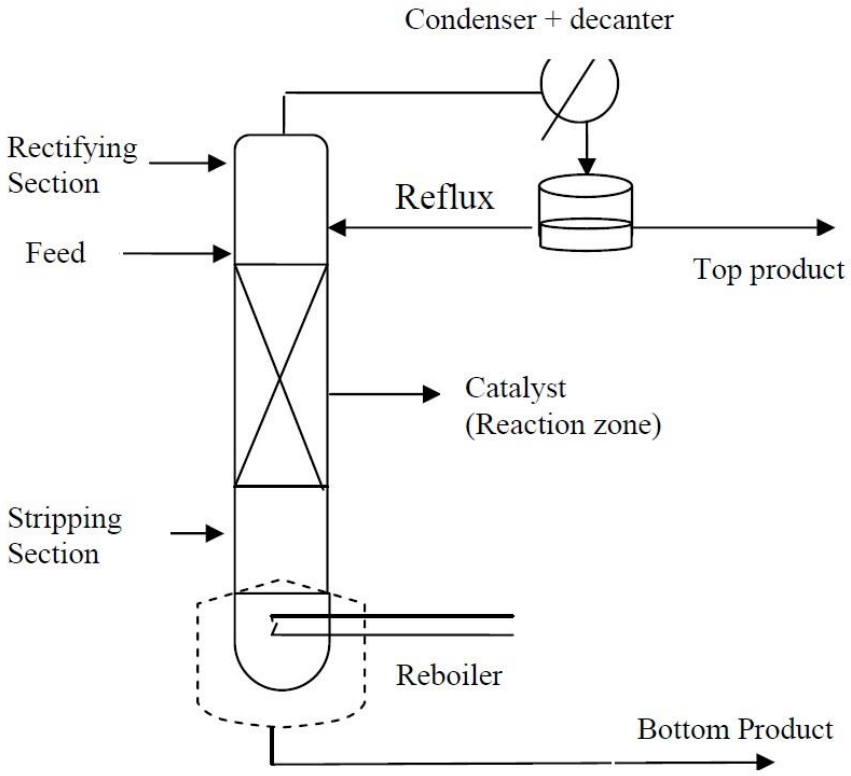

Figure 5.6: A schematic diagram of a reactive distillation column [122]

Table 5.2: Examples of reactive separation processes

Process	Key features	Applications
Reactive distillation	Combination of separation and chemical reaction within a distillation apparatus where the production and removal of products are carried out simultaneously. Advantages: enhancing productivity and selectivity, consuming less energy and solvents while also keeping high efficiency of the reaction system. Disadvantages: limited application by operating constrains of both distillation and reaction, and more difficult control [123].	Synthesis of methyl acetate [121], biodiesel production [81], production of formic acid [124]

Reactive absorption	An equipment in which a selective absorption of gaseous species by liquid solutions is combined with simultaneous chemical reactions Advantages: improving the reaction conversion and the separation efficiency of absorption, capability to process gas mixtures, low thermal degradation of products. Disadvantage: higher capital investment and utility cost due to absorbent recovery units [120].	Production of nitric or sulfuric acid, treatment of industrial gases and elimination of CO_2, H_2S, ozone, and NO_x [120]
Reactive extraction	A single operating unit comprises liquid-liquid extraction and chemical reaction by adding a selective solvent to reaction zone. Advantages: higher yield and selectivity of reaction and liquid separation, lower waste generation, allowing extraction of difficult-to-separate products [120]. Disadvantages: loss of reactants because of emulsification, mixing and phase separation, technical and economic difficulties in the recovery of low concentration solutes, unsuitable for high viscous solutions [125].	Separation of carboxylic acids [126], production of renewable fuels [127]
Membrane reactors	Integration of a membrane separation into a reactor to overcome equilibrium limitations by continuously removal of reactants or products. Advantages: increasing reactor efficiency in term of productivity and purity of products, decreasing number of downstream processing units. Disadvantages: decline of production due to membrane fouling, lack of experience on equipment designing [128].	Production of biofuels, hydrogen and other basic chemical [129]

The reactive distillation process to produce methyl acetate by Eastman Kodak is a well-known example of successful industrial reactive separation [107]. Methyl acetate is produced through the catalyzed esterification of acetic acid with methanol [107]. Due to the reversible nature of the reaction and its azeotrope products, the conventional methyl acetate production requires large amounts of reactants for high conversion rate and an energy intensive purification process to separate the products [107]. The Eastman process uses 80% less energy and only 20% investment cost of the conventional process by replacing an entire plant of reactors, distillation columns and liquid-liquid extraction with a RD column and two separation columns [107].

In conclusion, the application of PI technologies in industry is one of the key components in the EU energy transition strategy. Besides significant cost reductions, PI technologies offer great energy savings and environmental benefits for many industries, especially energy intensive ones such as chemical, oil and gas industries [107]. Dividing wall column, static mixer reactor, reactive distillation and reverse osmosis filtration are examples from many successes of PI technologies at industrial scale [107]. However, the application of PI technologies is not always going smoothly. When scaling up from laboratory to industrial level, there are several technical and non-technical problems such as increasing fouling in membrane filtration, losing thermodynamics efficiency, new technologies being incompatible with existing infrastructure and the conservative of industrial management [107]. New PI technologies are usually compared with existing conventional chemical plants which are used as benchmarks for capital investment and operating costs [130]. Even though newer technologies have advantages of equipment size and costs, the operating costs can increase significantly in some cases [130]. Finding a balance of capital investment and operating costs is a considerable challenge for PI to replace the existing technologies [130].

5.3. The effects of digital twin on the energy transition of the process industries.

Digital twin has seen a wide range of researches and applications in many sectors, including but not limited to production, construction, aviation, education, automotive and meteorology with various scales from a single product to factories, cities and countries [131]. In the 2018 Tutzing Symposium of ProcessNet in Germany, DT was considered the foundation of digitalization and cooperation in process industries that can reduce production time, increase versatility and process efficiency [132]. Depending on its applications, the DT has different aspects and definitions [133]. The definition of DT for the applications in process industries is a set of virtual models which have a real-time connection with the physical production process and an ability of constant adaptation and update itself by getting real-time data from the physical process during its life cycle [133]. From this definition, the DT provides not just a digital replica but also abilities of control, prediction and optimization of the production process [133].

With the features as constantly updating and directly linking between the virtual model and the entire production line, one of notable DT applications in the process industries is production control. Novák et al. proposed a new production planning tool for production control by integrating a DT of a physical process into an automated planning system [134]. The real-time information of DT such as equipment states (ready, running, maintenance or failure), operating conditions (temperature, pressure), etc., enhances the speed, the flexibility and the adaptation of the production planning system [134]. The new planning tool is able to quickly reformulate a new plan in case of product change or technical failure, providing a global overview of the entire production line for further operating optimization [134].

Safety and risk management in process industries such as oil, gas and chemicals are usually considered of utmost importance [135]. The integration of DT into existing empirical process safety models can improve the process operation and safety [135]. Lee et al. proposed a concept of a "mega digital twin" model which linked different types of models with real-time data of a production process. The "mega digital twin" model was used to improve the performance of a process plant and give a depth safety and risk analysis through its entire life cycle, from design and construction to operation, maintenance, optimization and modifications, personnel development and environmental impact control [135].

Since 2018, the number of publications relating to applications of DT has increased, particularly in maintenance applications [136]. Because industrial process plants are usually enormous, complex and operating in high risk conditions, the maintenance is a crucial and costly operation to keep the plants running efficiently. The time-based or preventive maintenance which is generally based on operating experience or recommendation of equipment producers has been slowly replaced with condition-based or predictive maintenance [137]. The concept of predictive maintenance was introduced in 1975 to reduce maintenance costs by making decisions based on real-time assessments of the production process [138]. The DT is considered one of key enablers to achieve the transition from preventive to predictive maintenance by making the virtual models of equipment and production process more realistic [139]. With the constant updated models, the predictive maintenance becomes more accurate and adaptive through the life cycle of industrial process plants [139]. The integration of DT into the predictive maintenance model allows evaluation and prediction of the current- and after-maintenance states of the production process [136]. Optimized maintenance plans can reduce the operating costs, energy consumption and environmental impacts [139].

Process industries are highly susceptible to product market prices which fluctuate according to various factors including but not limited to seasonal changes, environmental policies, consumer demands and political issues. The integration of the DT into process models make them more adaptable to changes in the market due to the timely communication between the real process and the virtual model. The benefits of production optimization with

the DT have been presented in several studies. The study of Min et al. presents an approach and a frame work for applying the DT in optimization of the production process in petrochemical industry which is a typical process industry[140]. This study presents the DT based optimization experiment of MAYA, a Chinese refinery with capacity of multi-million tons (diesel, gasoline, LPG, propane, propylene, petroleum coke, oil slurry, naphtha, and sulphate MTBE) per year [140]. The case study results show an increase in the light oil daily yield of the refinery by 0.2 - 0.5% [140]. Shen et al. proposed a DT based optimization model in oil and gas industry [141]. The DT model provided an virtual environment which continuously connected the oil and gas supply capacity of oil wells with the working conditions and capacity of equipment [141]. The real time connection of different components in the production process allowed more precise prediction and control of the production capacity and energy requirements of refinery [141]. The proposed DT control model was applied to 35 oil wells which showed a reduction of daily average power consumption by 48.12 kWh and an increase of system efficiency from 11.02% to 16.43% [141].

Figure 5.7 presents search results from the website Scopus for keywords of “digital twin”, “process intensification”, combinations of “digital twin” or “process intensification” with “process industry” from 2012 to 2021. The number of publications relating to DT have increased significantly with 5860 papers . However, the applications of the DT in the process industries are still scarce and immature compared to other sectors [131]. There are several barriers for extensively applying the DT in process industries [131]. One of the main barriers can be identified as the high difficulty in application of the DT to the complexity of physical and chemical processes which are commonly used in process industries [131]. Another main barrier is the compatibility of existing industrial process plants which can be several decades old with new digital information and control systems [142]. With the exception of modern plants which are built with digital-ready designs, the investment costs for the DT in an existing plant can easily discourage most of the plant management [142]. Therefore, the deployment methodologies of DT are required to be innovative and adaptive with the situation of each process plant. After applied in the plant, the maintenance of DT model is quite a challenge in term of plant personnel who have the required know-how knowledge and experience.

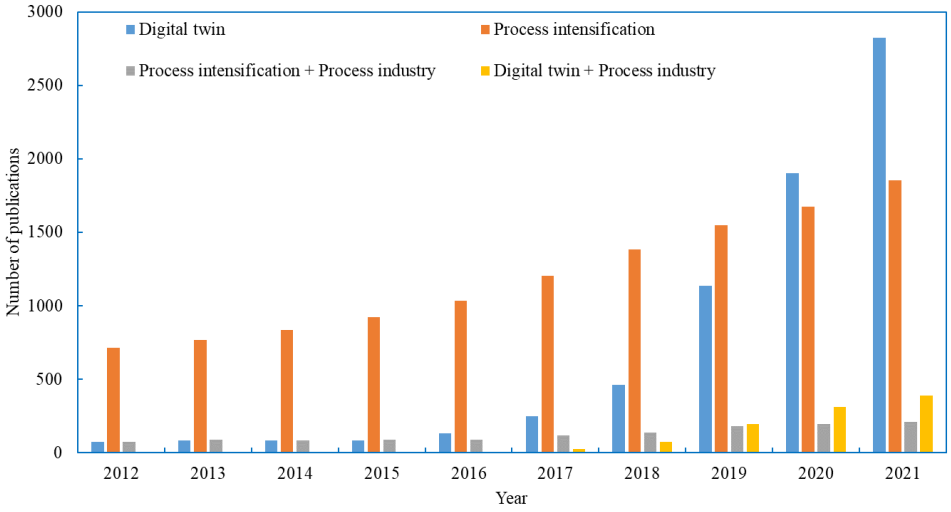

Figure 5.7: The number of publications relating to DT and PI over last 10 years

The DT approach for process industries is equally important as its applications. The method of DT application greatly depends on the size and state of the existing plant, the investment budget, the skills of operators and the available digital tools and data. Sierla et al. proposed a methodology of "semi-automatic generation of digital twins" for several decade old process plants or "brownfield process plants" where a large part of data was not available in digital format [142]. The method included nine steps to combine machine and human efforts in input and correction of data for setting up a DT model with reasonable investments [142]. Örs et al. presented a operational digital twin (ODT) focused on the optimization of plant operation and its generic development framework in chemical process industry [143]. The ODT was combined with artificial intelligence (AI) support to optimize the process model, schedule and control [143]. From the research, the application of AI-based ODT can improve the production flexibility and reduce the CO_2 emissions of chemical process plants [143]. Perno et al. systematically analysed the enablers and barriers and proposed a model for application of the DT in process industries [131]. The model connected the enabler with the right barrier to create a proper guidance of the DT deployment for process industry practitioners [131].

As its potential has been proven, the DT can play an important role in the energy transition of process industries. With the abilities of precise simulation and prediction, the DT can improve the design, control and maintenance plan from single equipment to entire processes. The application of DT through the lifecycle of industrial process plants increases production efficiency and reduces unnecessary costs and energy requirement.

5.4. The combination of PI and DT in process industries, a winning formula?

The barriers of PI applications in process industries can be overcome by connecting it to DT. The DT creates a virtual environment of the process plant where the PI strategies can be simulated, predicted and optimized with real-time data [144]. The effects of PI can be evaluated in the research and development phases, thus, saving the costs of prototypes and adjustments after physical implementation [144]. The analysis of a high quality DT model helps understand the chemical and physical limitations of the production process and improve PI designs [144]. With the knowledge from the DT, the need of many testing and pilot steps can be reduced during the scale-up while still ensuring the performance of PI equipment [144].

Due to the integration of two or more processes into a single equipment, operation and control are challenging issues of intensified processes [145]. With a real-time exchange between virtual model and real operating plant data, the DT is an advanced tool for control, simulation and optimization of the operating conditions of intensified equipment and production systems [145]. The high accurate simulation using the DT model allows process industry practitioners to optimize the operation and control of a PI system at the conceptual design stage [145].

López-Guajardo et al. have presented the concept of Process Intensification 4.0 which is the integration between PI, Industry 4.0 and Circular Chemistry [146]. The real-time data based simulation and prediction of the DT are identified as important tools to achieve the next generation of PI [146]. The PI 4.0 takes advantages of Industry 4.0 data-driven tools and algorithms to develop, improve and deploy innovative technologies and circular processes, thus, improving the viability of sustainable transitions in process industries [146].

The advances in PI allow the development of more sophisticated equipment and process designs, thus creating more complex physical and chemical systems. The challenges of understanding and describing high complex systems become the drive for developing advanced sensors, accurate and reliable simulation tools and updated modelling methods. These then lead to improve the depth, reliability and accuracy of the DT.

Figure 5.7 shows an upward trend in the number of PI and DT researches in process industries recently, leading to more attentions on the concept of integrating advanced computational and data-centric tools into process design, control and maintenance. Although the combination of PI and DT has been vaguely mentioned in a few publications, it is proven that process intensification can be evolved by integrating Industry 4.0 toolboxes, especially the digital twin model. Advances in process and equipment designs, intelligent technologies and big data management are applied to develop more flexible, environmentally friendly and efficient production processes.

5.5. Conclusion

The process intensification and the digital twin are potential tools to reduce the environmental impact of process industries. Besides economic benefits, they can increase the energy saving, enhance process safety and reduce unnecessary material consumption in production and equipment manufacturing. The concept of combining the PI and the DT can further improve their capabilities. The data based model and real-time data interaction of the DT and the physical process play important roles in the development of the next generation PI, which in turn has an impact on the sensory system, data management and simulation software. However, the applications of the PI and DT in process industries are not without difficulties such as lack of capital investment, insufficient skilled workforce, legacy equipment, conservative plant management, etc. Nonetheless, the deployment of PI, DT and their combination can accelerate the energy transition in process industries and the barriers can be overcome by identifying and communicating the solutions, combining different approaches and technologies, publishing new development in PI and DT openly and increasing public awareness of the impact of energy transition in process industries.

To conclude, there are important topics and future perspectives requiring our attention:

1) The human-machine interface which gives access, details and explanation of DT knowledge to different level of industrial practitioners, from operator to supply chain manager, is a key to bring out all the knowledge of the DT. Finding a simple and effective communication method between user and virtual environment can be an important topic for DT developers.
2) While various patented DT platforms have been developed by large companies such as IBM, Microsoft, General Electrics and Siemens [133], open-source software is a more economic option for implementing DT in small and medium size plants. A notable examples of open source DT framework is the project Eclipse Ditto™ which is sponsored mainly by Robert Bosch GmbH [147]. Another platform is iTwin.js of Bentley Systems for setting up and managing the DTs of infrastructures such as buildings, airports, bridges, industrial and power plants and railroad [148].
3) The development of more effective methods to collect, process and communicate data are urgently needed because data availability is one of the key enablers for the implementation of PI and DT in process industries.
4) In addition to DT, the combination of PI and different tools of Industrial 4.0 such as machine learning and data-driven simulation and modelling is crucial for developing more effective processes and a direction for the future chemical engineering.
5) The energy transition in process industries requires a joint effort of different disciplines and management levels. A worldwide digital platform for sharing data and knowledge of PI and DT can reduce costs and time of their development and application.

6) Beyond the traditional process industries, the PI and DT can transform the production paradigm of other sectors such as renewable energy (solar, wind, biofuels, etc.), agriculture, and high-value biochemicals from microalgae. Therefore, studies to widen the applications of PI and DT are important in the long term strategy of energy transition.

6. Conclusion and outlook

“The end is just the beginning” – Thomas Stearns Eliot

6.1. Conclusions

This study addresses the challenges of biodiesel production such as high costs, food-or-fuel debates and environment impacts with process intensification technology such as membrane reactor and reactive distillation. Three new models for applying process intensification in the biodiesel production have been developed:

The first model is a novel mathematical model for the membrane reactor which integrate the dynamic fouling states. The model has been used to describe the cyclic operation of membrane reactor in biodiesel production.

Secondly, from the membrane cleaning model of Zondervan et al. [33], a new cleaning model for the membrane reactor has been developed for biodiesel reaction and fouling. The cleaning duration and costs of cleaning including production lost, chemical and energy costs can be determined from the model.

The superstructure model for the biodiesel production is the third model. The first new feature of this model is the wide range of feedstocks from three biodiesel generations and innovative technologies such membrane reactor, reactive distillation and supercritical reaction. The second novel feature is the heat integration which allows the model to match the hot and cold product streams to reduce the heating and cooling requirements.

The membrane reactor for biodiesel production is not a new study in the literature [23]. Although the fouling is an intrinsic problem of the membrane operation, the effects of fouling on the membrane reactor in biodiesel production has not received adequate attentions. After a certain period called operating cycle, the membrane has to be physical cleaning to remove the reversible fouling [29]. The accumulation of irreversible fouling requires a complete stop of the reactor operation to do a chemical cleaning [29]. In chapter 2, the membrane reactor model in combination with the membrane cleaning model is used to simulate the reactor operating under effects of fouling with different operating cycles. Then, the cleaning costs which contribute greatly to the operating cost are calculated. From the results, an optimal operating cycle is identified to minimize the operating cost per weight of biodiesel produced.

Even though the reaction is important to produce biodiesel, the feedstock and purification process contribute more than 80% of the total production cost [9]. With a network of different feedstock and process technologies, the superstructure model set up in chapter 3 has been used effectively to optimize the biodiesel production. The tallow is the chosen feedstock due to its low cost and non-edible status. The optimal process of producing biodiesel from tallow is using reactive distillation which is a process intensification technology. The heat integration and glycerol treatment process reduce the cost and environmental impacts of biodiesel production further.

The membrane reactor has the advantage of high reaction rate and product purity. However, its biodiesel yield is lower than other reactors such as continuous stirred tank or reactive distillation, thus making it not cost effective for biodiesel production.

The production of biodiesel has been affected by many uncertainties. Based on the production cost breakdown in chapter 3, chapter 4 identifies that the market prices of biodiesel and feedstock, and production capacity are most influencing uncertainties. The assessment of different technology and feedstocks shows that process intensification such as reactive distillation greatly improves the biodiesel production in term of costs and flexibility.

The application of process intensification technologies in the process industries including biodiesel production is very difficult as management is conservative (business as usual) or the new technology is incompatible with old production lines. One potential solution to overcome those difficulties is the combination of process intensification with digital twin as presented in chapter 5. By creating a virtual environment, the DT helps evaluate the effects of PI technology in the early stages of the project such as research and development. Therefore, the DT model can be used to prove the advantages of PI design and analysing the compatibility with the existing plant without spending additional costs for protypes or adjustments after physical deployment of the new technology.

6.2. Outlook

Validation with experiments in pilot scale with different membrane materials and operating conditions is the next step to improve the membrane reactor model. The current model has been proven that it can reliably simulate the biodiesel reaction in combination with fouling activities. However, it is fitted with only one set of experimental data which provides essential data such as the permeate flux and the biodiesel yield over time [27]. This experiment does not reflect the advances in membrane material and technology [27]. While there are new membrane technologies for different fields such as water treatment, medical and food applications, the reports in biodiesel production are scarce. The model can be improved greatly in terms of accuracy, biodiesel yield and selectivity with sufficient data of new membrane technologies, especially the data in the pilot scale.

Improving the accuracy of the superstructure model with more detailed cost calculation, heat exchanger network design, and accounting the uncertainty in the product and raw material prices, the availability of technologies. The current accuracy is limited to 30% to 35%. The first reason is the Lang's factor method to calculate the capital investment which is a study estimate [68]. The second reason is the heat integration feature which does not calculate heat exchanger costs, thus reducing the accuracy in the equipment cost result. The third reason is the uncertainty which is still an issue and requires to be integrate into the superstructure model. From the initial optimization result, more accurate and detailed

biodiesel production can be designed by using more detailed methods such as preliminary estimate and definitive estimate for capital investment and cost spread sheet for annual costs [69]. The heat integration results can be used to design a heat exchanging network and calculate the heat exchanger costs. The recommended calculations can be done after the initial estimate study. Optimization under uncertainty has been received more attentions in the field of process systems engineering [149]. The sensitivity analysis and technological assessment in chapter 4 are important preconditions for solving the superstructure model under uncertainty.

Supply chain optimization integrating the developed superstructure is an interesting work to improve the production costs of biodiesel. The models developed in this study are useful for initial estimate studies of the biodiesel production design and optimization. They can answer the questions relating to the direction of biodiesel production. The limitations of those models can be overcome with more data and improvement in modelling and calculation methods which cannot be address in the finite time of this study. It is interesting to note that the superstructure is modelled in AIMMS which is a powerful tool for supply chain optimization, thus opening opportunities to integrate the superstructure in future biodiesel supply chains and making an enterprise level optimization.

Bibliography

1. Yoro, K.O. and M.O. Daramola, *Chapter 1 - CO2 emission sources, greenhouse gases, and the global warming effect*, in *Advances in Carbon Capture*, M.R. Rahimpour, M. Farsi, and M.A. Makarem, Editors. 2020, Woodhead Publishing. p. 3-28.
2. Ritchie, H. and M. Roser, *CO_2 and Greenhouse Gas Emissions.* Our World in Data, 2020.
3. EurObserv'ER, *Renewable Energy in Transport Barometer*. 2021.
4. Hanaki, K. and J. Portugal-Pereira, *The Effect of Biofuel Production on Greenhouse Gas Emission Reductions*, in *Biofuels and Sustainability: Holistic Perspectives for Policy-making*, K. Takeuchi, et al., Editors. 2018, Springer Japan: Tokyo. p. 53-71.
5. Knothe, G., *2 - History of Vegetable Oil-Based Diesel Fuels*, in *The Biodiesel Handbook (Second Edition)*, G. Knothe, J. Krahl, and J. Van Gerpen, Editors. 2010, AOCS Press. p. 5-19.
6. Kiss, A.A., *Biodiesel and Fatty Esters*, in *Process Intensification Technologies for Biodiesel Production: Reactive Separation Processes*, A.A. Kiss, Editor. 2014, Springer International Publishing: Cham. p. 9-24.
7. Knothe, G., *1 - Introduction*, in *The Biodiesel Handbook (Second Edition)*, G. Knothe, J. Krahl, and J. Van Gerpen, Editors. 2010, AOCS Press. p. 1-3.
8. Fazal, M.A., S. Rubaiee, and A. Al-Zahrani, *Overview of the interactions between automotive materials and biodiesel obtained from different feedstocks.* Fuel Processing Technology, 2019. **196**: p. 106178.
9. Zhang, Y., et al., *Biodiesel production from waste cooking oil: 2. Economic assessment and sensitivity analysis.* Bioresource Technology, 2003. **90**(3): p. 229-240.
10. *4 - Biodiesel Production*, in *The Biodiesel Handbook (Second Edition)*, G. Knothe, J. Krahl, and J. Van Gerpen, Editors. 2010, AOCS Press. p. 31-96.
11. Atadashi, I.M., et al., *Refining technologies for the purification of crude biodiesel.* Applied Energy, 2011. **88**(12): p. 4239-4251.
12. Rezania, S., et al., *Review on transesterification of non-edible sources for biodiesel production with a focus on economic aspects, fuel properties and by-product applications.* Energy Conversion and Management, 2019. **201**: p. 112155.
13. Chhandama, M.V.L., et al., *Microalgae as a feedstock for the production of biodiesel: A review.* Bioresource Technology Reports, 2021. **15**: p. 100771.
14. Galanopoulos, C., P. Kenkel, and E. Zondervan, *Superstructure optimization of an integrated algae biorefinery.* Computers & Chemical Engineering, 2019. **130**: p. 106530.
15. Rodríguez-Palacio, M.C., et al., *The cultivation of five microalgae species and their potential for biodiesel production.* Energy, Sustainability and Society, 2022. **12**(1).
16. Mulyatun, M., et al., *Production of non-food feedstock based biodiesel using acid-base bifunctional heterogeneous catalysts: A review.* Fuel, 2022. **314**: p. 122749.
17. Budiman Abdurakhman, Y., et al., *Techno-economic analysis of biodiesel production process from waste cooking oil using catalytic membrane reactor and realistic feed composition.* Chemical Engineering Research and Design, 2018. **134**: p. 564-574.

18. Adeniyi, A.G., J.O. Ighalo, and O.A.A. Eletta, *Process Integration and Feedstock Optimisation of a Two-Step Biodiesel Production Process from Jatropha Curcas Using Aspen Plus.* Chemical Product and Process Modeling, 2019. **14**(2).
19. Petrescu, L., et al., *Modelling and Simulation of Methanol and Biodiesel Production Processes Using Innovative Technologies.* Chemical Engineering Transactions, 2020. **80**: p. 181-186.
20. Dubé, M.A., A.Y. Tremblay, and J. Liu, *Biodiesel production using a membrane reactor.* Bioresource Technology, 2007. **98**(3): p. 639-647.
21. Cao, P., A.Y. Tremblay, and M.A. Dubé, *Kinetics of Canola Oil Transesterification in a Membrane Reactor.* Industrial & Engineering Chemistry Research, 2009. **48**(5): p. 2533-2541.
22. Cheng, L.-H., et al., *Study on membrane reactors for biodiesel production by phase behaviors of canola oil methanolysis in batch reactors.* Bioresource Technology, 2010. **101**(17): p. 6663-6668.
23. Chong, M.F., et al., *Modeling analysis of membrane reactor for biodiesel production.* AIChE Journal, 2013. **59**(1): p. 258-271.
24. Gao, L., W. Xu, and G. Xiao, *Modeling of biodiesel production in a membrane reactor using solid alkali catalyst.* Chemical Engineering and Processing: Process Intensification, 2017. **122**: p. 122-127.
25. Hapońska, M., et al., *Membrane reactors for biodiesel production with strontium oxide as a heterogeneous catalyst.* Fuel Processing Technology, 2019. **185**: p. 1-7.
26. Cao, P., M.A. Dubé, and A.Y. Tremblay, *High-purity fatty acid methyl ester production from canola, soybean, palm, and yellow grease lipids by means of a membrane reactor.* Biomass and Bioenergy, 2008. **32**(11): p. 1028-1036.
27. Cheng, L.-H., et al., *Modeling and simulation of biodiesel production using a membrane reactor integrated with a prereactor.* Chemical Engineering Science, 2012. **69**(1): p. 81-92.
28. Xu, W., et al., *Biodiesel production in a membrane reactor using MCM-41 supported solid acid catalyst.* Bioresource Technology, 2014. **159**: p. 286-291.
29. Cheryan, M., *Fouling and Cleaning*, in *Ultrafiltration and Microfiltration Handbook (2nd ed.)*, M. Cheryan, Editor. 1998, CRC Press: Boca Raton. p. 56.
30. Popović, S., et al., *Application of an ultrasound field in chemical cleaning of ceramic tubular membrane fouled with whey proteins.* Journal of Food Engineering, 2010. **101**(3): p. 296-302.
31. Li, H. and V. Chen, *Chapter 10 - Membrane Fouling and Cleaning in Food and Bioprocessing*, in *Membrane Technology*, Z.F. Cui and H.S. Muralidhara, Editors. 2010, Butterworth-Heinemann: Oxford. p. 213-254.
32. Wang, Z., et al., *Membrane cleaning in membrane bioreactors: A review.* Journal of Membrane Science, 2014. **468**: p. 276-307.
33. Zondervan, E., B.H.L. Betlem, and B. Roffel, *Development of a dynamic model for cleaning ultra filtration membranes fouled by surface water.* Journal of Membrane Science, 2007. **289**(1): p. 26-31.
34. Madaeni, S.S., et al., *Optimization of Chemical Cleaning for Removal of Biofouling Layer.* Chemical Product and Process Modeling, 2009. **4**(1).
35. Popović, S.S., M.N. Tekić, and M.S. Djurić, *Kinetic models for alkali and detergent cleaning of ceramic tubular membrane fouled with whey proteins.* Journal of Food Engineering, 2009. **94**(3): p. 307-315.

36. Patel, N.K. and S.N. Shah, *11 - Biodiesel from Plant Oils*, in *Food, Energy, and Water*, S. Ahuja, Editor. 2015, Elsevier: Boston. p. 277-307.
37. Darnoko, D. and M. Cheryan, *Kinetics of palm oil transesterification in a batch reactor*. Journal of the American Oil Chemists' Society, 2000. **77**(12): p. 1263-1267.
38. Rashid, U. and F. Anwar, *Production of biodiesel through optimized alkaline-catalyzed transesterification of rapeseed oil.* Fuel, 2008. **87**(3): p. 265-273.
39. Gomes, M.C.S., N.C. Pereira, and S.T.D.d. Barros, *Separation of biodiesel and glycerol using ceramic membranes.* Journal of Membrane Science, 2010. **352**(1): p. 271-276.
40. Alves, M.J., et al., *Biodiesel purification using micro and ultrafiltration membranes.* Renewable Energy, 2013. **58**: p. 15-20.
41. Noriega, M.A., P.C. Narváez, and A.C. Habert, *Biodiesel separation using ultrafiltration poly(ether sulfone) hollow fiber membranes: Improving biodiesel and glycerol rich phases settling.* Chemical Engineering Research and Design, 2018. **138**: p. 32-42.
42. Buonomenna, M.G. and J. Bae, *Membrane processes and renewable energies.* Renewable and Sustainable Energy Reviews, 2015. **43**: p. 1343-1398.
43. Rahimpour, M.R., *10 - Membrane reactors for biodiesel production and processing*, in *Membrane Reactors for Energy Applications and Basic Chemical Production*, A. Basile, et al., Editors. 2015, Woodhead Publishing. p. 289-312.
44. Choi, H., et al., *Influence of cross-flow velocity on membrane performance during filtration of biological suspension.* Journal of Membrane Science, 2005. **248**(1): p. 189-199.
45. Cheryan, M., *Performance and Engineering Models*, in *Ultrafiltration and Microfiltration Handbook (2nd ed.)*, M. Cheryan, Editor. 1998, CRC Press: Boca Raton. p. 58.
46. Iritani, E. and N. Katagiri, *Developments of Blocking Filtration Model in Membrane Filtration.* KONA Powder and Particle Journal, 2016. **33**: p. 179-202.
47. Ghaffour, N., *Modeling of fouling phenomena in cross-flow ultrafiltration of suspensions containing suspended solids and oil droplets.* Desalination, 2004. **167**: p. 281-291.
48. Das, B., B. Chakrabarty, and P. Barkakati, *Separation of oil from oily wastewater using low cost ceramic membrane.* Korean Journal of Chemical Engineering, 2017. **34**(10): p. 2559-2569.
49. Salama, A., et al., *A new modeling approach for flux declining behavior during the filtration of oily-water systems due to coalescence and clustering of oil droplets: Experimental and multicontinuum investigation.* Separation and Purification Technology, 2019. **227**: p. 115688.
50. Ariono, D., et al., *Fouling mechanism in ultrafiltration of vegetable oil.* Materials Research Express, 2018. **5**(3): p. 034009.
51. Daniel, R.C., et al., *Integrated pore blockage-cake filtration model for crossflow filtration.* Chemical Engineering Research and Design, 2011. **89**(7): p. 1094-1103.
52. Portha, J.F., et al., *Simulation and kinetic study of transesterification of triolein to biodiesel using modular reactors.* Chemical Engineering Journal, 2012. **207-208**: p. 285-298.
53. Baker, R.W., *Concentration Polarization*, in *Membrane Technology and Applications*, R.W. Baker, Editor. 2012. p. 179-206.

54. *What Is the Genetic Algorithm?* [cited 2022 14/1/2022]; Available from: https://nl.mathworks.com/help/gads/what-is-the-genetic-algorithm.html.
55. Fayyazi, E., et al., *Genetic Algorithm Approach to Optimize Biodiesel Production by Ultrasonic System.* Chemical Product and Process Modeling, 2014. **9**(1): p. 59-70.
56. Zondervan, E., *Data regression and curve fitting*, in *A Numerical Primer for the Chemical Engineer (2nd ed.)*, E. Zondervan, Editor. 2019, CRC Press: Boca Raton. p. 109-116.
57. Zondervan, E., *Case studies*, in *A Numerical Primer for the Chemical Engineer (2nd ed.)*, E. Zondervan, Editor. 2019, CRC Press: Boca Raton.
58. Jepsen, K.L., et al., *Membrane Fouling for Produced Water Treatment: A Review Study From a Process Control Perspective.* Water, 2018. **10**(7): p. 847.
59. Tula, A.K., et al., *A computer-aided software-tool for sustainable process synthesis-intensification.* Computers & Chemical Engineering, 2017. **105**: p. 74-95.
60. A. Kiss, A., A. C. Dimian, and G. Rothenberg, *Biodiesel production by integrated reactive-separation design*, in *Computer Aided Chemical Engineering*, V. Pleşu and P.Ş. Agachi, Editors. 2007, Elsevier. p. 1283-1288.
61. Gomez-Castro, F.I., et al., *Alternatives for the Production of Biodiesel by Supercritical Technologies: A Comparative Study*, in *Computer Aided Chemical Engineering*, A. Kraslawski and I. Turunen, Editors. 2013, Elsevier. p. 7-12.
62. Myint, L.L. and M.M. El-Halwagi, *Process analysis and optimization of biodiesel production from soybean oil.* Clean Technologies and Environmental Policy, 2009. **11**(3): p. 263-276.
63. Mencarelli, L., et al., *A review on superstructure optimization approaches in process system engineering.* Computers & Chemical Engineering, 2020. **136**: p. 106808.
64. AlNouss, A., G. McKay, and T. Al-Ansari, *Superstructure Optimization for the Production of Fuels, Fertilizers and Power using Biomass Gasification*, in *Computer Aided Chemical Engineering*, A.A. Kiss, et al., Editors. 2019, Elsevier. p. 301-306.
65. Kenkel, P., et al., *A generic superstructure modeling and optimization framework on the example of bi-criteria Power-to-Methanol process design.* Computers & Chemical Engineering, 2021. **150**: p. 107327.
66. West, A.H., D. Posarac, and N. Ellis, *Assessment of four biodiesel production processes using HYSYS.Plant.* Bioresource Technology, 2008. **99**(14): p. 6587-6601.
67. Bart, J.C.J., N. Palmeri, and S. Cavallaro, *13 - Valorisation of the glycerol by-product from biodiesel production*, in *Biodiesel Science and Technology*, J.C.J. Bart, N. Palmeri, and S. Cavallaro, Editors. 2010, Woodhead Publishing. p. 571-624.
68. Seider, W.D., et al., *Chapter 16 - Cost Accounting and Capital Cost Estimation*, in *Product and Process Design Principles: Synthesis, Analysis and Evaluation, 4th Edition*, S. Rajan, M. O'Sullivan, and L. Ratts, Editors. 2016, John Wiley & Sons, Inc.: New Jersey. p. 426-494.
69. Seider, W.D., et al., *Chapter 17 - Annual Costs, Earnings, and Profitability Analysis*, in *Product and Process Design Principles: Synthesis, Analysis and*

Evaluation, 4th Edition, S. Rajan, M. O'Sullivan, and L. Ratts, Editors. 2016, John Wiley & Sons, Inc.: New Jersey. p. 498-546.
70. Sahinidis, N.V., *BARON: A general purpose global optimization software package.* Journal of Global Optimization, 1996. **8**(2): p. 201-205.
71. Zhang, Y., et al., *Biodiesel production from waste cooking oil: 1. Process design and technological assessment.* Bioresource Technology, 2003. **89**(1): p. 1-16.
72. Boon-anuwat, N.-n., et al., *Process design of continuous biodiesel production by reactive distillation: Comparison between homogeneous and heterogeneous catalysts.* Chemical Engineering and Processing: Process Intensification, 2015. **92**: p. 33-44.
73. *Palm and rapeseed oil prices*. [cited 2022 17/3]; Available from: https://www.neste.com/investors/market-data/palm-and-rapeseed-oil-prices#1fb175e1.
74. *Biodiesel prices (SME & FAME)*. [cited 2022 17/3]; Available from: https://www.neste.com/investors/market-data/biodiesel-prices-sme-fame#1fb175e1.
75. *Waste - based market performance*. Available from: http://www.greenea.com/en/market-analysis/.
76. Karuppiah, R. and I.E. Grossmann, *Global optimization of multiscenario mixed integer nonlinear programming models arising in the synthesis of integrated water networks under uncertainty*, in *Computer Aided Chemical Engineering*, W. Marquardt and C. Pantelides, Editors. 2006, Elsevier. p. 1747-1752.
77. Sahinidis, N.V., *Optimization under uncertainty: state-of-the-art and opportunities.* Computers & Chemical Engineering, 2004. **28**(6): p. 971-983.
78. Clay, R.L. and I.E. Grossmann, *A disaggregation algorithm for the optimization of stochastic planning models.* Computers & Chemical Engineering, 1997. **21**(7): p. 751-774.
79. Reay, D., C. Ramshaw, and A. Harvey, *Chapter 1 - A Brief History of Process Intensification*, in *Process Intensification (Second Edition)*, D. Reay, C. Ramshaw, and A. Harvey, Editors. 2013, Butterworth-Heinemann: Oxford. p. 1-25.
80. Zondervan, E., C. Almeida-Rivera, and K.V. Camarda, *2. Performance products in a challenging environment*, in *Product-Driven Process Design: From Molecule to Enterprise*. 2020, De Gruyter. p. 9-88.
81. Kiss, A.A., *Process Intensification Technologies for Biodiesel Production - Reactive Separation Processes*. 1 ed. SpringerBriefs in Applied Sciences and Technology. 2014, Heidelberg, Germany: Springer, Cham. XV, 103.
82. Dubé, M.A., A.Y. Tremblay, and J. Liu, *Biodiesel production using a membrane reactor.* Bioresour Technol, 2007. **98**(3): p. 639-47.
83. Kiss, A.A., *Novel Catalytic Reactive Distillation Processes for a Sustainable Chemical Industry.* Topics in Catalysis, 2019. **62**(17): p. 1132-1148.
84. Kim, Y.-h., et al., *Modular Chemical Process Intensification: A Review.* Annual Review of Chemical and Biomolecular Engineering, 2017. **8**(1): p. 359-380.
85. Grieves, M. and J. Vickers, *Digital Twin: Mitigating Unpredictable, Undesirable Emergent Behavior in Complex Systems*, in *Transdisciplinary Perspectives on Complex Systems*, F.S. Kahlen FJ., Alves A. , Editor. 2017, Springer, Cham: Heidelberg, Germany. p. 85-113.

86. Wang, Y., X. Wang, and A. Liu, *Digital Twin-driven Supply Chain Planning.* Procedia CIRP, 2020. **93**: p. 198-203.
87. Tao, F., et al., *Digital Twin in Industry: State-of-the-Art.* IEEE Transactions on Industrial Informatics, 2019. **15**(4): p. 2405-2415.
88. VanDerHorn, E. and S. Mahadevan, *Digital Twin: Generalization, characterization and implementation.* Decision Support Systems, 2021. **145**: p. 113524.
89. Cimino, C., E. Negri, and L. Fumagalli, *Review of digital twin applications in manufacturing.* Computers in Industry, 2019. **113**: p. 103130.
90. Safdarnejad, S.M., J.F. Tuttle, and K.M. Powell, *Development of a roadmap for dynamic process intensification by using a dynamic, data-driven optimization approach.* Chemical Engineering and Processing - Process Intensification, 2019. **140**: p. 100-113.
91. *ERPI: European Roadmap for Process Intensification: Creative Energy - Energy Transition*. 2008.
92. Sitter, S., Q. Chen, and I.E. Grossmann, *An overview of process intensification methods.* Current Opinion in Chemical Engineering, 2019. **25**: p. 87-94.
93. Sholl, D.S. and R.P. Lively, *Seven chemical separations to change the world.* Nature, 2016. **532**(7600): p. 435-437.
94. Abdulrahman, I., V. Máša, and S.Y. Teng, *Process intensification in the oil and gas industry: A technological framework.* Chemical Engineering and Processing - Process Intensification, 2021. **159**: p. 108208.
95. Harmsen, J. and M. Verkerk, *16 Intensified ethanol production by cyclic distillation*, in *Process Intensification: Breakthrough in Design, Industrial Innovation Practices, and Education*. 2020, De Gruyter. p. 176-187.
96. Yildirim, Ö., A.A. Kiss, and E.Y. Kenig, *Dividing wall columns in chemical process industry: A review on current activities.* Separation and Purification Technology, 2011. **80**(3): p. 403-417.
97. Kiss, A.A., J.J. Pragt, and C.J.G.v. Strien, *Reactive Dividing-Wall Columns - Defying Equilibrium Restrictions.* Chemical Product and Process Modeling, 2009. **4**(5).
98. Maleta, V.N., et al., *Understanding process intensification in cyclic distillation systems.* Chemical Engineering and Processing: Process Intensification, 2011. **50**(7): p. 655-664.
99. Wiessner, F.G., *Basics and industrial applications of pressure swing adsorption (PSA), the modern way to separate gas.* Gas Separation & Purification, 1988. **2**(3): p. 115-119.
100. Tondeur, D. and P.C. Wankat, *Gas Purification by Pressure Swing Adsorption.* Separation and Purification Methods, 1985. **14**(2): p. 157-212.
101. Fahim, M.A., T.A. Alsahhaf, and A. Elkilani, *Chapter 11 - Hydrogen Production*, in *Fundamentals of Petroleum Refining*, M.A. Fahim, T.A. Alsahhaf, and A. Elkilani, Editors. 2010, Elsevier: Amsterdam. p. 285-302.
102. Marcinek, A., J. Guderian, and D. Bathen, *Process intensification of the high-purity nitrogen production in twin-bed Pressure Swing Adsorption plants.* Adsorption, 2021. **27**(6): p. 937-952.
103. Rodrigues, A.E., et al., *Chapter 1 - Principles of Simulated Moving Bed*, in *Simulated Moving Bed Technology*, A.E. Rodrigues, et al., Editors. 2015, Butterworth-Heinemann: Oxford. p. 1-30.

104. Migliorini, C., et al., *Analysis of simulated moving-bed reactors.* Chemical Engineering Science, 1999. **54**(13): p. 2475-2480.
105. Shi, Q., et al., *Simulated moving bed reactor for p-xylene production: Modeling, simulation, and optimization.* Chemical Engineering Science, 2020. **225**: p. 115802.
106. Keil, F.J., *Process intensification.* Reviews in Chemical Engineering, 2018. **34**(2): p. 135-200.
107. Kiss, A.A., *Process intensification: Industrial applications*, in *Process Intensification in Chemical Engineering: Design Optimization and Control*. 2016, Springer: Netherlands.
108. van der Schaaf, J. and J.C. Schouten, *High-gravity and high-shear gas–liquid contactors for the chemical process industry.* Current Opinion in Chemical Engineering, 2011. **1**(1): p. 84-88.
109. Reay, D., C. Ramshaw, and A. Harvey, *Chapter 5 - Reactors*, in *Process Intensification (Second Edition)*, D. Reay, C. Ramshaw, and A. Harvey, Editors. 2013, Butterworth-Heinemann: Oxford. p. 121-204.
110. Reay, D., C. Ramshaw, and A. Harvey, *Chapter 8 - Application Areas – Petrochemicals and Fine Chemicals*, in *Process Intensification (Second Edition)*, D. Reay, C. Ramshaw, and A. Harvey, Editors. 2013, Butterworth-Heinemann: Oxford. p. 259-321.
111. Berg, J.v.d., *SPINID.* Green Processing and Synthesis, 2014. **3**(1): p. 77-79.
112. Thakur, R.K., et al., *Static Mixers in the Process Industries—A Review.* Chemical Engineering Research and Design, 2003. **81**(7): p. 787-826.
113. Bayer, T. and K. Himmler, *Mixing and Organic Chemistry.* Chemical Engineering & Technology, 2005. **28**(3): p. 285-289.
114. Hayes, R.E. and I. Cornejo, *Multi-scale modelling of monolith reactors: A 30-year perspective from 1990 to 2020.* The Canadian Journal of Chemical Engineering, 2021. **99**(12): p. 2589-2606.
115. Zamaniyan, A., et al., *Tube fitted bulk monolithic catalyst as novel structured reactor for gas–solid reactions.* Applied Catalysis A: General, 2010. **385**(1): p. 214-223.
116. Baharudin, L., et al., *Process intensification in multifunctional reactors: A review of multi-functionality by catalytic structures, internals, operating modes, and unit integrations.* Chemical Engineering and Processing - Process Intensification, 2021. **168**: p. 108561.
117. Schubert, K., et al., *MICROSTRUCTURE DEVICES FOR APPLICATIONS IN THERMAL AND CHEMICAL PROCESS ENGINEERING.* Microscale Thermophysical Engineering, 2001. **5**(1): p. 17-39.
118. Neuberg, S., et al., *Effect of oxygen addition on the water–gas shift reaction over Pt/CeO2 catalysts in microchannels – Results from catalyst testing and reactor performance in the kW scale.* International Journal of Hydrogen Energy, 2014. **39**(31): p. 18120-18127.
119. Yao, X., et al., *Review of the applications of microreactors.* Renewable and Sustainable Energy Reviews, 2015. **47**: p. 519-539.
120. Alzate, C.A.C., M.O. Sanchez, and Y. Pisarenko, *Reactive Separation for Process Intensification and Sustainability*. 1 ed. 2019, Boca Raton: CRC Press.
121. Krishna, R., *Reactive separations: more ways to skin a cat.* Chemical Engineering Science, 2002. **57**(9): p. 1491-1504.

122. Sharma, N. and K. Singh, *Control of Reactive Distillation Column: A Review.* International Journal of Chemical Reactor Engineering, 2010. **8**(1).
123. Shah, M.R., et al., *Evaluation of configuration alternatives for multi-product polyester synthesis by reactive distillation.* Computers and Chemical Engineering, 2013. **52**: p. 10.
124. Novita, F.J., H.-Y. Lee, and M. Lee, *Self-heat recuperative dividing wall column for enhancing the energy efficiency of the reactive distillation process in the formic acid production process.* Chemical Engineering and Processing: Process Intensification, 2015. **97**: p. 144-152.
125. Wieszczycka, K., *Reactive extraction at liquid–liquid systems.* Physical Sciences Reviews, 2018. **3**(3).
126. Djas, M. and M. Henczka, *Reactive extraction of carboxylic acids using organic solvents and supercritical fluids: A review.* Separation and Purification Technology, 2018. **201**: p. 106-119.
127. Mederos-Nieto, F.S., et al., *Renewable fuels production from the hydrotreating over NiMo/γ-Al2O3 catalyst of castor oil methyl esters obtained by reactive extraction.* Fuel, 2021. **285**: p. 119168.
128. Basile, A., et al., *Membrane Reactor Engineering: Applications for a Greener Process Industry*. 2016, West Sussex: John Wiley & Sons.
129. Basile, A., et al., *Membrane Reactors for Energy Applications and Basic Chemical Production*. 2015, Amsterdam: Woodhead Publishing.
130. van der Wielen, L.A.M., S.I. Mussatto, and J. van Breugel, *Bioprocess intensification: Cases that (don't) work.* New Biotechnology, 2021. **61**: p. 108-115.
131. Perno, M., L. Hvam, and A. Haug, *Implementation of digital twins in the process industry: A systematic literature review of enablers and barriers.* Computers in Industry, 2022. **134**: p. 103558.
132. Kockmann, N., *Digital methods and tools for chemical equipment and plants.* Reaction Chemistry & Engineering, 2019. **4**(9): p. 1522-1529.
133. Semeraro, C., et al., *Digital twin paradigm: A systematic literature review.* Computers in Industry, 2021. **130**: p. 103469.
134. Novák, P., J. Vyskočil, and B. Wally, *The Digital Twin as a Core Component for Industry 4.0 Smart Production Planning.* IFAC-PapersOnLine, 2020. **53**(2): p. 10803-10809.
135. Lee, J., I. Cameron, and M. Hassall, *Improving process safety: What roles for Digitalization and Industry 4.0?* Process Safety and Environmental Protection, 2019. **132**: p. 325-339.
136. Errandonea, I., S. Beltrán, and S. Arrizabalaga, *Digital Twin for maintenance: A literature review.* Computers in Industry, 2020. **123**: p. 103316.
137. Wen, Y., et al., *Recent advances and trends of predictive maintenance from data-driven machine prognostics perspective.* Measurement, 2022. **187**: p. 110276.
138. Ahmad, R. and S. Kamaruddin, *An overview of time-based and condition-based maintenance in industrial application.* Computers & Industrial Engineering, 2012. **63**(1): p. 135-149.
139. Damant, L., et al. *Exploring the transition from preventive maintenance to predictive maintenance within ERP systems by utilising digital twins*. in *Advances in Transdisciplinary Engineering*. 2021. IOS Press.

140. Min, Q., et al., *Machine Learning based Digital Twin Framework for Production Optimization in Petrochemical Industry.* International Journal of Information Management, 2019. **49**: p. 502-519.
141. Shen, F., et al., *A Digital Twin-Based Approach for Optimization and Prediction of Oil and Gas Production.* Mathematical Problems in Engineering, 2021. **2021**: p. 3062841.
142. Sierla, S., et al., *Roadmap to semi-automatic generation of digital twins for brownfield process plants.* Journal of Industrial Information Integration, 2021: p. 100282.
143. Örs, E., et al. *A Conceptual Framework for AI-based Operational Digital Twin in Chemical Process Engineering*. in *2020 IEEE International Conference on Engineering, Technology and Innovation (ICE/ITMC)*. 2020.
144. Aglave, R., J. Nixon, and J. Lusty, *Using Simulation and Digitalization for Modular Process Intensification.* Chemical Engineering Progress, 2019. **2019**: p. 45.
145. Pistikopoulos, E.N., Y. Tian, and R. Bindlish, *Operability and control in process intensification and modular design: Challenges and opportunities.* AIChE Journal, 2021. **67**(5): p. e17204.
146. López-Guajardo, E.A., et al., *Process intensification 4.0: A new approach for attaining new, sustainable and circular processes enabled by machine learning.* Chemical Engineering and Processing - Process Intensification, 2021: p. 108671.
147. *ditto*. 2021 21/4/2022 [cited 2022 9/5/2022]; Available from: https://www.eclipse.org/ditto/.
148. Systems, B. *iTwin.js*. [cited 2022 9/5/2022]; Available from: https://www.itwinjs.org/.
149. Grossmann, I.E., et al., *Recent advances in mathematical programming techniques for the optimization of process systems under uncertainty.* Computers & Chemical Engineering, 2016. **91**: p. 3-14.
150. Poddar, T., A. Jagannath, and A. Almansoori, *Use of reactive distillation in biodiesel production: A simulation-based comparison of energy requirements and profitability indicators.* Applied Energy, 2017. **185**: p. 985-997.
151. Sotoft, L.F., et al., *Process simulation and economical evaluation of enzymatic biodiesel production plant.* Bioresource Technology, 2010. **101**(14): p. 5266-5274.
152. Baroi, C. and A.K. Dalai, *Process sustainability of biodiesel production process from green seed canola oil using homogeneous and heterogeneous acid catalysts.* Fuel Processing Technology, 2015. **133**: p. 105-119.
153. Santibáñez, C., M.T. Varnero, and M. Bustamante, *Residual Glycerol from Biodiesel Manufacturing, Waste or Potential Source of Bioenergy: A Review.* Chilean journal of agricultural research, 2011. **71**: p. 469-475.
154. Ruy, A.D.d.S., et al., *Market Prospecting and Assessment of the Economic Potential of Glycerol from Biodiesel*, in *Biotechnological Applications of Biomass*, T.P. Basso, T.O. Basso, and L.C. Basso, Editors. 2020, IntechOpen: London.

Appendixes

Appendix A-2.1

The diffusion coefficient of a component in a solvent is more difficult to determine or estimate than viscosity and density by experimental methods. The Wilke-Chang equation can be used as a semi-theoretical to estimate diffusivity [52].

$$D_{AB} = \frac{(117.3\times10^{-18})(\emptyset M_B)^{0.5}T}{\mu V_A^{0.6}}$$

Where D_{AB} is diffusivity of component *A* in solvent *B*, MB is molecular weight of solvent, *T* is temperature, μ is solution viscosity, V_A is solute molar volume at normal boiling point and ϕ is association constant for solvent.

There are 6 components including TG, MeOH, FAME, DG, MG and GL in the membrane reactor. Methanol which is used with excessive amount becomes the continuous phase. In this case, MeOH is regarded as solvent and other components are regarded as solutes [23].

The research on kinetics of transesterification of Portha et al. (2012) [52] gives the values Φ_{MeOH} = 1.9 and M_{MeOH} = 32 g/mol for methanol. The molar volumes at normal boiling point of other components are shown in Table A-1.

Table A-1: The molar volume of component at its normal boiling temperature (m^3/kmol) [52]:

Component	TG	MeOH	DG	MG	GL	FAME
V	1.2118	0.048	0.826	0.4578	0.096	0.4077

Appendix A-3.1

The description of superstructure options includes name, cost, reference capacity and equipment size exponent.

Option	Name	Cost (USD)	Reference capacity (kg/h)	Chemical Engineering Index	Equipment Size Exponent	Reference
1	Waste cooking oil	740 (USD/t)				Price in 2020
2	Tallow	625 (USD/t)				Price in 2020
3	Linseed oil	1127 (USD/t)				Price in 2020
4	Rapeseed oil	1050 (USD/t)				Price in 2020
5	Canola oil	950 (USD/t)				Price in 2020
6	Algae oil	1500 (USD/t)				Price in 2020
7	Waste cooking oil	740 (USD/t)				Price in 2020
8	Tallow	625 (USD/t)				Price in 2020
9	Linseed oil	1127 (USD/t)				Price in 2020
10	Rapeseed oil	1050 (USD/t)				Price in 2020
11	Canola oil	950 (USD/t)				Price in 2020
12	Algae oil	1,500 (USD/t)				Price in 2020
13	Esterification / Pretreatment	677,000	1,268	401.7	0.6	[71]
14	Transesterification CSTR Homogeneous alkali-catalyzed	292,000	1,175.71	401.7	0.53	[66]
15	Reactive distillation column Homogeneous alkali-catalyzed	232,000	4,892.95	556.8	0.78	[150]
16	Transesterification CSTR Homogeneous alkali-catalyzed	292,000	1,175.71	401.7	0.53	[66]
17	Reactive distillation column	232,000	4,892.95	556.8	0.78	[150]

	Homogeneous alkali-catalyzed					
18	Transesterification CSTR Homogeneous acid-catalyzed	680,000	2,819	401.7	0.53	[66]
19	Transesterification multiphase reactor Heterogeneous acid-catalyzed	75,000	1,168.84	401.7	0.53	[66]
20	Reactive distillation column Heterogeneous acid-catalyzed	236,400	4,456.89	556.8	0.78	[72]
21	CSTR Supercritical MeOH	639,000	2,572	401.7	0.53	[66]
22	Heterogeneous enzyme CSTR	328,320	2,054.4	521.9	0.53	[151]
23	Membrane reactor Heterogeneous acid-catalyzed	336,000	1,971	596.2	0.68	[17]
24	Neutralization reactor + Decanter H2SO4	150,000	2,811.17	576.1	0.53	[152]
25	Neutralization reactor + Decanter CaO	150,000	2,811.17	576.1	0.53	[152]
26	Distillation column MeOH recovery Homogeneous alkali-catalyzed	38,000	1,227	401.7	0.78	[66]
27	Distillation column MeOH recovery Homogeneous acid-catalyzed	152,000	2,819	401.7	0.78	[66]
28	Distillation column MeOH recovery Homogeneous alkali-catalyzed	38,000	1,227	401.7	0.78	[66]
29	Distillation column MeOH recovery Homogeneous acid-catalyzed	152,000	2,819	401.7	0.78	[66]
30	Hydrocyclone	15,000	1,172.88	401.7	0.6	[66]
31	Decanter glycerol separation	113,200	4,457	556.8	0.72	[150]

	reactive distillation process					
32	Decanter glycerol separation Enzymatic process	32,850	1,160	521.9	0.72	[151]
33	Distillation column MeOH recovery Supercritical process	167,000	2,529	401.7	0.78	[66]
34	Decanter glycerol separation	113,200	4,457	556.8	0.72	[150]
35	Distillation MeOH purification homogeneous acid catalyzed	380,000	2,811	576.1	0.78	[152]
36	L-L extraction column Water washing Homogeneous alkali-catalyzed	84,000	1,120	401.7	0.78	[66]
37	Decanter glycerol separation	113,200	4,457	556.8	0.72	[150]
38	Neutralization reactor + Decanter H2SO4	150,000	2,811.17	576.1	0.53	[152]
39	Neutralization reactor + Decanter CaO	150,000	2,811.17	576.1	0.53	[152]
40	Distillation MeOH recovery Heterogeneous acid-catalyzed	28,000	1,163	401.7	0.78	[66]
41	Distillation MeOH removal	140,000	1,288.4	401.7	0.78	[71]
42	Decanter Glycerol separation Supercritical alcohol process	58,000	1,170.33	401.7	0.72	[66]
43	Distillation MeOH separation Catalytic membrane reactor	38,000	1,227	401.7	0.78	[17]
44	Decanter Glycerol homogeneous acid catalyzed	30,000	1,107.67	576.1	0.72	[152]

45	Distillation FAME purification Pre-treated alkali-catalyzed	102,000	1,059.14	401.7	0.78	[66]
46	Distillation FAME purification homogeneous acid catalyzed Including hexane distillation	256,000	1,153.5	401.7	0.78	[71]
47	L-L extraction column Water washing homogeneous acid-catalyzed	113,000	1,313.95	401.7	0.78	[66]
48	Decanter glycerol separation Heterogeneous acid-catalyzed	57,000	1,149.8	401.7	0.72	[66]
49	Distillation FAME purification Heterogeneous acid-catalyzed	95,000	1,049.4	401.7	0.78	[66]
50	Distillation FAME purification Supercritical process	146,000	1,060.23	401.7	0.78	[66]
51	Distillation FAME purification (Without oil) Catalytic membrane reactor	324,000	2,990.37	401.7	0.78	[17]
52	Distillation FAME purification homogeneous acid-catalyzed	560,000	1,016	576.1	0.78	[152]
53	Distillation FAME purification heterogeneous acid-catalyzed	95,000	1,049.4	401.7	0.78	[66]
54	Biodiesel sales	1,060 (USD/t)				Price in 2020
55	Waste glycerol disposal	15 (USD/t)				[153]
56	Neutralization reactor Glycerol	21,000	128	401.7	0.53	[71]
57	Crude glycerol sales	170 (USD/t)				[154]

58	Neutralization reactor Glycerol	21,000	128	401.7	0.53	[71]
59	Crude glycerol sales	170 (USD/t)				[154]
60	Distillation Glycerol purification MeOH, water removal	140,000	1,288.4	401.7	0.78	[71]
61	Distillation Glycerol purification MeOH, water removal	140,000	1,288.4	401.7	0.78	[71]
62	Technical glycerol sales	895 (USD/t)				[154]
63	Distillation Glycerol purification MeOH, water removal	140,000	1,288.4	401.7	0.78	[71]
64	Distillation Glycerol purification MeOH, water removal	140,000	1,288.4	401.7	0.78	[71]
65	Distillation Glycerol purification MeOH, water removal	140,000	1,288.4	401.7	0.78	[71]
66	Technical glycerol sales	895 (USD/t)				[154]
67	Distillation Glycerol purification MeOH, water removal	140,000	1,288.4	401.7	0.78	[71]
68	Pure glycerol sales	1,275 (USD/t)				[154]

Appendix A-3.2

The split factor, $SF_{j,k}$, of each component *k* in option *j*.

k \ j	1	2	3	4	5	6	7	8	9	10	11	12	13	14	15	16	17	18	19	20	21	22	23	24
FAME	1	1	1	1	1	1	1	1	1	1	1	1	1	1	0.99	1	0.99	1	1	1	1	1	0.51	1
MeOH	1	1	1	1	1	1	1	1	1	1	1	1	0	1	0.35	1	0.35	1	1	0.18	1	1	0.46	1
Oil	1	1	1	1	1	1	1	1	1	1	1	1	1	1	0.85	1	0.85	1	1	0.98	1	1	0	1
Glycerol	1	1	1	1	1	1	1	1	1	1	1	1	1	1	1	1	1	1	1	1	1	1	0.38	1
H_2SO_4	1	1	1	1	1	1	1	1	1	1	1	1	0	1	1	1	1	1	1	1	1	1	1	
Water	1	1	1	1	1	1	1	1	1	1	1	1	1	1	1	1	1	1	1	1	1	1	1	1
Hexane	1	1	1	1	1	1	1	1	1	1	1	1	1	1	1	1	1	1	1	1	1	1	1	1
NaOH	1	1	1	1	1	1	1	1	1	1	1	1	1	1	1	1	1	1	1	1	1	1	1	0
SnO	1	1	1	1	1	1	1	1	1	1	1	1	1	1	1	1	1	1	1	1	1	1	1	1
CaO	1	1	1	1	1	1	1	1	1	1	1	1	1	1	1	1	1	1	1	1	1	1	1	1
$C_2H_6MgO_2$	1	1	1	1	1	1	1	1	1	1	1	1	1	1	1	1	1	1	1	0	1	1	1	1
WO_x/Al_2O_3	1	1	1	1	1	1	1	1	1	1	1	1	1	1	1	1	1	1	1	1	1	1	1	1
Enzymes	1	1	1	1	1	1	1	1	1	1	1	1	1	1	1	1	1	1	1	1	1	1	1	1

k \ j	25	26	27	28	29	30	31	32	33	34	35	36	37	38	39	40	41	42
FAME	1	1	1	1	1	1	1	1	1	1	1	1	1	1	1	1	1	1
MeOH	1	0.06	0.01	0.06	0.01	1	0.47	0.51	0.01	1	0	0.46	0	1	1		0.06	0.45
Oil	1	1	1	1	1	1	0.98	0.99	1	1	1	1	1	1	1	1	1	1
Glycerol	1	1	1	1	1	1	0.03	0	1	0	1	0	0	1	1	1	1	0.01
H_2SO_4	0	1	1	1	1	1	1	1	1	1	1	0	0	0	0	1	1	1
Water	1	1	1	1	1	1	1	1	1	1	0.89	1	0.12	1	1	1	1	1
Hexane	1	1	1	1	1	1	1	1	1	1	1	1	1	1	1	1	1	1
NaOH	1	1	1	1	1	1	0.06	0.06	1	0.06	1	1	1	0	1	1	1	1
SnO	1	1	1	1	1	0	1	1	1	1	1	1	1	1	1	1	1	1
CaO	0	1	1	1	1	1	1	1	1	1	1	1	1	1	0	1	1	1
$C_2H_6MgO_2$	1	1	1	1	1	1	1	1	1	1	1	1	1	1	1	1	1	1
WO_x/Al_2O_3	1	1	1	1	1	1	1	1	1	1	1	1	1	1	1	1	1	1
Enzymes	1	1	1	1	1	1	1	1	1	1	1	1	1	1	1	1	1	1

k \ j	43	44	45	46	47	48	49	50	51	52	53	54	55	56	57	58	59	60
FAME	1	1	1	0.975	1	1	1	1	1	1	1	1	1	1	1	1	1	0
MeOH	0.01	0.57	0.03	0	1	0.34	1	1		1	1	1	1	1	1	1	1	0
Oil	0	1	0	0	1	0.99	0	0	0	0	0	1	1	1	1	1	1	0
Glycerol	0	0.1	0	0	0	0.01	1	1	0	1	1	1	1	1	1	1	1	1
H_2SO_4	1	1	1	1	0	1	1	1	1	1	1	1	1	0	1	0	1	0
Water	0	0.94	0	1	0	1	1	1	0	1	0	1	1	1	1	1	1	0
Hexane	1	1	1	0.035	1	1	1	1	1	1	1	1	1	0	1	0	1	0
NaOH	1	0.06	0	1		0.06	1	1	1	0	1	1	1	0	1	0	1	0
SnO	1	1	1	1	1	1	1	1	1	1	1	1	1	0	1	0	1	0
CaO	1	1	1	1	1	1	1	1	1	1	1	1	1	0	1	0	1	0
$C_2H_6MgO_2$	1	1	1	1	1	1	1	1	1	1	1	1	1	0	1	0	1	0
WO_x/Al_2O_3	1	1	1	1	1	1	1	1	1	1	1	1	1	0	1	0	1	0
Enzymes	1	1	1	1	1	1	1	1	1	1	1	1	1	0	1	0	1	0

k \ j	61	62	63	64	65	66	67	68
FAME	0	1	0	1	0	1	0	1
MeOH	0	0	0	0.04	0	1	0	1
Oil	0	1	0	0	0	1	0	1
Glycerol	1	1	1	1	1	1	1	1
H_2SO_4	0	1	0	0	0	1	0	1
Water	0	1	0	0.06	0.03	1	0.03	1
Hexane	0	1	0	0	0	1	0	1
NaOH	0	1	0	0	0	1	0	1
SnO	0	1	0	0	0	1	0	1
CaO	0	1	0	0	0	1	0	1
$C_2H_6MgO_2$	0	1	0	0	0	1	0	1
WO_x/Al_2O_3	0	1	0	0	0	1	0	1
Enzymes	0	1	0	0	0	1	0	1

Appendix A-4.1

Table A-4.1: Sensitivity factors according to the parameters of the superstructure model

Parameter	S
Biodiesel price	2.36
Glycerol price	0.28
Feedstock price	1.41
Equipment price	0.061
Production capacity (infeed)	1.06

Appendix A-4.2

Table A-4.2: The total annual profit and production costs of the base case and scenarios

	Total annual profit (USD)	Equipment cost (USD)	Chemical cost (USD)	Utility cost (USD)	Operating and maintenance cost (USD)
Base case	3,539,026	211,525	297,302	190,886	124,231
1	3,134,732	301,589	255,353	185,617	126,032
2	2,973,252	837,099	244,897	248,385	136,742
3	2,295,976	909,503	756,482	336,741	138,190
4a	2,006,746	1,274,505	607,250	124,806	145,490
4b	2,691,673	847,137	574,504	186,276	136,943
5	1,033,043	209,843	288,822	180,665	124,197
6	333,871	637,211	321,567	133,440	132,744

Can process intensification change the future of biodiesel? presents the answers for improving biodiesel production with process systems engineering tools such as membrane reactor modelling and superstructure optimization. A novel membrane reactor model with dynamic functions of reversible and irreversible fouling and a new dynamic membrane cleaning model have been developed for biodiesel production. The superstructure model which is a network of different alternative options brings the optimization of biodiesel production from equipment level to process level. From the technical assessment with the superstructure, process intensification technologies such as reactive distillation are important for biodiesel production in particular and the process industry in general. This thesis discusses the potential of combining process intensification and digital twin in the energy transition of the process industry.

ISBN: 978-90-365-5421-3